PONTIFICIA UNIVERSIDAD CATÓLICA DE CHILE
FACULTY OF PHYSICS

COSMIC INFLATION IN MODIFIED MODELS OF GRAVITY AND AN ANALYSIS ON GRAVITATIONAL WAVES

MAURICIO GAMONAL SAN MARTÍN

Thesis submitted to the Faculty of Physics of Pontificia Universidad Católica de Chile in partial fulfillment of the requirements for the degree of Master in Physics.

Advisor:
PROF. JORGE ALFARO (Pontificia Universidad Católica de Chile)

Examining Committee:
PROF. GONZALO PALMA (Universidad de Chile)
PROF. BENJAMIN KOCH (Technische Universität Wien)
PROF. MARCO AURELIO DÍAZ (P. Universidad Católica de Chile)

Santiago de Chile, 29 Mayo 2021

"(...) And no one showed us to the land

And no one knows the where's or why's

But something stirs and something tries

And starts to climb toward the light (...)"

– Pink Floyd in Echoes (1971)

CONTENTS

FIGURES

TABLES

ACKNOWLEDGEMENTS

This thesis could not have been completed if it were not for the enormous support of Prof. Alfaro, whom I will always thank for teaching me to fearlessly expand my mind into the unknown, for telling me his stories and showing me the human facet of science, and for making me a much more resilient person.

I want to thank the important support of Prof. Víctor Cortés, Prof. Nelson Padilla, and Prof. Alfaro for writing the letter of recommendation that I needed to pursue a PhD in the United States. Additionally, I acknowledge the support from the Fulbright Commission during the application process. If I was admitted at Penn State, it is in part because of all of you.

During my stay in the master's degree, many people accompanied me on the way. I want to give my sincere gratefulness to those who have been part of my life during this adventure, for tolerating my absence in my moments of greatest anxiety and for being there when I needed it: Juan Manuel González, Maximiliano Cerda, Sebastián Moya, Jennifer Fienco, Loreto Osorio, Javiera Díaz Diego García, Melissa Aguilar, Cristóbal Vallejos, Trinidad Lantaño, Rafael Riveros, Sixto Acuña, Sebastián González, Carolina Morales, Diego Pinar, among many others; and, in particular, Almendra Mendizábal, for pushing me to be a better person. All of you can always count on me.

Finally, I want to thank my family. But above all, to my grandmother, Ruth Velásquez, I am what I am because of her. She taught me the importance of hard work, never settling or ever giving up on always looking for the best possible solution. I also want to thank the love that Nicky, my beautiful dog, has given me over the years. I never thought that I could be able to love a little animal so much. I will be in eternal debt to you two.

Abstract

This work comprises three different lines of research related to the study of cosmological inflation and the propagation of gravitational waves. In the first issue, we developed -for the first time in a systematic way- the slow-roll approximation for a single field inflaton within the framework of $f(R,T)$ gravity, a modified model of gravity such that the Lagrangian is a function of the scalar curvature and the trace of the energy-momentum tensor. We obtained the modified slow-roll parameters and the spectral indices by choosing a minimal coupling between matter and gravity. We computed these quantities for several models and contrasted the predictions with the constraints of the Planck data, obtaining corrections to the Starobinsky model.

In the second line of research, we studied how a free Lorentz-valued bosonic 0-form coupled to Einstein-Cartan gravity's action can be considered the inflaton field. In this model, the interacting terms of the fields come directly from the torsionful contributions of the action. Hence, the inflationary dynamics can be extended so that we can define an effective potential that describes the evolution of the background fields. We found that for a particular combination of initial conditions, the model could adequately guarantee the slow-roll conditions over more than 55 e-folds. However, a more detailed analysis is required to confirm the viability of this inflationary scenario.

Finally, we addressed a different problem related to the propagation of low-frequency gravitational waves coming from sources located at cosmological distances. Within the linearized regime of gravity, we performed a coordinate system transformation between a frame which origin is the source of gravitational waves and the comoving frame of the FLRW metric. Then, we studied the observational consequences in Pulsar Timing Arrays experiments, finding a non-trivial modification to the timing residual of pulsars that depends on the value of the Hubble constant.

NOTATION AND CONVENTIONS

Along this thesis, natural units will be used (i.e. $c = \hbar = 1$) except where is indicated; with c as the speed of light in vacuum, while $\hbar$ is the reduced Planck constant. In this units, the reduced Planck mass is given by $M_{\rm Pl} = (8\pi G)^{-1/2}$.

In general, latin indices (e.g. i, j, $k, \ldots$) will correspond to the three-dimensional spatial coordinates and they will take the values 1, 2 or 3 (x, y or z)

On the other hand, greeks indices (e.g. μ, $\nu, \ldots$) will correspond to the four-dimensional spacetime coordinates and they will take the values 0, 1, 2 o 3 (t, x, y o z). The component x^0 will be generally considered as the temporal coordinate of the system.

Additionally, we will use the Einstein summation convention: The appearance of two repeated indices implies the sum in these indices. For example, $p^\mu p_\mu = \sum_\mu p^\mu p_\mu$.

A metric of spacetime will be denoted by $g_{\mu\nu}$ and the spacetime interval will defined as $\mathrm{d}s^2 = g_{\mu\nu}\mathrm{d}x^\mu \mathrm{d}x^\nu$. The metric of Minkowski flat spacetime will be $\eta_{\alpha\beta} \equiv \mathrm{diag}(-1, 1, 1, 1)$.

Some abbreviations used:

GR: General Relativity

EFE: Einstein Field Equations

EC: Einstein-Cartan

Λ**CDM**: Cosmological Constant + Cold Dark Matter

FLRW: Friedmann–Lemaître–Robertson–Walker

GW: Gravitational Wave

PTA: Pulsar Timing Array

Motivation and Outline

Understanding the laws that govern the dynamics of the Universe has always been the primary goal of physics. In that sense, two regimes encompass a vast range of phenomena: The fundamental particles regime, accurately described by different Quantum Field Theories (QFTs), and the cosmological regime, which can be described by the equations of General Relativity (GR). Since full GR cannot be described by a renormalizable QFT [1], the relationship between these two regimes of the Universe is not fully understood, and sadly, no quantum theory of gravity has been derived yet.

Nonetheless, there is a period where these two regimes played an important role, i.e., during the early epoch of the Universe. The classical theory of the Big Bang describes a much hotter and denser Universe 13.3 billion years ago, and in the last decades, we have gathered a lot of observational evidence of this description [2]. However, some theoretical problems remain if we consider that the existence started with an initial singularity at the Big Bang. These problems (Flatness, Horizon, and Monopoles problems are just some of them) were addressed by the pioneering inflationary models proposed by Starobinsky [3], Guth [4], and Linde [5], among many others during the early eighties. In the most straightforward realization of this model, a quantum scalar field produces an epoch of exponential expansion before reaching the period of reheating (which is how now we understand the big-bang). The quantum fluctuations of this field provide the seeds of the large-scale structure of matter within the Universe and produce a mechanism for the generation of primordial gravitational waves, i.e., tensor perturbations in spacetime that propagates through the entire Universe. Therefore, the quantum description of the inflaton field can explain the dynamics of the cosmos at larges scales, combining both regimes beautifully.

Although GR still has great predictive power and provides the framework of many astrophysical events, there are many cosmological puzzles where we cannot provide a natural explanation. For instance, the accelerated expansion of the Universe [6] requires the addition of a strange component into the field equations, the so-called Dark Energy [7]. We also have problems at the galactic scale since the rotational speed of galaxies requires an extra ingredient, i.e., Dark Matter, to be accurately described [8]. These puzzles have been addressed mainly from different perspectives. First, by considering new particles, like Axions [9] and WIMPS [10], or contributions from Primordial Black Holes [11]. Another -and maybe a more intriguing- alternative has been revisiting the equations of GR and considering modified models of gravity. Since we do not have a full quantum theory of gravitation, it is expected that at the quantum scale, some corrections arise, which can account for the solution of the puzzles.

In this thesis, we will study two different models of gravity that differ from standard General Relativity. The first one is called $f(R,T)$ gravity, developed by Harko et al. [12], which in its more general form can be understood as a generalization of the Einstein-Hilbert action of GR by including an arbitrary function depending on the Ricci scalar R and the trace of the energy-momentum tensor T. In this model, many authors have addressed the cosmological puzzles, but here we will discuss the consequences of cosmic inflation. Secondly, we will study the Einstein-Cartan model of gravity, which was developed by Élie Cartan in 1924 [13]. He extended the Riemannian geometry by including a contribution of torsion, which gives an intrinsic characterization of how tangent spaces twist about a curve when they are parallel transported, while curvature describes how the tangent spaces roll along the curve. This generalization has different consequences at the cosmological scale, e.g., it avoids the occurrence of an initial singularity and, by considering spinor-fields, could mimic the dynamics of inflation [14]. However, here we will discuss how a bosonic 0-form coupled to EC gravity can be considered a source of inflation.

Finally, we will change the subject a little bit. We will discuss the tensor perturbations, i.e., gravitational waves not sourced by primordial fluctuations but with an astrophysical origin. The first observation of gravitational waves was done by LIGO in 2015 [15], where the merger of two black holes produced enough gravitational radiation to be measured at Earth. In particular, it is expected that the ground-based detectors can measure GWs with a frequency between $1-10^4$ Hz. However, there are other kinds of sources, like binary systems of Supermassive Black Holes, that could produce gravitational waves with a frequency between $10^6 - 10^{-10}$ Hz. These systems are usually located at intermediate cosmological distances, so it is expected that the accelerated expansion of the Universe could generate some modifications in the observed wave. This is the problem that we will address in the final part of this thesis. By analyzing the linearized regime of GR and using a coordinate transformation, we will relate the comoving frame of the cosmology expansion with a frame at the source. Thus, we will describe how the Universe's expansion changes the timing residual of pulsars, having several consequences for Timing Pulsar Arrays experiments

This thesis is structured as follows: In Chapter 1 we will review the foundations of General Relativity, the linearized regime, gravitational waves, and the description of the cosmological evolution of the Universe, including the formalism of cosmic inflation and primordial fluctuations. In Chapter 2 we will discuss the model of $f(R,T)$ gravity and develop the slow-roll inflation formalism within this theory, applying the results to well-known inflationary models and comparing the predictions with the data from the Planck collaboration. In Chapter 3 we will review the foundations of Einstein-Cartan gravity and discuss how a bosonic 0-form can be the source of a two-field model of inflation. In Chapter 4 we will address the problem of studying gravitational waves propagating through an expanding Universe and discuss the consequences of this expansion to Pulsar Timing Arrays experiments. Finally, in Chapter 5 we will give the main conclusions of this thesis.

Some of the results included in this thesis were published in Refs. [16] and [17], and they were presented in the following conferences:

a) **XII SILAFAE**: Latin American Symposium of High Energy Physics, Nov. 2018, Lima, Perú.
b) **XXI Simposio Chileno de Física**, Nov. 2018, Antofagasta, Chile.
c) **La parte y el Todo VII & VIII**: Tópicos Avanzados en Física de Altas Energías y Gravitación, Jan. 2019 & Jan. 2021, Afunalhue, Chile.
d) **CosmoSur V**, Oct. 2019, Valparaíso, Chile.
e) **XXII Simposio Chileno de Física**, Nov. 2020, Chile.

1. INTRODUCTION

The best theoretical description of the classical gravitational interaction is given by the Theory of General Relativity (GR), developed by Albert Einstein between 1905 and 1915, and where the Newtonian concept of gravitational force was replaced by a much more elegant geometric explanation: The acceleration felt by a free-falling body is, in fact, an inertial consequence of moving along a geodesic on a curved spacetime.

The predictions of General Relativity have been tested for decades: From the precession of the perihelion of Mercury [18], passing by the deflection of light during a solar eclipse [19], to the development of GPS [20] and, more lately, the detection of gravitational waves [21], the measurement of the accelerated expansion of the Universe, and the observation of a Black Hole. Thus, it is commonly accepted that General Relativity is the most robust theory of gravity, at least at the classical scale.

In this chapter, we will briefly discuss the foundations of GR and some applications to the study of the Universe. A detailed development of the theory can be found in the classic textbooks of Weinberg [22] and Carroll [23], which are the primary references of this chapter.

1.1. General Relativity

In order to introduce the gravitational interaction to the Special Theory of Relativity, which only applies to inertial frames, Einstein postulated the *Principle of Equivalence*, i.e., an accelerating reference frame is identical to an equivalent gravitational field in small enough regions of space, and the *Principle of General Covariance*, i.e., equations must be covariant, preserving their form under general coordinate transformations [24].

The Equivalence Principle induces us to describe the *spacetime* as a 4-dimensional differentiable curved Lorentzian manifold, which is a topological space equipped with a metric tensor $g_{\mu\nu}(x^\mu)$, that satisfies the following properties as a second rank tensor,

$$g_{\mu\nu} = g_{\nu\mu}, \qquad g_{\mu'\nu'} = \frac{\partial x^\rho}{\partial x^{\mu'}}\frac{\partial x^\sigma}{\partial x^{\nu'}} g_{\rho\sigma}, \qquad g^{\mu\lambda} g_{\lambda\nu} = \delta^\mu_\nu, \tag{1.1}$$

such that the line element between two events in spacetime is given by,

$$\mathrm{d}s^2 = g_{\mu\nu}\,\mathrm{d}x^\mu\,\mathrm{d}x^\nu = -\,\mathrm{d}\tau^2\,, \tag{1.2}$$

where τ is the proper time.

1.1.1. Geodesics on the spacetime

If we want to find the path between two time-like separated events, we can use the following action principle: *The world line of a free test particle between two time-like separated events extremizes the proper time between them.* Thus,

$$\tau = \int_A^B \sqrt{-\,\mathrm{d}s^2} = \int_{\lambda_1}^{\lambda_2} \sqrt{-g_{\mu\nu}\frac{\mathrm{d}x^\mu}{\mathrm{d}\lambda}\frac{\mathrm{d}x^\nu}{\mathrm{d}\lambda}}\,\mathrm{d}\lambda \tag{1.3}$$

where λ describes an affine parametrization of the 4-coordinates. Therefore, varying τ,

$$\delta\tau = \int_{\lambda_A}^{\lambda_B} \delta\left(\sqrt{-g_{\mu\nu}\frac{\mathrm{d}x^\mu}{\mathrm{d}\lambda}\frac{\mathrm{d}x^\nu}{\mathrm{d}\lambda}}\right)\mathrm{d}\lambda = \int_{\lambda_A}^{\lambda_B} \frac{\delta\left(-g_{\mu\nu}\frac{\mathrm{d}x^\mu}{\mathrm{d}\lambda}\frac{\mathrm{d}x^\nu}{\mathrm{d}\lambda}\right)}{2\sqrt{-g_{\mu\nu}\frac{\mathrm{d}x^\mu}{\mathrm{d}\lambda}\frac{\mathrm{d}x^\nu}{\mathrm{d}\lambda}}}\,\mathrm{d}\lambda = 0, \tag{1.4}$$

where we applied the Hamilton's Principle, i.e., $\delta\tau = 0$. Using that $\delta g_{\mu\nu} = \frac{\partial g_{\mu\nu}}{\partial x^\alpha}\delta x^\alpha$, and

$$\frac{\mathrm{d}\tau}{\mathrm{d}\lambda} = \sqrt{-g_{\mu\nu}\frac{\mathrm{d}x^\mu}{\mathrm{d}\lambda}\frac{\mathrm{d}x^\nu}{\mathrm{d}\lambda}}, \tag{1.5}$$

we can exploit the product rule to obtain

$$\begin{aligned}
\delta\tau = 0 &= \int_{\lambda_A}^{\lambda_B}\left(\frac{\mathrm{d}x^\mu}{\mathrm{d}\lambda}\frac{\mathrm{d}x^\nu}{\mathrm{d}\tau}\partial_\alpha g_{\mu\nu}\delta x^\alpha + 2g_{\mu\nu}\frac{\mathrm{d}(\delta x^\mu)}{\mathrm{d}\lambda}\frac{\mathrm{d}x^\nu}{\mathrm{d}\tau}\right)\mathrm{d}\lambda\\
&= \int_{\lambda_A}^{\lambda_B}\left(\frac{\mathrm{d}x^\mu}{\mathrm{d}\tau}\frac{\mathrm{d}x^\nu}{\mathrm{d}\tau}\partial_\alpha g_{\mu\nu}\delta x^\alpha - 2\delta x^\mu\frac{\mathrm{d}}{\mathrm{d}\tau}\left[g_{\mu\nu}\frac{\mathrm{d}x^\nu}{\mathrm{d}\tau}\right]\right)\mathrm{d}\tau\\
&= \int_{\lambda_A}^{\lambda_B}\left(g_{\mu\nu}\frac{\mathrm{d}^2x^\nu}{\mathrm{d}\tau^2} + \frac{1}{2}\frac{\mathrm{d}x^\alpha}{\mathrm{d}\tau}\frac{\mathrm{d}x^\nu}{\mathrm{d}\tau}(\partial_\alpha g_{\mu\nu} + \partial_\nu g_{\mu\alpha} - \partial_\mu g_{\alpha\nu})\right)\delta x^\mu\,\mathrm{d}\tau\,,
\end{aligned}$$

Therefore, the Euler-Lagrange equation for this action, after multiplying by the inverse of the metric tensor $g^{\mu\beta}$, is known as the **geodesic equation**,

$$\frac{\mathrm{d}^2x^\beta}{\mathrm{d}\tau^2} + \Gamma^\beta{}_{\alpha\nu}\frac{\mathrm{d}x^\alpha}{\mathrm{d}\tau}\frac{\mathrm{d}x^\nu}{\mathrm{d}\tau} = 0, \tag{1.6}$$

where the components of the *Christoffel symbol* are defined as

$$\Gamma^{\beta}_{\ \alpha\nu} = \frac{1}{2} g^{\mu\beta}(\partial_\alpha g_{\mu\nu} + \partial_\nu g_{\mu\alpha} - \partial_\mu g_{\alpha\nu}). \tag{1.7}$$

Notice that the geodesic equation can also be expressed in terms of an affine parameter (which is commonly used in null geodesics),

$$\frac{\mathrm{d}^2 x^\beta}{\mathrm{d}\lambda^2} + \Gamma^{\beta}_{\ \alpha\nu}\frac{\mathrm{d}x^\alpha}{\mathrm{d}\lambda}\frac{\mathrm{d}x^\nu}{\mathrm{d}\lambda} = 0. \tag{1.8}$$

1.1.2. The Field Equations

Furthermore, from the study of curved differential manifolds, we can assign a tensor to each point of the Lorentzian manifold that measures the extent to which the metric tensor is not locally isometric to the Minkowski spacetime. This tensor field is known as the *Riemann curvature tensor*, and its components are given by the following expression

$$R^{\rho}_{\ \sigma\mu\nu} = \partial_\mu \Gamma^{\rho}_{\ \nu\sigma} - \partial_\nu \Gamma^{\rho}_{\ \mu\sigma} + \Gamma^{\rho}_{\ \mu\lambda}\Gamma^{\lambda}_{\ \nu\sigma} - \Gamma^{\rho}_{\ \nu\lambda}\Gamma^{\lambda}_{\ \mu\sigma}. \tag{1.9}$$

Additionally, we can define the components of the *Ricci Tensor* as,

$$R_{\mu\nu} \equiv R^{\alpha}_{\ \mu\alpha\nu} \tag{1.10}$$

Similarly, the *Ricci scalar* is defined as the trace of the Ricci Tensor,

$$R \equiv g^{\mu\nu} R_{\mu\nu} = R^{\mu}_{\ \mu}. \tag{1.11}$$

With the above objects, we can ask ourselves what the equations of motion of the gravitational field are. Again, we can use the action principle to obtain the dynamics of the gravitational interaction for an arbitrary manifold. The simplest action of gravity was found by David Hilbert in 1915 and is currently known as the *Einstein-Hilbert* action, given by

$$S_{\mathrm{EH}}[g] \equiv \int \left[\frac{R - 2\Lambda}{2\kappa} + \mathcal{L}_m\right]\sqrt{-g}\,\mathrm{d}^4 x\,, \tag{1.12}$$

where $g = \det(g_{\mu\nu})$, $\kappa = \frac{8\pi G}{c^4}$ while G is the Newtonian gravitational constant, $\mathcal{L}_m$ is the Lagrangian of the matter fields contained within the spacetime, and Λ is the so-called *cosmological constant*. Therefore, by taking variations with respect to the inverse of the metric, we obtain,

$$\delta S_{\text{EH}} = \int \left[\frac{\sqrt{-g}}{2\kappa} \frac{\delta R}{\delta g^{\mu\nu}} + \frac{R}{2\kappa} \frac{\delta\sqrt{-g}}{\delta g^{\mu\nu}} - \frac{\Lambda}{\kappa} \frac{\delta\sqrt{-g}}{\delta g^{\mu\nu}} + \frac{\delta(\sqrt{-g}\mathcal{L}_m)}{\delta g^{\mu\nu}} \right] \delta g^{\mu\nu} \, \mathrm{d}^4 x \,. \tag{1.13}$$

We have three different terms to compute:

a) The variation of R: The Palatini identity states that the variation of the Ricci tensor is given by,

$$\delta R_{\mu\nu} = \delta R^{\rho}_{\mu\rho\nu} = \nabla_\rho(\delta\Gamma^{\rho}_{\nu\mu}) - \nabla_\nu(\delta\Gamma^{\rho}_{\rho\mu}), \tag{1.14}$$

where ∇_μ represents the covariant derivative acting on a certain tensor[1]. For a (r, s) tensor $\mathbf{T}$, it has the following components

$$\begin{aligned} \nabla_c(T^{a_1,\ldots,a_r}_{b_1,\ldots,b_s}) = \partial_c T^{a_1,\ldots,a_r}_{b_1,\ldots,b_s} + \Gamma^{a_1}_{dc} T^{d\,a_2,\ldots,a_r}_{b_1,\ldots,b_s} + \ldots + \Gamma^{a_r}_{dc} T^{a_1,\ldots,a_{r-1}d}_{\phantom{a_1,\ldots,a_{r-1}d}b_1,\ldots,b_s} \\ - \Gamma^{d}_{b_1 c} T^{a_1,\ldots,a_r}_{d\,b_2,\ldots,b_s} - \ldots - \Gamma^{d}_{b_s c} T^{a_1,\ldots,a_r}_{b_1,\ldots,b_{s-1}d}. \end{aligned} \tag{1.15}$$

Therefore, the variation of the Ricci scalar becomes,

$$\begin{aligned} \delta R = \delta(g^{\mu\nu}R_{\mu\nu}) &= R_{\mu\nu}\delta g^{\mu\nu} + g^{\mu\nu}\delta R_{\mu\nu} \\ &= R_{\mu\nu}\delta g^{\mu\nu} + g^{\mu\nu}\Big[\nabla_\rho(\delta\Gamma^{\rho}_{\nu\mu}) - \nabla_\nu(\delta\Gamma^{\rho}_{\rho\mu})\Big] \\ &= R_{\mu\nu}\delta g^{\mu\nu} + \nabla_\rho(g^{\mu\nu}\delta\Gamma^{\rho}_{\nu\mu} - g^{\mu\rho}\delta\Gamma^{\lambda}_{\lambda\mu}). \end{aligned} \tag{1.16}$$

where in the last equation we used the metric compatibility of General Relativity, i.e., $\nabla_\sigma g^{\mu\nu} = 0$. The last term in the above equation is a total derivative in the action, so it only yields a boundary term when is integrated. If we assume that the variation $\delta g^{\mu\nu}$ vanishes in a neighborhood of the boundary[2], the variation of the Ricci scalar

[1] The Christoffel symbol does not transform like a tensor, but its variation does.
[2] We are, in fact, neglecting the Gibbons-Hawking-York boundary term.

simply becomes,

$$\frac{\delta R}{\delta g^{\mu\nu}} = R_{\mu\nu}. \tag{1.17}$$

b) Variation of $\sqrt{-g}$: According to the Jacobi's formula, the differentiation of a determinant is of the form,

$$\delta g = g g^{\mu\nu} \delta g_{\mu\nu}. \tag{1.18}$$

Hence, we get

$$\delta\sqrt{-g} = -\frac{1}{2\sqrt{-g}}\delta g = \frac{\sqrt{-g}}{2} g^{\mu\nu}\delta g_{\mu\nu} = -\frac{\sqrt{-g}}{2} g_{\mu\nu}\delta g^{\mu\nu} \tag{1.19}$$

where we used in the last equality the differentiating rule of the inverse metric,

$$\delta g^{\mu\nu} = -g^{\mu\alpha}(\delta g_{\alpha\beta})g^{\beta\nu}. \tag{1.20}$$

Therefore, the variation of the determinant becomes,

$$\frac{\delta\sqrt{-g}}{\delta g^{\mu\nu}} = -\frac{\sqrt{-g}}{2} g_{\mu\nu}. \tag{1.21}$$

c) The variation of $\mathcal{L}_m$: We will define the components of the *Energy-Momentum tensor* as

$$T_{\mu\nu} \equiv -\frac{2}{\sqrt{-g}}\frac{\delta(\sqrt{-g}\mathcal{L}_m)}{\delta g^{\mu\nu}} = -2\frac{\delta \mathcal{L}_m}{\delta g^{\mu\nu}} + g_{\mu\nu}\mathcal{L}_m, \tag{1.22}$$

where in the last expression we used the product rule and the result for the variation of the determinant. This tensor comprises all the information related to the matter fields, including the conservation of energy and 4-momentum, i.e., $\nabla^\mu T_{\mu\nu} = 0$.

Putting all the pieces together, the variation of the Einstein-Hilbert action becomes

$$\delta S_{\text{EH}} = \int \left[\frac{R_{\mu\nu}}{2\kappa} - \frac{R}{4\kappa} g_{\mu\nu} + \frac{\Lambda}{2\kappa} g_{\mu\nu} - \frac{T_{\mu\nu}}{2}\right]\delta g^{\mu\nu}\sqrt{-g}\,\mathrm{d}^4x\,. \tag{1.23}$$

After combining the Hamilton's Principle, i.e., $\delta S_{\text{EH}} = 0$, with the fact that the resulting equation will hold for any variation $\delta g^{\mu\nu}$, we obtain the **Einstein Field Equations** (EFE),

$$R_{\mu\nu} - \frac{1}{2} g_{\mu\nu} R + \Lambda g_{\mu\nu} = \kappa T_{\mu\nu}. \tag{1.24}$$

This expression comprise a set of ten nonlinear partial differential equations and describe the gravitational interaction at the classical level. Therefore, General Relativity tell us how spacetime is curved by the presence of matter/energy (field equations) and how matter/energy moves through the curved spacetime (geodesic equation).

1.2. Linearized Gravity and Gravitational Waves

Gravitational waves were predicted for the first time by Einstein himself in 1916 [25]. These ripples in spacetime come from the linearization of the Field Equations around the flat spacetime, and they were measured by the LIGO collaboration in 2015 [15].

1.2.1. Linearization of General Relativity

Let us consider a small fluctuation described by a symmetric tensor $h_{\mu\nu}$, such that the metric tensor reads,

$$g_{\mu\nu} = \eta_{\mu\nu} + h_{\mu\nu}, \qquad |h_{\mu\nu}| \ll 1. \tag{1.25}$$

The strategy reduces to expand the Christoffel symbols, the Riemann and Ricci tensors, and the curvature scalar, as we show in Appendix A. Therefore, the linearized EFE is given by the following expression (for the case $\Lambda = 0$),

$$\Box \bar{h}_{\mu\nu} = -2\kappa T_{\mu\nu}, \tag{1.26}$$

where $\Box \equiv \partial_\mu \partial^\mu$ is the d'Alembert operator in the Minkowski spacetime, and $\bar{h}_{\mu\nu}$ is the trace-reversed perturbation defined by

$$\bar{h}_{\mu\nu} \equiv h_{\mu\nu} - \frac{1}{2}\eta_{\mu\nu} h, \quad h \equiv \eta^{\mu\nu} h_{\mu\nu}, \tag{1.27}$$

which satisfies the Lorenz gauge condition

$$\partial_\beta \bar{h}^{\beta\alpha} = 0. \tag{1.28}$$

As any symmetric tensor has 10 degrees of freedom, and we have eliminated 4 with the Lorenz gauge, there is residual gauge freedom. In a vacuum, and neglecting the cosmological constant, we can completely fix the gauge by imposing the Transverse-Traceless (TT) gauge, where the perturbation satisfies the following conditions,

$$h^{0\mu} = 0, \quad h = 0, \quad \partial^j h_{ij} = 0. \tag{1.29}$$

Hence, $\bar{h}_{\mu\nu} = h_{\mu\nu}$, and since the 0μ components vanish, we can denote the TT gauge as h_{ij}^{TT}, such that in vacuum the gravitational waves satisfies a homogeneous wave equation,

$$\Box h_{ij}^{\mathrm{TT}} = 0. \tag{1.30}$$

In general, any symmetric tensor S_{ij} has a Transverse-Traceless part given by,

$$S_{ij}^{\mathrm{TT}} = \Lambda_{ij,kl} S_{kl}, \tag{1.31}$$

where $\Lambda_{ij,kl} = P_{ik}P_{jl} - (1/2)P_{ij}P_{kl}$, while the projector tensor is defined as $P_{ij} = \delta_{ij} - n_i n_j$. Thus, given any plane wave $h_{\mu\nu}$ in the Lorenz gauge, we can recast the perturbation in the TT gauge by doing $h_{ij}^{\mathrm{TT}} = \Lambda_{ij,kl} h_{kl}$. In general, and by construction, the TT gauge cannot be chosen within the source (for details, see Appendix A) and its use is valid only outside the source.

1.2.2. Plane Wave Expansion in the TT gauge

The result of the linear perturbation of the field equations of gravity is the propagation of **Gravitational Waves** (GWs): The homogeneous wave equation have plane wave solutions given by,

$$h_{ij}^{\mathrm{TT}}(x^\mu) = e_{ij}(\mathbf{k})\,\mathrm{Re}\Big\{e^{ik_\mu x^\mu}\Big\}, \tag{1.32}$$

where $e_{ij}(\mathbf{k})$ is called the polarization tensor, and k_μ are the covariant components of the 4–wavevector, such that k_0 is the angular frequency of a monochromatic gravitational wave. By inserting the plane wave ansatz into the wave equation, we deduce that the 4-wavevector has to be light-like, i.e., $k_\mu k^\mu = 0$, so gravitational waves propagate with the speed of light. Furthermore, if the wavefront has the same direction of the GW propagation, i.e.,

$\hat{\mathbf{n}} = \mathbf{k}/|\mathbf{k}|$, then the TT gauge condition $\partial^j h_{ij}^{\mathrm{TT}} = n^i h_{ij}^{\mathrm{TT}} = 0$ implies that the non-zero components of h_{ij}^{TT} are in a plane transverse to $\hat{\mathbf{n}}$. Therefore, without loss of generality, we can choose $\hat{\mathbf{n}} = \hat{\mathbf{z}}$, so the perturbation becomes

$$h_{ij}^{\mathrm{TT}}(x^\mu) = \begin{pmatrix} h_+ & h_\times & 0 \\ h_\times & -h_+ & 0 \\ 0 & 0 & 0 \end{pmatrix} \cos(k_\mu x^\mu). \tag{1.33}$$

The two possible polarizations, h_+ and $h_\times$, have those names as a consequence of the motion of test particles when a gravitational wave is propagating, e.g., see Fig. 1.1.

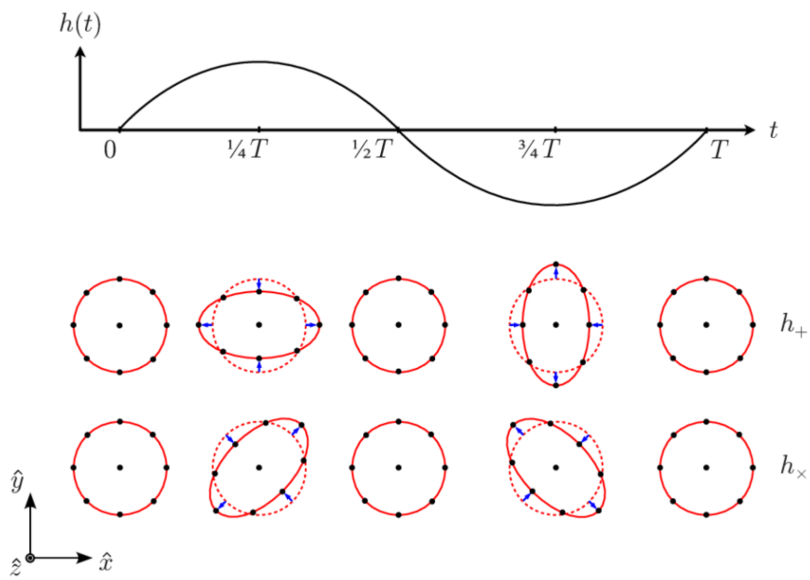

FIGURE 1.1. A monochromatic gravitational wave of frequency $k_0 = 2\pi/T$ propagating along the $\hat{\mathbf{z}}$ direction. The lower panel shows the effects of the $+$ and $\times$ polarizations on a ring of freely falling particles which are in a local inertial frame. Image obtained from Ref. [26].

Furthermore, the metric perturbation can be decomposed in Fourier modes as follows

$$h_{ij}^{\mathrm{TT}}(x^\mu) = \int \frac{\mathrm{d}^3 k}{(2\pi)^3} \Big(\mathcal{A}_{ij}(\mathbf{k}) e^{ik_\mu x^\mu} + \mathcal{A}_{ij}^*(\mathbf{k}) e^{-ik_\mu x^\mu} \Big). \tag{1.34}$$

By considering that $\mathrm{d}^3k = |\mathbf{k}|^2\,\mathrm{d}|\mathbf{k}|\,\mathrm{d}\Omega = (2\pi)^3 f^2\,\mathrm{d}f\,\mathrm{d}\Omega$, $k_0 = 2\pi f$ and $\mathrm{d}^2\hat{\mathbf{n}} = \mathrm{d}(\cos(\theta))\,\mathrm{d}\phi$, we have

$$h_{ij}^{\mathrm{TT}}(t,\mathbf{x}) = \int_0^\infty \mathrm{d}f\,f^2 \int \mathrm{d}^2\hat{\mathbf{n}}\,\Big(\mathcal{A}_{ij}(f,\hat{\mathbf{n}})e^{-2\pi i f(t-\hat{\mathbf{n}}\cdot\mathbf{x})} + \mathcal{A}_{ij}^*(f,\hat{\mathbf{n}})e^{2\pi i f(t-\hat{\mathbf{n}}\cdot\mathbf{x})}\Big). \tag{1.35}$$

If the GW is emitted by a single astrophysical source, the direction of propagation $\hat{\mathbf{n}}_0$ is well-defined and $\mathcal{A}_{ij}(\mathbf{k}) = A_{ij}(f)\delta^{(2)}(\hat{\mathbf{n}} - \hat{\mathbf{n}}_0)$. Furthermore, for the case of ground based interferometers, the scale of the detector is usually much smaller than the wavelength of GWs, i.e., $L \ll \lambda/2\pi$. Thus, $e^{2\pi i f\hat{\mathbf{n}}\cdot\hat{\mathbf{x}}} \sim 1$, and we can neglect the $\mathbf{x}$-dependence, such that

$$h_{ij}^{\mathrm{TT}}(t) = \int_0^\infty \mathrm{d}f\,f^2\Big(A_{ij}(f)e^{-2\pi i f t} + A_{ij}^*(f)e^{2\pi i f t}\Big). \tag{1.36}$$

1.2.3. The graviton

As the Standard Model of particles explains it, the fundamental interactions are carried by gauge bosons, e.g., photons (electromagnetic), gluons (strong), Z and $W^{\pm}$ (electroweak). Thus, we can also expect to have a particle that carries the gravitational interaction. According to several experiments at the solar system scale and beyond, gravity has certain features that can give us a hint about its quantum description:

a) Is a long range interaction $\rightarrow$ The particle has to be **massless**.
b) For static sources there is a static field $\rightarrow$ The particle has an integer spin (a **boson**).
c) Is universally attractive $\rightarrow$ The particle has an **even spin** (0, 2, 4, etc).
d) Light is deflected by a gravitational field $\rightarrow$ The particle's spin **cannot be** 0.
e) There are theoretical problems for particles with spin $\geq 5/2$.
f) The source of gravity is a 2nd-rank tensor $T_{\mu\nu}$ $\rightarrow$ **The particle's spin should be** 2**.**

Therefore, we can expect that the gravitational interaction is carried by a massless bosonic particle of spin 2, which is usually denoted as the *graviton*. The hypothetical quantum of gravity has not been observed yet, and, in fact, after several decades of research, there is still no complete quantum field theory of gravitons, mainly because General Relativity is not a renormalizable theory. Different proposed models intend to give a quantum description of the gravitational interaction, e.g., Loop Quantum Gravity [27], String Theory [28], Causal Dynamical Triangulation [29], and many others, but without success, *yet*.

However, since the Minkowski spacetime is an excellent approximation in many situations, it could be of interest to have a relativistic quantum field theory living in flat spacetime, such that the non-relativistic limit reduces to Newtonian gravity. Pauli and Fierz found that the more general gauge-invariant action of a free symmetric tensor subject to the local gauge symmetry $h_{\mu\nu} \to h_{\mu\nu} - (\partial_\mu \xi_\nu + \partial_\nu \xi_\mu)$ is given by [30],

$$S_{\text{PF}} = \frac{1}{2}\int \mathrm{d}^4x \, (-\partial_\rho h_{\mu\nu}\partial^\rho h^{\mu\nu} + 2\partial_\rho h_{\mu\nu}\partial^\nu h^{\mu\rho} - 2\partial_\nu h^{\mu\nu}\partial_\mu h + \partial^\mu h \partial_\mu h). \tag{1.37}$$

The above expression, after a rescaling, is precisely the linearized version of the E-H action. Therefore, we can conclude that the linearized version of GR describes a free massless particle with spin 2 propagating in the flat spacetime. On the other hand, as the gravitational field should couple to the mass, we can write the gauge-invariant interaction term as

$$S_{\text{int}} = \frac{\bar{\kappa}}{2}\int \mathrm{d}^4x \, h_{\mu\nu}T^{\mu\nu}. \tag{1.38}$$

where $\bar{\kappa}$ is a coupling constant that could be fixed *a posteriori*. In order to find the graviton propagator, we must add a gauge-fixing term. The Lorenz gauge can be incorporated by adding the following term,

$$S_{\text{gf}} = -\int \mathrm{d}^4x \, (\partial^\nu \bar{h}_{\mu\nu})^2 = \int \mathrm{d}^4x \left(-\partial_\rho h_{\mu\nu}\partial^\nu h^{\mu\rho} + \partial_\nu h^{\mu\nu}\partial_\mu h - \frac{1}{4}\partial^\mu h \partial_\mu h\right). \tag{1.39}$$

After putting all the terms together, we get

$$S = S_{\text{PF}} + S_{\text{gf}} + S_{\text{int}} = \int \mathrm{d}^4x \left[-\frac{1}{2}\partial_\rho h_{\mu\nu}\partial^\rho h^{\mu\nu} + \frac{1}{4}\partial^\mu h \partial_\mu h + \frac{\bar{\kappa}}{2}h_{\mu\nu}T^{\mu\nu}\right]. \tag{1.40}$$

Hence, the equations of motion obtained by performing the variation of this action are,

$$\Box \bar{h}_{\mu\nu} = -\frac{\bar{\kappa}}{2}T_{\mu\nu}, \tag{1.41}$$

recovering the linearized field equation under the rescaling $h_{\mu\nu} \to (32\pi G)^{-1/2}h_{\mu\nu}$, so the coupling constant is fixed to be $\bar{\kappa} = (32\pi G)^{1/2}$. Furthermore, the propagator of the graviton can be obtained by integrating by parts the free part of the action,

$$\int \mathrm{d}^4x \left[-\frac{1}{2}\partial_\rho h_{\mu\nu}\partial^\rho h^{\mu\nu} + \frac{1}{4}\partial^\mu h \partial_\mu h\right] = \frac{1}{2}\int \mathrm{d}^4x\, h^{\mu\nu} A_{\mu\nu\rho\sigma}\partial^2 h^{\rho\sigma}, \tag{1.42}$$

where $A_{\mu\nu\rho\sigma} = \frac{1}{2}(\eta_{\mu\rho}\eta_{\nu\sigma} + \eta_{\mu\sigma}\eta_{\nu\rho} - \eta_{\mu\nu}\eta_{\rho\sigma})$. Since the inverse of A is A itself,

$$A_{\mu\nu\alpha\beta}A^{\alpha\beta}{}_{\rho\sigma} = \frac{1}{2}(\eta_{\mu\rho}\eta_{\nu\sigma} + \eta_{\mu\sigma}\eta_{\nu\rho}),$$

then, the propagator of the graviton is given by

$$\tilde{D}_{\mu\nu\rho\sigma}(k) = \frac{1}{2}(\eta_{\mu\rho}\eta_{\nu\sigma} + \eta_{\mu\sigma}\eta_{\nu\rho} - \eta_{\mu\nu}\eta_{\rho\sigma})\left(\frac{-i}{k^2 - i\epsilon}\right), \tag{1.43}$$

where the $i\epsilon$ is the standard prescription of the Feynman propagator. In particular, we have $\tilde{D}_{0000}(k) = -i/(2k^2)$ and $D_{0000} = -i/(8\pi r)$. Hence, in the non-relativistic limit, the static interaction potential $V(\mathbf{x})$ reduces to the Newtonian limit of gravity [31],

$$\begin{aligned} V(\mathbf{x}) &= -\int \frac{\mathrm{d}^3q}{(2\pi)^3} M_{fi}(\mathbf{q}) e^{i\mathbf{q}\cdot\mathbf{x}} = -i\frac{\bar{\kappa}^2}{4}\int \frac{\mathrm{d}^3q}{(2\pi)^3}\tilde{T}_1^{00}(\mathbf{q})\tilde{D}_{0000}(\mathbf{q})\tilde{T}_2^{00}(-\mathbf{q})e^{i\mathbf{q}\cdot\mathbf{x}} \\ &= -i\frac{\bar{\kappa}^2}{4}m_1 m_2 D_{0000}(\mathbf{x}) = -\frac{Gm_1m_2}{r}, \end{aligned} \tag{1.44}$$

where $iM_{fi} = (-ig)^2\tilde{T}_1(\mathbf{q})\tilde{D}(\mathbf{q})\tilde{T}_2(-\mathbf{q})$ is the $2 \to 2$ scattering amplitude, and where we used the energy momentum tensor of relativistic classical particles moving on the trajectory $\mathbf{x}_0(t)$, so $T^{\mu\nu}(\mathbf{x}, t) = \frac{p^\mu p^\nu}{p^0}\delta^{(3)}(\mathbf{x} - \mathbf{x}_0)$, while p^μ is the 4-momentum.

1.3. Cosmology in General Relativity

We have discussed perturbations (GWs) around the flat background of the Minkowski metric. However, to study the evolution and dynamics of the Universe, we must consider a different background spacetime. According to the *Cosmological Principle*, when viewed on a sufficiently large scale, the Universe should be isotropic and homogeneous, i.e., there is no preferred direction or preferred position. Thus, the Friedmann-Lemaître-Robertson-Walker (FLRW) spacetime was developed between 1922 and 1937 [32]–[35], which in spherical coordinates is given by the following expression,

$$ds^2 = g_{\mu\nu}dx^\mu dx^\nu = -dt^2 + a^2(t)\left(\frac{dr^2}{1-Kr^2} + r^2 d\Omega^2\right), \tag{1.45}$$

where $a(t)$ is a dimensionless function of time known as the scale factor, and K is the Gaussian curvature of space. When we work in a flat geometry and, and if we normalize the scale factor such that at the present epoch t_0 reads $a_0 \equiv a(t_0) = 1$, the radial coordinate r and the cosmic time t are comoving coordinates.

In order to solve the Einstein Field Equations, we need an expression for the Energy-Momentum tensor. If we treat the Universe as a giant pool filled with a perfect fluid (which is not viscous and does not transport heat), the Energy-Momentum tensor becomes,

$$T_{\mu\nu} = (\rho + p)U_\mu U_\nu + p g_{\mu\nu}, \tag{1.46}$$

where ρ is the rest energy density (i.e. volumetric mass density), p is the isotropic volumetric pressure and U_μ is the four-velocity of the fluid. Moreover, it is common to use a *equation of state* that relates both quantities,

$$p_i = \chi_i \rho_i, \tag{1.47}$$

Where we used the subscript i as a label, e.g. $i = d$ (non–relativistic matter), $i = r$ (radiation) and $i = \Lambda$ (cosmological constant). Hence, each of these fluids has a density ρ_i, an isotropic pressure p_i and an equation of state $p_i = \chi_i \rho_i$, with χ_i constant.

In Appendix B we derive the well-known **Friedmann Equations** in the case of a single fluid with density ρ_i and pressure p_i, which read

$$H^2 = \left(\frac{\dot{a}}{a}\right)^2 = \frac{8\pi G}{3}(\rho_i + \rho_\Lambda) - \frac{K}{a^2} \tag{1.48a}$$

$$\left(\frac{\ddot{a}}{a}\right) = 8\pi G\left(\frac{\rho_\Lambda}{3} - \frac{\rho_i}{6} - \frac{p_i}{2}\right), \tag{1.48b}$$

where $\rho_\Lambda \equiv \Lambda/8\pi G$, $(\dot{\ })$ means derivative with respect to the cosmic time t, and $H \equiv \dot{a}/a$ is known as the *Hubble parameter*. Having the above in mind, it is commonly accepted that the most successful[3] cosmological model is ΛCDM, which total effective density is,

$$\rho_{\text{eff}} = \rho_\Lambda + \rho_K + \rho_d + \rho_r = \rho_\Lambda + \rho_{K0} a^{-2} + \rho_{d0} a^{-3} + \rho_{r0} a^{-4}, \tag{1.49}$$

where $\rho_\Lambda = \Lambda/\kappa$ is the density of dark energy ($\chi_\Lambda = -1$), $\rho_{K0} = \rho_K(t_0)$ is the density associated to the curvature ($\chi_K = -1/3$), $\rho_{d0} = \rho_d(t_0)$ is the current density of non-relativistic matter (i.e. Cold Dark Matter and baryonic matter: $\chi_d = 0$) and $\rho_{r0} = \rho_r(t_0)$ is the current density of radiation (photons and neutrinos: $\chi_r = 1/3$); all of them are constants measured at the present epoch t_0 and whose latest values were constrained with the Planck Data [2]. If we define the critical density as the value of ρ such that $K = 0$,

$$\rho_{\text{cr}} \equiv \frac{3H^2}{8\pi G}, \tag{1.50}$$

then, we can define the density parameters for each kind of fluid as follows,

$$\Omega_i \equiv \frac{\rho_i}{\rho_{\text{cr}}} = \frac{8\pi G \rho_i}{3H^2}. \tag{1.51}$$

Therefore, from the Friedmann equations, we have a closure relation of the form

$$\Omega_{K0} + \sum_i \Omega_{i0} = 1, \tag{1.52}$$

where Ω_{i0} indicates the present-time value of the i-th density parameter. Likewise, we can write an alternative expression for the Hubble parameter,

$$H^2 = \frac{8\pi G \rho_{\text{eff}}(t)}{3} = H_0^2 \left(\Omega_\Lambda + \frac{\Omega_{K0}}{a^2} + \frac{\Omega_{d0}}{a^3} + \frac{\Omega_{r0}}{a^4} \right), \tag{1.53}$$

where $H_0 = H(t_0)$ is the present-time value of the Hubble parameter and is widely known as the *Hubble Constant*. From the latest observations of the Planck collaboration [37], we

[3] However, in the last years, considerable evidence has been gathered, suggesting tensions between the early and late Universe descriptions. Probably the more important is the 4.2σ tension in the value of the Hubble constant. For an updated review of proposals that intend to solve this tension, see Ref. [36].

have the following constraints:

$$\Omega_{K0} = 0.0007 \pm 0.0019$$
$$\Omega_{\Lambda} = 0.6889 \pm 0.0056$$
$$\Omega_{d0} = 0.3111 \pm 0.0056$$
$$\Omega_{r0} \sim 8.97 \cdot 10^{-5}.$$

Due to their particularly small values, in this work we will neglect the contributions from curvature and radiation.

On the other hand, as a consequence of the Bianchi identities[4], we can ensure the local conservation law of Energy-Momentum, which implies that

$$\nabla^{\mu} T_{\mu\nu} = 0. \tag{1.54}$$

After replacing (1.46) into (1.54), the $\nu = 0$ component is another way to express the *continuity equation*, which has the following form

$$\dot{\rho}_i + 3H(\rho_i + p_i) = 0 \rightarrow \frac{\mathrm{d}\rho_i}{\rho_i} = -3(\chi_i + 1)\frac{\mathrm{d}a}{a},$$

where we used the equation of state (1.47). After the integration, we get

$$\rho_i = \begin{cases} \rho_{i0}\, a^{-3(\chi_i+1)}, & \text{if } \chi_i \neq -1 \\ \rho_{\Lambda} & \text{if } \chi_i = -1 \end{cases}, \tag{1.55}$$

where $\rho_{i0} = \rho_i(t_0)$ is the rest energy density of the i-th fluid measured at the present time t_0. By replacing the last expression into (1.48a), we get the temporal dependence of the scale factor,

$$a(t) = \begin{cases} \left(\dfrac{t}{t_0}\right)^{\frac{2}{3(\chi_i+1)}}, & \text{if } \chi_i \neq -1 \\ e^{\sqrt{\Lambda/3}(t-t_0)}, & \text{if } \chi_i = -1 \end{cases} \tag{1.56}$$

[4]The contracted Bianchi identities are given by: $\nabla_{\mu} R^{\mu}_{\ \nu} = \frac{1}{2}\nabla_{\nu} R$

Combining (1.55) with (1.56) we obtain the general dependence of the density in terms of cosmic time,

$$\rho_i(t) = \begin{cases} \dfrac{4}{3(\chi_i+1)^2\kappa t^2}, & \text{if } \chi_i \neq -1 \\ \rho_\Lambda & \text{if } \chi_i = -1 \end{cases}, \tag{1.57}$$

One important aspect of the FLRW spacetime is to determine how light propagates through the Universe. Let us consider the geodesic equation for light. If we define the 4-momentum of a photon as $P^\mu \equiv \mathrm{d}x^\mu \,/\, \mathrm{d}\lambda$, where λ is an affine parameter, then the geodesic equation can be recast in terms of 4-momentum as follows,

$$\frac{\mathrm{d}P^\mu}{\mathrm{d}\lambda} + \Gamma^\mu{}_{\nu\rho} P^\nu P^\rho = 0. \tag{1.58}$$

Since the Christoffel symbols for the FLRW metric are given by,

$$\Gamma^0{}_{00} = 0, \quad \Gamma^0{}_{0i} = 0, \quad \Gamma^0{}_{ij} = a\dot{a}\,\delta_{ij}, \quad \Gamma^i{}_{0j} = H\delta^i{}_j, \tag{1.59}$$

the computation of the 0-component of the geodesic equation reads,

$$\frac{\mathrm{d}\bar{P}}{\mathrm{d}\lambda} + H\bar{P}^2 = \frac{\mathrm{d}}{\mathrm{d}\lambda}\big(\bar{P}a\big) = 0, \tag{1.60}$$

where $\bar{P}^2 = g_{ij}P^iP^j$ such that $P^\mu P_\mu = -E^2 + \bar{P}^2 = 0$ ($= -m^2$ for massive particles). Therefore the energy of a photon goes as $E \propto a^{-1}$. From this relationship, in combination with the expression of the photon's energy in quantum theory, i.e., $E = hf$, we get,

$$\frac{a_{\text{em}}}{a_{\text{obs}}} = \frac{E_{\text{obs}}}{E_{\text{em}}} = \frac{f_{\text{obs}}}{f_{\text{em}}} = \frac{\lambda_{\text{em}}}{\lambda_{\text{obs}}} \equiv \frac{1}{1+z}. \tag{1.61}$$

This is the well-known relation between the redshift, z, and the scale factor. We can use this parametrization of the scale factor to compute different quantities. For instance, the age of the Universe reads,

$$t_0 = \int_0^{t_0} \mathrm{d}t = \int_0^1 \frac{\mathrm{d}a}{\dot{a}} = \int_0^\infty \frac{\mathrm{d}z}{H(z)(1+z)} \sim 13.8\,\text{Gyr}, \tag{1.62}$$

where

$$H(z) = H_0\sqrt{\Omega_{r0}(1+z)^4 + \Omega_{d0}(1+z)^3 + \Omega_{K0}(1+z)^2 + \Omega_\Lambda}. \tag{1.63}$$

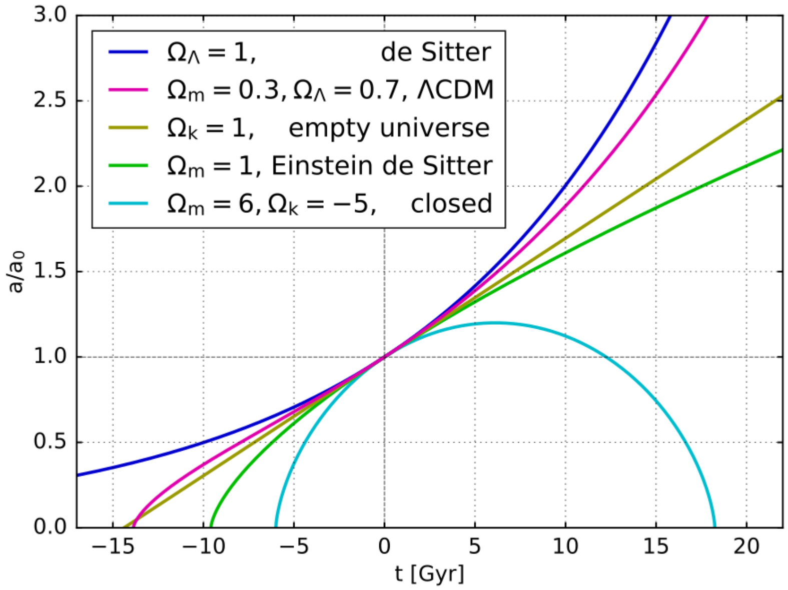

FIGURE 1.2. Temporal evolution of the scale factor $a(t)$ for different models of the Universe. Image elaborated by Geek3 and licensed under CC BY-SA 4.0.

The Hot Big Bang model is usually described by the evolution of the scale factor in different stages, from the radiation dominated epoch to the Dark Energy dominated epoch, as follows,

$$a(t) \propto \begin{cases} t^{1/2} & \text{Radiation-dominated era,} \\ t^{2/3} & \text{Matter-dominated era,} \\ e^{H_0 t} & \text{Dark Energy-dominated era,} \end{cases} \tag{1.64}$$

In Fig. 1.2 we have a pictorial visualization of the scale factor evolution through cosmic time in universes with different material contents.

1.4. Thermal History of the Universe and the Standard Model of Cosmology

The history of the Universe is, in fact, much broader than the radiation, matter, and dark energy-dominated epochs. To start, the Big Bang model predicts a hot and dense early Universe, and the FLRW metric has a singularity at $t = 0$, where the classical model of General Relativity collapses. However, it is widely believed that a consistent and complete theory of quantum gravity may allow an accurate description of that event and the first 10^{-43} seconds (where the four fundamental forces are expected to be unified), but no such theory has yet been developed. After 10^{-36} seconds, we expect that the electroweak and strong forces remain unified, being described by a Grand Unification Theory (GUT). However, at 100 GeV, is expected a symmetry breaking between the electromagnetic and weak interactions, so the Z and $W^{\pm}$ acquire mass. A couple of seconds after this event, as the spacetime expands and the temperature decreases below the electron rest mass, we expect that the electrons and positrons annihilate each other. Then, at 100 KeV, the strong interaction becomes relevant, and the first nucleons form light isotopes of Hydrogen, Helium, and Lithium during Big Bang Nucleosynthesis (BBN).

Event	**Time**	**Redshift**	**Temperature**
Present	13.7 Gyr	0	0.24 meV
Dark Energy/Matter Equality	9 Gyr	0.4	0.33 meV
Reionization	100 Myr	11	2.6 meV
Recombination	260 kyr	1100	0.26 eV
Matter/Radiation Equality	60 kyr	3200	0.75 eV
Big Bang Nucleosynthesis	180 s	10^{8}	100 KeV
Electron-Positron Annihilation	6 s	10^{9}	500 KeV
QCD Phase Transition	10^{-9} s	10^{12}	150 MeV
Electroweak Phase Transition	10^{-10} s	10^{15}	100 GeV
Grand Unification Scale	10^{-36} s	10^{28}	$\sim 10^{16}$ GeV
Quantum Gravity Scale	10^{-43} s	10^{32}	$\sim 10^{19}$ GeV

TABLE 1.1. The thermal history of the Universe, from the quantum gravity scale to present day. Temperature is in natural units, i.e., 1 K $= 8.62 \cdot 10^{-14}$ GeV.

After 380.000 years, protons and electrons combine into neutral hydrogen atoms during an epoch called recombination. Then, as the Universe keeps cooling and expanding, the mean free path of photons becomes much larger than the Hubble length. Once photons decoupled from matter, they traveled freely through the Universe and constitute what is observed today as Cosmic Microwave Background radiation (CMB). Today, we observe these photons coming from all directions with a temperature of $T_0 \sim 2.73$ K, and it was measured for the first time by Wilson and Penzias in 1965 [38]. A summary of the history of the Universe is shown in Table 1.1.

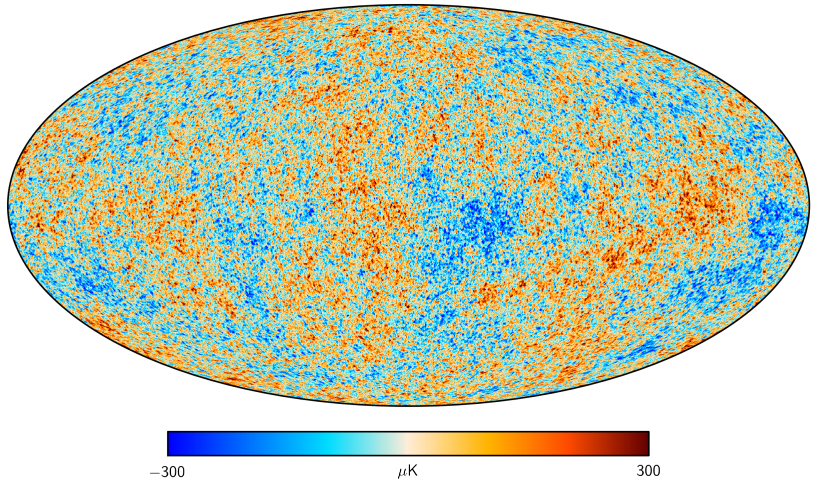

FIGURE 1.3. All-sky map of the CMB temperature fluctuations as obtained by ESA and the Planck Collaboration [37].

The CMB is nearly but not perfectly isotropic. The last data obtained by the Planck Collaboration, published in 2018 [37], shows how the temperature fluctuations are distributed across the sky, e.g., see Fig. 1.3. It is widely used the expansion in terms of spherical harmonics to describe the anisotropy of the CMB,

$$\frac{\Delta T}{T} = \sum_{\ell=1}^{\infty} \sum_{m=-\ell}^{\ell} a_{\ell m} Y_{\ell m}(\theta, \phi). \tag{1.65}$$

To simplify the data visualization is standard to define the rotationally invariant angular spectrum as,

$$C_\ell = \frac{1}{2\ell+1} \sum_m |a_{\ell m}|^2. \tag{1.66}$$

The first contribution, $\ell = 1$, gives the dipole and $(\Delta T/T)_{\ell=1} \sim 10^{-3}$. The COBE mission observed, in the early 90's, that $(\Delta T/T)_{\ell>1} \sim 10^{-5}$. It is commonly accepted that these perturbations grow and are the seeds of the large-scale structures observed in the Universe.

The ΛCDM model, the standard and more accepted theoretical framework of cosmology, is based on a couple of assumptions: (1) That GR is an adequate description of gravity, (2) The cosmological principle, (3) The Big Bang hypothesis of a hotter and denser Universe in the past, (4) Five primary cosmological constituents (DE, DM, baryonic matter, photons, and

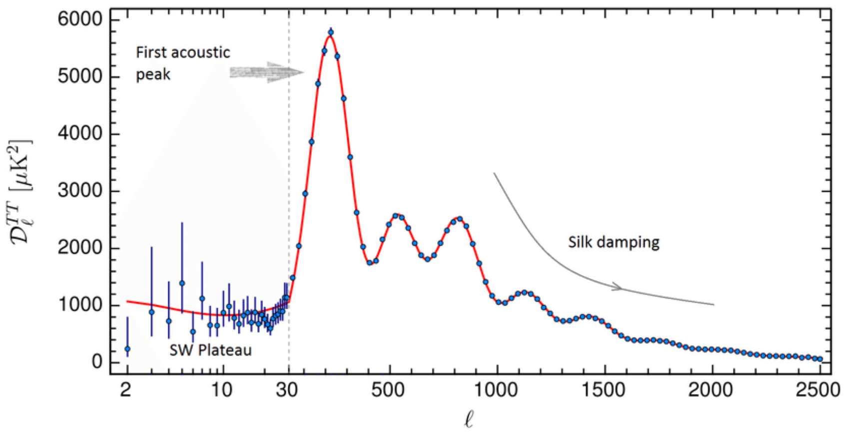

FIGURE 1.4. Best-fit of the CMB temperature power spectrum as obtained by Planck [37]. The vertical axis is given by $\mathcal{D}_\ell^{TT} = \frac{\ell(\ell+1)}{2\pi} C_\ell^{TT}$. In red line, the best fit of the ΛCDM model according to the parameters of Tab. 1.2.

neutrinos), (5) Flat geometry, (6) Perturbations are Gaussian, adiabatic and nearly scale-invariant, (7) The observable Universe has a trivial topology. With these assumptions, it is possible to predict a wide range of observations with just six parameters (see Tab. 1.2). For instance, Fig. 1.4 shows how well is fitted the temperature power spectrum within the framework of the ΛCDM model.

Parameter	**Planck+BAO value**
$\Omega_b h^2$	0.02242 ± 0.00014
$\Omega_c h^2$	0.11933 ± 0.00091
$100\theta_{\mathrm{MC}}$	1.04101 ± 0.00029
τ	0.0561 ± 0.00071
$\ln(10^10 A_s)$	3.047 ± 0.014
n_s	0.9665 ± 0.0038

TABLE 1.2. Parameter limits from Planck: CMB temperature, polarization, lensing power spectra, and the inclusion of BAO data. The parametrization includes the fraction of baryonic matter $\Omega_b h^2$, cold dark matter $\Omega_c h^2$, the angular distance τ, the optical depth at reionization $100\theta_{\mathrm{MC}}$, the spectral index n_s and the amplitude of the initial scalar perturbation A_s.

1.5. Cosmic Inflation

1.5.1. Motivation

Although the Big Bang model can describe much of the Universe's evolution, there are some problems during the primordial epoch that were addressed during the late '70s and early '80s, which required the inclusion of an epoch of a quasi-exponential expansion. Let us review what these problems are and how they can be solved by *cosmic inflation*.

a) **The Flatness Problem**:

Let us consider the definition of the curvature density parameter,

$$\Omega_K = -\frac{K}{H^2 a^2}.$$

According to the latest observations, we can assert with an enormous level of confidence that $|\Omega_{K0}| < 1$. However, from the definition, we have,

$$|\Omega_K| = \left| -\frac{K}{H^2 a^2} \right| = \left| -\frac{K}{H^2 a^2} \frac{H_0^2 a_0^2}{H_0^2 a_0^2} \right| = |\Omega_{K0}| \frac{H_0^2}{H^2 a^2} < \frac{H_0^2}{H^2 a^2}, \tag{1.67}$$

where we used $a_0 = 1$. In the epoch of radiation dominance the right hand side of the above equation goes as a^2, so in the primordial epoch Ω_K gets close to zero. For instance, at the Planck time, e.g., $z \sim 10^{32}$, $\Omega_K < 10^{-60}$. Therefore, we have a fine-tuning problem since, to match the value observed today, the curvature density parameter has to be determined at the Planck scale with a precision of 60 decimals. This problem was addressed by Guth [4], considering that if before the radiation-dominated era the early Universe had a phase where H is approximately constant, we will have $\Omega_K \propto a^{-2}$, and it would be possible to explain the current geometrical flatness. If the curvature was a relevant portion of the content of the Universe at the initial stage of the inflationary epoch, i.e.,

$$\frac{|K|}{a_i^2 H_i^2} \sim \mathcal{O}(1), \tag{1.68}$$

where the subscript i indicates the beginning of the inflationary phase, at the end of inflation, the scale factor $a_{\text{end}} \sim a_i e^N$, where N is called the e-folds number. Then,

$$\frac{|K|}{a_{\text{end}}^2 H_{\text{end}}^2} \sim \frac{|K|}{a_i^2 H_i^2} e^{-2N} \sim e^{-2N}. \tag{1.69}$$

Thus, the current curvature density parameter reads

$$|\Omega_{K0}| = \frac{|K|}{H_0^2} = \frac{|K|}{a_{\text{end}}^2 H_{\text{end}}^2} \left(\frac{a_{\text{end}} H_{\text{end}}}{H_0}\right)^2 \sim e^{-2N} \left(\frac{a_{\text{end}} H_{\text{end}}}{H_0}\right)^2 \tag{1.70}$$

Hence, since today we have $|\Omega_{K0}| < 1$, we require that

$$\frac{a_{\text{end}} H_{\text{end}}}{H_0} < e^N \tag{1.71}$$

If we take that inflation ends just at the beginning of the radiation epoch, the above constraint becomes,

$$e^N > \Omega_{r0}^{1/4} \sqrt{\frac{H_{\text{end}}}{H_0}} = \Omega_{r0}^{1/4} \left(\frac{\rho_{\text{end}}}{\rho_0}\right)^{1/4} \tag{1.72}$$

Since $\rho_0 = 3H_0^2/\kappa \sim 8.69 \cdot 10^{-23}$ kg/m^3, at the Planck scale, where the Planck density is $\rho_{\text{P}} = m_{\text{P}}/\ell_{\text{P}}^3 = \frac{c^5}{\hbar G^2} \sim 5.15 \cdot 10^{96}$ kg/m^3, it will be required $e^N > 3.18 \cdot 10^{28}$, i.e, $N > 66$.

b) **The Horizon Problem**:

After the discovery of the Cosmic Microwave Background, another problem arose. According to the observations, the microwave background is nearly perfect isotropic at large angular scales, which the standard Big Bang model cannot explain. Let us consider the proper particle horizon in a Universe dominated by matter and radiation,

$$d_{\text{H}} \equiv a(t) \int_0^t \frac{\mathrm{d}t'}{a(t')} = \frac{2a}{H_0 \Omega_{m0}} \left(\sqrt{a\Omega_{m0} + \Omega_{r0}} - \sqrt{\Omega_{r0}}\right). \tag{1.73}$$

On the other hand, the angular diameter distance in a matter/radiation-dominated Universe becomes

$$d_{\text{A}} \equiv a(t) \int_t^{t_0} \frac{\mathrm{d}t'}{a(t')} = \frac{2a}{H_0} \left(\sqrt{\Omega_{m0} + \Omega_{r0}} - \sqrt{a\Omega_{m0} + \Omega_{r0}}\right). \tag{1.74}$$

The ratio $d_{\rm H}/d_{\rm A}$ defines the angular radius of the particle horizon at a given a. Therefore, at the end of the epoch of recombination ($z \sim 1100$), where the surface of last scattered photons is formed, we have

$$\left.\frac{d_{\rm H}}{d_{\rm A}}\right|_{a=a_{\rm rec}} = \left.\frac{\sqrt{a\Omega_{m0}+\Omega_{r0}}-\sqrt{\Omega_{r0}}}{\sqrt{\Omega_{m0}+\Omega_{r0}}-\sqrt{a\Omega_{m0}+\Omega_{r0}}}\right|_{a=a_{\rm rec}} \sim 0.018 \;\to\; 1.03^\circ \tag{1.75}$$

Therefore, any two points on the surface of last-scattering that are separated by more than 1° appear never to have been in causal contact, which seems contradictory when we observe the nearly perfect isotropy of the CMB at large angular scales. Surpris-

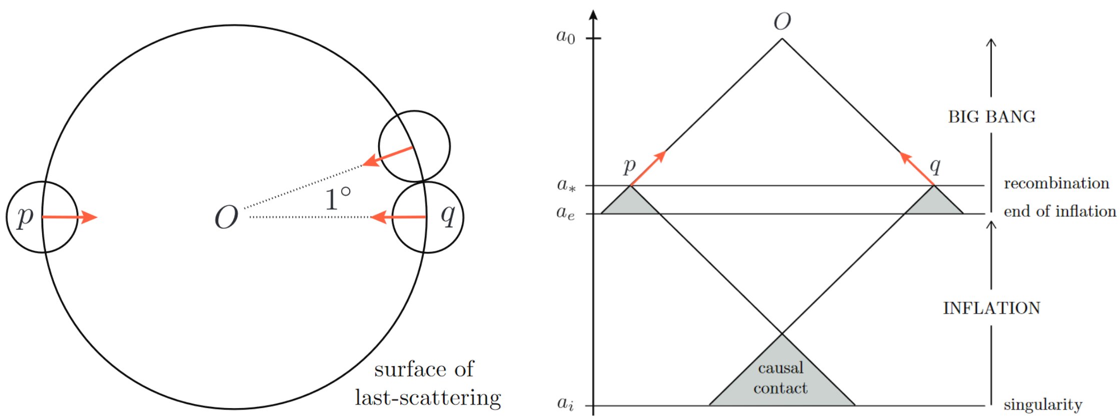

FIGURE 1.5. (a). Let us consider opposite points on the sky labelled p and q. As we shown, only regions separated by $\sim 1^\circ$ are causally connected at the surface of last-scattering, in the absence of inflation. How then could the CMB be isotropic? (b). The solution provided by an inflationary epoch, in comoving coordinates and conformal time. All points in the sky have overlapping past light cones and therefore came from a causally connected region of space. Figures obtained from [39].

ingly, we can address this problem just in the same way as with the flatness problem. If we assume an inflationary phase at a constant rate, i.e., $H = H_i = H_{\rm end}$, such that $a(t) = a_i e^{H_{\rm end}(t-t_i)} = a_{\rm end} e^{-H_{\rm end}(t_{\rm end}-t)}$, then

$$d_{\rm H} \sim a \int_{t_i}^{t_{\rm end}} {\rm d}t\, \frac{e^{H_{\rm end}(t_{\rm end}-t)}}{a_{\rm end}} = \frac{a}{a_{\rm end}H_{\rm end}}(e^N - 1) \sim \frac{a}{a_{\rm end}H_{\rm end}} e^N, \tag{1.76}$$

where $N = H_{\text{end}}(t_{\text{end}} - t_i)$ such that $N \gg 1$. Since $d_{\text{A}} \sim a/H_0$ in the limit $a \to 0$, the angular radius becomes,

$$\frac{d_{\text{H}}}{d_{\text{A}}} \sim \frac{H_0}{a_{\text{end}} H_{\text{end}}} e^N. \tag{1.77}$$

Thus, in order to have $d_{\text{H}} > d_{\text{A}}$, i.e., an isotropic microwave background, we require that

$$\frac{a_{\text{end}} H_{\text{end}}}{H_0} < e^N,$$

which is exactly the same condition as in eq. (1.71). The spacetime diagram of Fig. 1.5 shows how the inflationary model solves the isotropy in the CMB.

c) **The Monopoles Problem**

A magnetic monopole is a hypothetical elementary particle that is an isolated magnet with only one magnetic pole, i.e., a modification in the Maxwell equations such that $\nabla \cdot \mathbf{B} \neq 0$. In grand unified theories local symmetry, under some simple symmetry group, is spontaneously broken at an energy $\sim 10^{16}$ GeV to the gauge symmetry of the Standard Model, under the group $SU(3) \times SU(2) \times U(1)$. Early models predicted an enormous density of monopoles, in clear contradiction to the experimental evidence. However, and in a very similar manner, an exponential rate of expansion at the primordial epoch can explain the non-observance of monopoles at the present time.

1.5.2. Single-Field Inflation

The simplest inflationary scenario can be induced by the inclusion of a spatially homogeneous scalar field called *inflaton*, denoted by $\varphi = \varphi(t)$, which can be introduced by a Lagrangian of the form,

$$\mathcal{L}_m^{(\varphi)} = -\frac{1}{2} g^{\mu\nu} \partial_\mu \varphi \partial_\nu \varphi - V(\varphi) = \frac{1}{2}\dot{\varphi}^2 - V(\varphi), \tag{1.78}$$

where $V(\varphi)$ is some potential. Therefore, the components of the energy-momentum tensor can be computed from (1.22) and read,

$$T^{(\varphi)}_{\mu\nu} = \partial_\mu\varphi\partial_\nu\varphi + g_{\mu\nu}\left(\frac{1}{2}\dot{\varphi}^2 - V(\varphi)\right), \tag{1.79}$$

which can be expressed as a perfect fluid with energy density ρ_φ and pressure p_φ,

$$T^{(\varphi)}_{00} = \frac{\dot{\varphi}^2}{2} + V(\varphi) = \rho_\varphi, \quad T^{(\varphi)}_{ij} = \left(\frac{\dot{\varphi}^2}{2} - V(\varphi)\right)g_{ij} = p_\varphi g_{ij}. \tag{1.80}$$

Moreover, the trace of the energy-momentum tensor is given by,

$$T^{(\varphi)} = g^{\mu\nu}T^{(\varphi)}_{\mu\nu} = \dot{\varphi}^2 - 4V(\varphi). \tag{1.81}$$

Thus, if we introduce equation (1.80) into the 00 component of the EFE, we get

$$H^2 = \frac{8\pi G\rho_\varphi}{3} = \frac{8\pi G}{3}\left(\frac{\dot{\varphi}^2}{2} + V(\varphi)\right), \tag{1.82}$$

commonly known as the first Friedmann equation and where we have defined the Hubble parameter as $H \equiv \dot{a}/a$. On the other hand, the trace of the field equations reads $R = -\kappa T$. Hence, by rearranging the trace equation, we obtain the second Friedmann equation (or acceleration equation),

$$\frac{\ddot{a}}{a} = -\frac{8\pi G}{6}(3p_\varphi + \rho_\varphi) = -\frac{8\pi G}{3}\left(\dot{\varphi}^2 - V(\varphi)\right). \tag{1.83}$$

Furthermore, from the definition of the Hubble parameter, the continuity equation for the energy density and the pressure reads,

$$\dot{\rho}_\varphi + 3H(\rho_\varphi + p_\varphi) = 0, \tag{1.84}$$

which is, as a matter of fact, the $\mu = 0$ component of the conservation of the energy-momentum tensor, i.e., $\nabla_\nu T^{\mu\nu} = 0$. Moreover, by inserting (1.80) into (1.84), we get the Klein–Gordon equation for the inflaton field (which can also be obtained from a variation on the action with respect to φ), given by the expression,

$$\ddot{\varphi} + 3H\dot{\varphi} + V_{,\varphi} = 0, \tag{1.85}$$

where $V_{,\varphi} = \frac{\mathrm{d}V}{\mathrm{d}\varphi}$. As we discussed before, the inflationary scenario at the early stages of the Universe is characterized by a quasi–exponential rate of expansion, i.e., $\frac{\mathrm{d}(H^{-1})}{\mathrm{d}t} \ll 1$, which implies the slow–roll condition,

$$\dot{\varphi}^2 \ll V(\varphi). \tag{1.86}$$

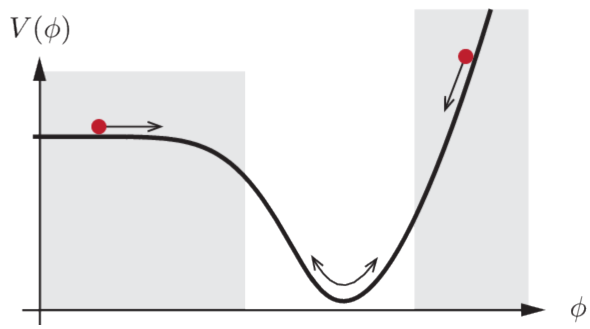

FIGURE 1.6. This is an example of a slow-roll potential. Inflation can occur in the shaded parts of the plot. The non-shaded region corresponds to the reheating epoch. Image obtained from Ref. [39].

Therefore, we can define the first slow–roll parameter, denoted by ϵ, as

$$\epsilon = -\frac{\dot{H}}{H^2} = \frac{3\dot{\varphi}^2}{\dot{\varphi}^2 + 2V(\varphi)}, \tag{1.87}$$

such that the minimum requirement to develop inflation is $|\epsilon| \ll 1$. If we apply the slow-roll approximation (1.86) and use the Friedmann equations, we can define at first order a similar slow-roll parameter, denoted by $\epsilon_{\rm V}$ which depends only in the potential $V(\varphi)$,

$$\epsilon \approx \frac{3\dot{\varphi}^2}{2V(\varphi)} = \frac{1}{16\pi G}\left(\frac{V_{,\varphi}}{V}\right)^2 \equiv \epsilon_{\rm V}, \tag{1.88}$$

If we take the derivative with respect to cosmic time, we can define the second slow-roll parameter, denoted by η, which guarantees the slow variation of ϵ in time,

$$\dot{\epsilon} = 2\frac{\dot{H}^2}{H^3} - \frac{\ddot{H}}{H^2} = 2H\epsilon(\epsilon - \eta), \quad \eta \equiv -\frac{\ddot{\varphi}}{H\dot{\varphi}}. \tag{1.89}$$

Similarly to the case of ϵ_V, we can define an η_V that depends only on the potential. Using (1.85) and the Friedmann equations we have,

$$\eta_V = \eta + \epsilon \approx \frac{1}{8\pi G}\left(\frac{V_{,\varphi\varphi}}{V}\right), \tag{1.90}$$

where $V_{,\varphi\varphi} = \mathrm{d}^2 V/\mathrm{d}\varphi^2$. These slow–roll parameters approximately describe the dynamics of inflation and the observational features of different models. Another important quantity is the number of e–folds, defined as $N = \ln(a)$, which measures the amount of spacetime expansion. The slow–roll approximation yields a N given by,

$$N = \int_{t_1}^{t_2} H\,\mathrm{d}t = \int_{\varphi_{\text{end}}}^{\varphi} \frac{H}{\dot{\varphi}}\,\mathrm{d}\varphi \approx 8\pi G \int_{\varphi_{\text{end}}}^{\varphi} \frac{V(\varphi')}{V_{\varphi}(\varphi')}\,\mathrm{d}\varphi'\,, \tag{1.91}$$

where φ_{end} is the inflaton value at the end of inflation, i.e. when ϵ_V or η_V is close to 1, and the integral upper limit usually refers to the value of φ at the horizon crossing. In summary, knowing the functional form of the potential $V(\varphi)$ would yield predictions susceptible to experimental verification by measuring the primordial power spectrum.

1.6. Primordial Fluctuations

As we discussed in the previous sections, the assumption of a homogeneous and isotropic Universe is reliable only at very large scales. However, the study of structures such as galaxies and clusters shows small deviations from the cosmological principle at a local scale, possibly caused by quantum fluctuations in the primordial epoch. Hence, here we will present some useful results on the theory of cosmological perturbations. For further details, see Refs. [40], [41].

1.6.1. Cosmological Perturbation Theory

Let us consider the FLRW metric, with $K = 0$, as the background spacetime. Using the conformal time, i.e., $\mathrm{d}\eta = \mathrm{d}t\,/a$, we have

$$\bar{g}_{\mu\nu} = a^2(\eta)(-\,\mathrm{d}\eta^2 + \delta_{ij}\,\mathrm{d}x^i\,\mathrm{d}x^j). \tag{1.92}$$

As we are considering deviations from homogeneity and isotropy, the actual physical spacetime is a different manifold, described by a metric $g_{\mu\nu}$ such that,

$$g_{\mu\nu}(x) = \bar{g}_{\mu\nu}(x) + \delta g_{\mu\nu}(x). \tag{1.93}$$

Since $g_{\mu\nu}$ and $\bar{g}_{\mu\nu}$ are tensors defined on different manifolds, the only way to make $\delta g_{\mu\nu}$ meaningful is to introduce a map between those two manifolds, i.e., a gauge, which allows us to use a fixed coordinate system -defined in the background manifold- also for the points in the physical manifold. In general, a symmetric tensor in 4D has 10 independent components that, in a generic gauge, can be written as

$$g_{\mu\nu} = a^2(\eta)\begin{pmatrix} -[1+2\psi] & w_i \\ w_i & \delta_{ij}[1+2\phi] + \chi_{ij} \end{pmatrix}, \tag{1.94}$$

where ψ and ϕ are two scalar fields, w_i is a vector field and χ_{ij} is a symmetric tensor field such that $\delta^{ij}\chi_{ij} = 0$, and all of them are functions of the background spacetime coordinates x^μ. Thus, we define $\delta g_{\mu\nu}$ as a *perturbation* if we choose a gauge such that $|g_{\mu\nu}| \ll |\delta g_{\mu\nu}|$. In particular, we shall write the physical metric as

$$g_{\mu\nu} = a^2(\eta_{\mu\nu} + h_{\mu\nu}), \tag{1.95}$$

so the perturbed Einstein field equations, obtained after an analogous procedure as we did in the above section, read

$$2a^2\delta G^0{}_0 = -6\mathcal{H}^2 h_{00} + 4\mathcal{H}h_{k0,k} - 2\mathcal{H}h'_{kk} + \nabla^2 h_{kk} - h_{kl,kl}, \tag{1.96a}$$

$$2a^2 G^0{}_i = 2\mathcal{H}h_{00,i} + \nabla h_{0i} - h_{k0,ki} + h'_{kk,o} - h'_{ki,k}, \tag{1.96b}$$

$$\begin{aligned} 2a^2\delta G^i{}_j = \Big[&-4\frac{a''}{a}h_{00} - 2\mathcal{H}h'_{00} - \nabla^2 h_{00} + 2\mathcal{H}^2 h_{00} - 2\mathcal{H}h'_{kk} + \nabla^2 h_{kk} \\ &-k_{kl,kl} + 2h'_{k0,k} + 4\mathcal{H}h_{k0,k} - h''_{kk}\Big]\delta^i{}_j + h_{00,ij} - \nabla^2 h_{ij} + h_{ki,kj} \\ &+ h_{kj,ki} - h_{kk,ij} + h''_{ij} + 2\mathcal{H}h'_{ij} - (h'_{0i,j} + h'_{0j,i}) - 2\mathcal{H}(h_{0i,j} + h_{0j,i}), \end{aligned} \tag{1.96c}$$

where $(\cdot)'$ indicates a derivative with respect to the conformal time η and $\mathcal{H} = a'/a$ is the conformal Hubble parameter. On the other hand, the most general energy-momentum tensor can be written as

$$T_{\mu\nu} = \rho U_\mu U_\nu + (P + \pi)\theta_{\mu\nu} + \pi_{\mu\nu}, \tag{1.97}$$

where $\theta_{\mu\nu} = g_{\mu\nu} + U_\mu U_\nu$, $\pi_{\mu\nu}$ is the anisotropic stress such that $\pi_{\mu\nu}U^\mu = 0$, and its trace π is the bulk viscosity. If we write $\delta U_i = aV_i$ for some 3-vector V_i, the perturbations of the energy-momentum tensor reads,

$$\delta T^0_{\ 0} = -\delta\rho \tag{1.98a}$$

$$\delta T^0_{\ i} = (\bar{\rho} + \bar{P})V_i = -\delta T^i_{\ 0} \tag{1.98b}$$

$$\delta T^i_{\ j} = \delta^i_{\ j}\delta P + \pi^i_{\ j}, \tag{1.98c}$$

where a bar indicates background quantities. Hence, the linearized version of the Einstein field equations becomes,

$$\delta G^\mu_{\ \nu} = \kappa \delta T^\mu_{\ \nu}. \tag{1.99}$$

After this process, an unexpected problem remains: We cannot assure, by only looking at a metric, that we have fluctuations about a known background or if the metric is written in a flawed coordinate system, i.e., physical perturbations cannot depend on the gauge. Let us consider a change from a gauge $\mathcal{G}$ to another gauge $\hat{\mathcal{G}}$, induced by the infinitesimal coordinate transformation.

$$x^\mu \to \hat{x}^\mu = x^\mu + \xi^\mu(x), \tag{1.100}$$

where x^μ are the background coordinates and ξ^μ is the gauge generator. Using the transformation property of any 2nd-rank tensor, we have that

$$\hat{g}_{\mu\nu}(x^\mu) = g_{\mu\nu}(x^\mu) - \nabla_\nu \xi_\mu - \nabla_\mu \xi_\nu. \tag{1.101}$$

Therefore, the following transformations for the perturbations hold,

$$\hat{\psi} = \psi - \mathcal{H}\xi^0 - \xi^{0\prime}, \qquad \hat{w}_i = w_i - \Xi_i' + \partial_i \xi^0 \tag{1.102a}$$

$$\hat{\phi} = \phi - \mathcal{H}\xi^0 - \frac{1}{3}\partial_i \xi^i, \quad \hat{\chi}_{ij} = \chi_{ij} - \partial_j \Xi_i - \partial_i \Xi_j + \frac{2}{3}\delta_{ij}\partial_k \xi^k, \tag{1.102b}$$

where $\Xi_i \equiv \delta_{ik}\xi^k$. By applying the gauge transformation to $T_{\mu\nu}$, we get

$$\hat{\delta\rho} = \delta\rho - \bar{\rho}'\xi^0, \qquad \hat{v}_i = v_i + \partial_i\xi^0 \tag{1.103a}$$

$$\hat{\pi} = \pi, \qquad \hat{\delta P} = \delta P - \bar{P}'\xi^0, \qquad \hat{\pi}_{ij} = \pi_{ij}. \tag{1.103b}$$

1.6.2. SVT Decomposition

We have seen that the perturbed metric depends on two scalars (ψ and ϕ), a 3-vector (w_i), and a 3-tensor χ_{ij}. Nonetheless, we can decompose even further the vector and tensor contributions to have a decoupled system where each kind of perturbation (scalar, vector, and tensor) can be analyzed separately. The Helmholtz theorem states that any spatial vector w_i can be decomposed as $w_i = w_i^{\parallel} + w_i^{\perp}$, where $\epsilon^{ijk}\partial_j w_k^{\parallel} = 0$ and $\partial^k w_k^{\perp} = 0$ (ϵ^{ijk} is the Levi-Civita symbol). By applying the Stokes theorem, we have $w_i^{\parallel} = \partial_i w$ for some scalar w. Hence, w_i can be expressed as follows,

$$w_i = \partial_i w + S_i, \tag{1.104}$$

where we defined $S_i \equiv w_i^{\perp}$ to simplify the notation. Here, w is the scalar part of w_i and S_i is the vector part of w_i. Thus, as S_i cannot be decomposed, we will say that is the *vector perturbation*. Similarly, for a 2nd-rank tensor χ_{ij} we can decompose it as $\chi_{ij} = \chi_{ij}^{\parallel} + \chi_{ij}^{\perp} + \chi_{ij}^{T}$, where $\epsilon^{ijk}\partial^m\partial_j\chi_{mk} = 0$, $\partial^i\partial^j\chi_{ij}^{\perp} = 0$ and $\partial^j\chi_{ij}^{T} = 0$. Following an analogously procedure, we can further decompose: $\chi_{ij}^{\parallel} = [\partial_i\partial_j - (1/3)\delta_{ij}\nabla^2](2\mu)$, $\chi_{ij}^{\perp} = \partial_j A_i + \partial_i A_j$, and $\partial^i A_i = 0$, where μ is some scalar and A_i is a divergenceless vector. Then, the tensor perturbation can be decomposed as follows,

$$\chi_{ij} = \Big(\partial_i\partial_j - (1/3)\delta_{ij}\nabla^2\Big)(2\mu) + \partial_j A_i + \partial_i A_j + \chi_{ij}^{T}. \tag{1.105}$$

Since the transverse part χ_{ij}^{T} cannot be further decomposed, we say that it is a *tensor perturbation*. Furthermore, by applying the Helmholtz theorem to ξ^μ, we can define $\alpha \equiv \xi^0$ and write $\Xi_i = \partial_i\beta + s_i$, where α and β are scalars and s_i a divergenceless vector. Thus, we obtain how the scalar perturbations transform:

$$\hat{\psi} = \psi - \mathcal{H}\alpha - \alpha', \qquad \hat{w} = w - \beta' + \alpha \tag{1.106a}$$

$$\hat{\phi} = \phi - \mathcal{H}\alpha - \frac{1}{3}\nabla^2\beta, \qquad \hat{\mu} = \mu - \beta. \tag{1.106b}$$

It is important to notice that we can construct certain combinations of scalar perturbations that are gauge-invariant. For instance, we have the famous *Bardeen's potentials*,

$$\Psi \equiv \psi + \frac{1}{a}[(w - \mu')]' \tag{1.107}$$

$$\Phi \equiv \phi + \mathcal{H}(w - \mu') - \frac{1}{3}\nabla^2\mu. \tag{1.108}$$

Moreover, by applying the same procedure to v_i, i.e, $v_i = \partial_i v + u_i$ with $\partial^i u_i = 0$, and to the matter perturbations, we can also obtain gauge-invariant variables. For instance,

$$\Gamma \equiv \delta P - \frac{\bar{P}'}{\bar{\rho}'}\delta\rho, \tag{1.109}$$

is known as the *entropy perturbation* since $\Gamma = 0$ implies adiabaticity. We also have,

$$\mathcal{R} \equiv \phi + \mathcal{H}v - \frac{1}{3}\nabla^2\mu \tag{1.110}$$

which is known as the *comoving curvature perturbation*, and

$$\zeta \equiv \phi + \frac{\delta\rho}{3(\bar{\rho} + \bar{P})} - \frac{1}{3}\nabla^2\mu. \tag{1.111}$$

These two quantities, $\mathcal{R}$ and ζ, are quite important in the context of inflation because they are conserved on large scales for adiabatic perturbations. In order to complete the analysis, we can also combine vector contributions to form new variables. In particular, we have the gauge-invariant vector potential $W_i = S_i - A_i'$ and the vector part of v_i, i.e., u_i, such that both are gauge-invariant. Finally, we have that χ_{ij}^T is also gauge-invariant since the gauge transformation on the metric cannot be accomplished by a tensor field.

In summary, we have that a generic perturbation can be split as: 4 scalar functions (ψ, ϕ, w and μ), 2 divergenceless 3-vectors (S_i and A_i, two independent components each), and a transverse-traceless spatial tensor (χ^T_{ij}, two independent components). Hence, we have $4+2+2+2=10$ independent components.

Since we introduced the transformation ξ^μ, we have the gauge freedom to set any 4 components of the metric to zero and fix the gauge. The most common choice is the Newtonian gauge, where we set $\hat{w}=\hat{\mu}=\hat{\chi}^\perp_{ij}=0$. With this election, we have that $\hat{\psi}=\Psi$ and $\hat{\phi}=\Phi$, i.e., the metric perturbations become identical to the Bardeen potentials.

1.6.3. Quantum Fluctuations and Spectral Indices

Once quantum fluctuations are considered in the context of inflation, something remarkable happens: It provides an elegant and clear mechanism for the generation of all the structures in the Universe. We can understand this mechanism using the interpretation developed by Guth and Pi, who considered that the inflaton field plays the role of a local clock describing the evolution of inflation. Since ϕ has a quantum nature, it will fluctuate: $\delta\phi(t,\mathbf{x}) = \phi(t,\mathbf{x})-\bar{\phi}(t)$. These quantum fluctuations imply that the instant when inflation ends will be different for different regions of space. As a consequence, local fluctuations in $\delta\rho(t,\mathbf{x})$ will be unavoidable, and these small perturbations will produce the structure of the Universe as it is seen today, e.g., the anisotropy in the CMB. However, not only scalar perturbations are expected to be generated by inflation but also tensor fluctuations. This fact implies that the model of cosmic inflation has a mechanism of generating *Primordial Gravitational Waves*. Thus, in the next paragraphs, we will discuss how tensor and scalar perturbations can be generated by cosmic inflation.

Primordial Tensor Fluctuations

The components of the perturbed FLRW metric, with only tensor perturbations, can be cast as,

$$g_{00}=-a^2, \qquad g_{0i}=0, \qquad g_{ij}=a^2(\delta_{ij}+h^T_{ij}), \tag{1.112}$$

where $h^T_{ij}=\chi^T_{ij}$ is the gauge-invariant divergenceless-traceless tensor. According to Eqs. (1.96a), (1.96b) and (1.96c), the only non-vanishing components of the linearized field equations are $\delta G^i{}_j = 0$, and therefore the tensor perturbations satisfy

$$h_{ij}^{T\prime\prime} + 2\mathcal{H}h_{ij}^{T\prime} - \nabla^2 h_{ij}^T = 0 \tag{1.113}$$

since scalar fields have a vanishing anisotropic stress contribution. The Fourier transform of the above expression becomes,

$$h'' + 2\mathcal{H}h' + k^2 h = 0, \tag{1.114}$$

where $h = h_{+,\times}$ represents both polarizations since they satisfy the same differential equation. It will be useful to introduce the following rescaling,

$$g \equiv \frac{ah}{\sqrt{32\pi G}} = \frac{M_{\rm Pl}}{2}ah, \tag{1.115}$$

where $M_{\rm Pl} = (8\pi G)^{-1/2}$ is the reduced Planck mass and the normalization is the same one used in Eq. (1.41). In this new variable, Eq. (1.113) reads,

$$g'' + \left(k^2 - \frac{a''}{a}\right)g = 0, \tag{1.116}$$

i.e, a harmonic oscillator without a dumping term. We can expand the GW as follows,

$$h_{ij}^T(\tau, \mathbf{x}) = \sum_{\lambda=\pm 2}\int \frac{\mathrm{d}^3\mathbf{k}}{(2\pi)^3}\Big[h(\tau,k)e^{i\mathbf{k}\cdot\mathbf{x}}a(\mathbf{k},\lambda)e_{ij}(\hat{k},\lambda) + h^*(\tau,k)e^{-i\mathbf{k}\cdot\mathbf{x}}a^*(\mathbf{k},\lambda)e_{ij}^*(\hat{k},\lambda)\Big], \tag{1.117}$$

where we will use τ as the conformal time (to avoid confusion with the 2nd slow roll parameter η), and the sum is over the helicity of the GW and $e_{ij}(\hat{k},\lambda)$ is the polarization tensor. Hence, we can assume that the initial state of the tensor fluctuation has a quantum nature on very small scales, i.e., $k \gg aH$. Thus, we promote $h_{ij}^T(\tau,\mathbf{x})$ and $a(\mathbf{k},\lambda)$ (do not confuse with the scale factor a) to quantum operators and impose the canonical commutation relations,

$$[a(\mathbf{k},\lambda), a(\mathbf{k}',\lambda')] = 0, \quad [a(\mathbf{k},\lambda), a^\dagger(\mathbf{k},\lambda')] = (2\pi)^3\delta^{(3)}(\mathbf{k}-\mathbf{k}')\delta_{\lambda\lambda'}. \tag{1.118}$$

The last expression can be understood as follows: $a^\dagger(\mathbf{k}, \lambda)$ creates a graviton of 4-momentum $\mathbf{k}$ and helicity λ, while $a(\mathbf{k}, \lambda)$ will destroy it. Since the quantum state of the Universe during inflation is the vacuum, $|0\rangle$, the expectation value of the vacuum is

$$\langle 0| \, h^T_{ij}(\tau, \mathbf{x}) h^T_{lm}(\tau, \mathbf{x}') \, |0\rangle = \int \frac{\mathrm{d}^3\mathbf{k}}{(2\pi)^3} |h(\tau, k)|^2 e^{i\mathbf{k}\cdot(\mathbf{x}-\mathbf{x}')} \Pi_{ij,lm}(\hat{k}), \tag{1.119}$$

where

$$\Pi_{ij,lm}(\hat{k}) \equiv \sum_{\lambda=\pm 2} e_{ij}(\hat{k}, \lambda) e^*_{lm}(\hat{k}, \lambda). \tag{1.120}$$

Let us recall, from the study of stochastic fluctuations, that if $G(\mathbf{x})$ is a random field such that its values are random variables for any $\mathbf{x}$, we define the 2-point correlation function as

$$\xi(\mathbf{x}_1, \mathbf{x}_2) = \langle G(\mathbf{x}_1) G(\mathbf{x}_2) \rangle \,, \tag{1.121}$$

where $\langle \cdot \rangle$ indicates the ensemble average. If $G(\mathbf{x})$ is a Gaussian random field, i.e., it has a statistical homogeneous and isotropic 2-point correlation function, then

$$\left\langle \tilde{G}(\mathbf{k}) \tilde{G}^*(\mathbf{k}') \right\rangle = (2\pi)^3 \delta^{(3)}(\mathbf{k} - \mathbf{k}') P_G(\mathbf{k}). \tag{1.122}$$

In the above expression $\tilde{G}(\mathbf{k})$ is the Fourier transform of the random field $G(\mathbf{x})$ and $P_G(\mathbf{k})$ is called the *Power Spectrum*, such that

$$\xi_G(r) = \int \frac{\mathrm{d}^3\mathbf{k}}{(2\pi)^3} P_G(k) e^{-i\mathbf{k}\cdot\mathbf{r}}, \tag{1.123}$$

since a homogeneous and isotropic random field satisfies $\xi(\mathbf{x}_1, \mathbf{x}_2) = \xi(\mathbf{x}_1 - \mathbf{x}_2) = \xi(|\mathbf{x}_1 - \mathbf{x}_2|) = \xi(r)$. We can also define the dimensionless power spectrum as,

$$\Delta^2_G(k) \equiv \frac{k^3 P_G(k)}{2\pi^2}. \tag{1.124}$$

Then, by a simple comparison, we can observe that the tensor quantum perturbations are Gaussian, with a power spectrum $P_h(\tau, k) \propto |h(\tau, k)|^2$. Thus, by solving the evolution equation for $h(\tau, k)$ we can get information about the power spectrum of the primordial tensor perturbations.

First, let us consider the slow roll parameter defined in Eq. (1.87). We can write it in terms of conformal time as follows,

$$\epsilon = -\frac{\dot{H}}{H^2} = \left(\frac{a}{\mathcal{H}}\right)' \frac{1}{a} = 1 - \frac{\mathcal{H}'}{\mathcal{H}^2} \tag{1.125}$$

Hence, by solving the differential equation for $\mathcal{H}$, we find that

$$\mathcal{H} = -\frac{1}{(1-\epsilon)\tau} \tag{1.126}$$

and, replacing the solution, that

$$\frac{a''}{a} = \mathcal{H}' + \mathcal{H}^2 = \frac{1}{(1-\epsilon)\tau^2} + \frac{1}{(1-\epsilon)^2\tau^2} \approx \frac{2+3\epsilon}{\tau^2}, \tag{1.127}$$

where we used the slow roll condition $\epsilon \ll 1$ as it should be during inflation. Therefore, the Eq. (1.116) becomes,

$$g'' + \left(k^2 - \frac{2+3\epsilon}{\tau^2}\right) g = 0. \tag{1.128}$$

This equation has a general solution given by a combination of Hankel functions,

$$g(\tau, k) = C_1(k)\sqrt{-\tau} H_\nu^{(1)}(-k\tau) + C_2(k)\sqrt{-\tau} H_\nu^{(2)}(-k\tau), \quad \nu = \frac{\sqrt{3}}{2}\sqrt{3+4\epsilon}, \tag{1.129}$$

where we introduced the minus since $\tau < 0$ during the inflationary epoch. But, according to [42], the asymptotic expansion on small scales of the Hankel function is given by,

$$H_\nu^{(1)}(-k\tau) \approx \sqrt{\frac{2}{-\pi k\tau}} e^{-ik\tau - i\nu(\pi/2) - i(\pi/4)}, \quad k|\tau| \gg 1. \tag{1.130}$$

Thus, if we want an initial condition of the form $g \sim (2k)^{-1/2} e^{-ik\tau}$, as the QFT procedure of quantization on Minkowski spacetime shows, we have to chose the integration constant to be $C_1(k) = (\sqrt{\pi}/2)e^{i\nu(\pi/2)+i(\pi/4)}$. Therefore, the solution that we are looking for, is

$$g(\tau, k) = \frac{\sqrt{\pi}}{2} e^{i\nu(\pi/2)+i(\pi/4)} \sqrt{-\tau} H_\nu^{(1)}(-k\tau), \quad \nu = \frac{\sqrt{3}}{2}\sqrt{3+4\epsilon}. \tag{1.131}$$

On the other hand, in the limit $k\tau \to 0$, i.e., on very large scales, the expansion becomes,

$$H_\nu^{(1)}(-k\eta) \approx -i\frac{\Gamma(\nu)}{\pi}\left(\frac{k|\tau|}{2}\right)^{-\nu}, \quad k|\tau| \to 0, \tag{1.132}$$

where $\Gamma(z)$ is the Euler gamma function. Therefore, the dimensionless power spectrum on large scales, according to Eq. (1.124), becomes

$$\Delta_h^2(\tau,k) = \frac{k^3}{2\pi^3}\frac{|\tau|\Gamma(\nu)^2}{M_{\rm Pl}^2 a^2}\left(\frac{k|\tau|}{2}\right)^{-2\nu} \approx \frac{1}{\pi^2 M_{\rm Pl}^2 a^2 |\tau|^2}(k|\tau|)^{n_T}, \quad k|\tau| \to 0, \tag{1.133}$$

where in the last expression we used the slow-roll condition and $n_T \equiv -2\epsilon$ is the *tensor spectral index*. It is important to emphasize that now the power spectrum is not exactly scale-invariant, and indeed, it has a small k-dependence with a tilt given by n_T. Conversely, on large scales, h is time-independent, so we can choose an arbitrary scale, e.g. $k = \mathcal{H}(\tau_*)$, where τ_* is the conformal time at the horizon crossing. Thus, as $k|\tau_*| \approx 1+\epsilon$, the dimensionless power spectrum can be cast as,

$$\Delta_h^2(k) = \left.\frac{H^2}{\pi^2 M_{\rm Pl}^2}\right|_{k=aH}. \tag{1.134}$$

From the above expression, it can be noticed that, if in the future, the gravitational wave background is measured, it would be possible to estimate the energy scale of inflation, i.e., $H^2 \sim V$.

Primordial Scalar Fluctuations

Now, let us consider the scalar perturbations on the FLRW spacetime. In principle, we can choose the conformal Newtonian gauge, where the metric can be cast as,

$$\mathrm{d}s^2 = a(\tau)^2\Big[-(1+2\Psi)\,\mathrm{d}\tau^2 + (1+2\Phi)\delta_{ij}\,\mathrm{d}x^i\,\mathrm{d}x^j\Big], \tag{1.135}$$

and consider perturbations on the inflaton field, i.e., $\varphi = \bar{\varphi}(\tau) = \delta\varphi(\tau,\mathbf{x})$. With this prescription, we can show that the perturbed Klein-Gordon equation becomes,

$$\delta\varphi'' + 2\mathcal{H}\delta\varphi' + (k^2 + V_{,\varphi\varphi}a^2)\delta\varphi = 2\Phi V_{,\varphi}a^2 - 4\Phi'\bar{\varphi}', \tag{1.136}$$

where we used that in the conformal Newtonian gauge $\Psi = -\Phi$. The contributions of the right hand side of the above expression makes solving the differential equation enormously difficult and there is no reason to neglect these terms. In fact, there are some reasons to not consider the evolution of $\delta\varphi$, e.g., inflaton should decay into ordinary matter during the post-inflationary epoch of reheating and the initial conditions are actually related to the comoving curvature perturbation $\mathcal{R}$. In fact, for adiabatic perturbations, i.e., fluctuations such that the local state of matter at some point of spacetime of $g_{\mu\nu}(\tau, \mathbf{x})$ are the same as in $\bar{g}_{\mu\nu}(\tau + \delta\tau, \mathbf{x})$, we have that all matter perturbations can be characterized by a single degree of freedom that we can choose it to be $\mathcal{R}$. In the conformal Newtonian gauge we have $\mathcal{R} = \Phi - (\mathcal{H}/\bar{\varphi}')\delta\varphi$. However, we can find a simpler way to write this object, by considering a gauge in which the perturbed scalar field vanishes,

$$\mathrm{d}s^2 = -a^2(1+E)\,\mathrm{d}\tau^2 + 2a^2 F_{,i}\,\mathrm{d}\tau\,\mathrm{d}x^i + a^2(1+A)\delta_{ij}\,\mathrm{d}x^i\,\mathrm{d}x^j\,, \quad \delta\hat{\varphi} = 0. \tag{1.137}$$

In this gauge, the curvature perturbation becomes $\mathcal{R} = A/2$, so we need to determine A from the perturbed Einstein field equations. The $0i$-component, i.e, $\delta G^i{}_0 = \kappa\delta T^0_i = 0$ becomes,

$$-\mathcal{H}E + A' = 0. \tag{1.138}$$

On the other hand, the ij component of the field equations gives,

$$-\frac{\mathcal{H}}{2}E' - (2\mathcal{H}^2 + \mathcal{H}')E - \frac{1}{2}\nabla^2 A + \frac{1}{2}A'' + \frac{5}{2}\mathcal{H}A' - \mathcal{H}\nabla^2 F = 0. \tag{1.139}$$

Furthermore, from the 0 component of the local conservation of the energy-momentum tensor, i.e., $\nabla_\nu T^\nu_0 = 0$, we have

$$\frac{a^2}{2}\left[\frac{E}{a^2}(\mathcal{H}^2 - \mathcal{H}')\right]' + (\mathcal{H}^2 - \mathcal{H}')\left(\nabla^2 F + 3\mathcal{H}E - \frac{3}{2}A'\right) = 0. \tag{1.140}$$

Hence, by combining (1.138), (1.139) and (1.140), we can eliminate E and F in order to find an equation for $\mathcal{R}$, which can be cast as follows,

$$\mathcal{R}'' + 2\frac{z'}{z}\mathcal{R}' + k^2\mathcal{R} = 0, \tag{1.141}$$

where we have defined $z \equiv (a\bar{\varphi}')/\mathcal{H}$. The above expression is commonly known as the *Mukhanov-Sasaki equation*. It is important to observe that z satisfies the following exact relationship,

$$z^2 = a^2\left(\frac{\bar{\varphi}'}{\mathcal{H}}\right)^2 = a^2\frac{3\bar{\varphi}'^2}{8\pi G(\bar{\varphi}'^2/2 + Va^2)} = a^2\frac{\epsilon}{4\pi G}. \tag{1.142}$$

Thus, the dumping term becomes $z'/z = \mathcal{H}(1+\epsilon-\eta)$, where η is the second slow-roll parameter, and for constant values of ϵ and η, the Mukhanov-Sasaki equation reads,

$$(z^2\mathcal{R})'' + \left(k^2 - \frac{2+6\epsilon-3\eta}{\tau}\right)(z^2\mathcal{R}) = 0. \tag{1.143}$$

Amazingly, the above expression is basically the same functional dependency that we had for tensor perturbations, i.e, Eq. (1.128). Therefore, the general solution of the differential equation is given by,

$$z^2(\tau)\mathcal{R}(\tau,k) = C_1(k)\sqrt{-\tau}H_\nu^{(1)}(-k\tau) + C_2(k)\sqrt{-\tau}H_\nu^{(2)}(-k\tau), \tag{1.144}$$

where the Hankel functions are of order $\nu = \frac{\sqrt{3}}{2}\sqrt{3+8\epsilon-4\eta}$. Thus, by following the same steps as we did in the case of tensor perturbations, we can show that the dimensionless power spectrum associated to the curvature perturbations is given by,

$$\Delta^2_{\mathcal{R}}(\tau,k) = \frac{1}{8\pi^2 M_{\rm Pl}^2\epsilon}\frac{1}{a^2\tau^2}(k|\tau|)^{n_{\rm S}}, \tag{1.145}$$

where $n_{\rm S} \equiv -4\epsilon + 2\eta$ is the scalar spectral index.

In summary, the dimensionless scalar and tensor power spectra can be written as,

$$\Delta^2_S \equiv \Delta^2_{\mathcal{R}} = \frac{k^3 P_{\mathcal{R}}(k)}{2\pi^2} = \left.\frac{H^2}{8\pi^2 M_{\rm Pl}^2\epsilon}\right|_{k=aH} \equiv A_S\left(\frac{k}{k_*}\right)^{n_{\rm S}(k)-1}, \tag{1.146}$$

$$\Delta^2_T \equiv 2\Delta^2_h = \frac{k^3 P_{\langle}(k)}{\pi^2} = \left.\frac{2H^2}{\pi^2 M_{\rm Pl}^2\epsilon}\right|_{k=aH} \equiv A_T\left(\frac{k}{k_*}\right)^{n_{\rm T}(k)-1}, \tag{1.147}$$

where now we explicit the k-dependence on the scalar and tensor spectral indices, we have introduced the pivot scale k_* which is usually take to be 0.002 Mpc^{-1} or 0.05 Mpc^{-1}, and the factor 2 in the tensor power spectrum comes from the two polarizations of Primordial Gravitational Waves. The spectral amplitudes, A_S and A_T, in principle are constrained by measurements of the CMB (scalar fluctuations) and, in the future, by the observation of the primordial Gravitational Wave Background (tensor fluctuations). As the spectral indices are not necessarily constant, in principle we can consider a running on the spectral indices,

$$\ln\left(\frac{\Delta_S^2}{A_S}\right) = \left[n_S - 1 + \frac{1}{2}\frac{\mathrm{d}n_S}{\mathrm{d}\ln k}\ln\left(\frac{k}{k_*}\right) + \dots\right]\ln\left(\frac{k}{k_*}\right) \tag{1.148}$$

$$\ln\left(\frac{\Delta_T^2}{A_T}\right) = \left[n_T + \frac{1}{2}\frac{\mathrm{d}n_T}{\mathrm{d}\ln k}\ln\left(\frac{k}{k_*}\right) + \dots\right]\ln\left(\frac{k}{k_*}\right). \tag{1.149}$$

At first order, when both spectral indices are constant, we have the following expressions,

$$n_\mathrm{S} - 1 = \frac{\mathrm{d}\ln(\Delta_S^2)}{\mathrm{d}\ln k} = \frac{\mathrm{d}\ln(H^2/\epsilon)}{\mathrm{d}\ln k} = -4\epsilon + 2\eta \approx -6\epsilon_V + 2\eta_V \tag{1.150a}$$

$$n_\mathrm{T} = \frac{\mathrm{d}\ln(\Delta_T^2)}{\mathrm{d}\ln k} = 2\,\frac{k}{H}\frac{\mathrm{d}H}{\mathrm{d}k}\bigg|_{aH=k} \approx -2\epsilon. \tag{1.150b}$$

It will also be useful to define the tensor-to-scalar ratio, which is given by,

$$r_* \equiv \frac{\Delta_T^2(k_*)}{\Delta_S^2(k_*)} = \frac{A_T}{A_S} = 16\epsilon = -8n_\mathrm{T}. \tag{1.151}$$

According to the last measurements of the Planck Collaboration [37],

$$n_\mathrm{S} = 0.9649 \pm 0.0042 \qquad \text{(at 68\% CL)}, \tag{1.152a}$$

$$r_{0.002} < 0.101 \qquad \text{(at 95\% CL)}, \tag{1.152b}$$

$$\ln\left(10^{10}A_s\right) = 3.044 \pm 0.014 \qquad \text{(at 68\% CL)}. \tag{1.152c}$$

2. Inflation in $f(R,T)$ Gravity

Although GR is the most important and accurate model of gravity that we currently have [43], it is not the more general theory of gravity that can be built. This serves as a motivation to study modified models to address the problems that cannot be included in the framework of GR. Among these theories, we will consider the approach of $f(R,T)$ gravity[1], a model proposed by Harko et al. [12], inspired in the interacting term of Eq. (1.38), and which considers an action described by a function of R (the scalar curvature) and T (the trace of the energy-momentum tensor). Different topics of contemporary cosmology have been widely studied within the framework of the $f(R,T)$ theory, for example: Cosmological models and Solar System consequences [46], [47], Scalar perturbations [48], Thermodynamics [49], The dark energy [50] or dark matter problems [51], a general description of the FLRW cosmology [52], the propagation of Gravitational Waves [53], [54] or the Hamiltonian formalism in Quantum Cosmology [55]. In that sense, a recent work addressed cosmic inflation triggered by a perfect fluid and by a specific quadratic potential [56]. This section aims to develop an exhaustive analysis of the slow-roll approximation in a single-field model of inflation within the framework of $f(R,T)$ gravity. With such a result, we will be able to determine the modification to the cosmological parameters and identify the physically meaningful corrections due to the action of the $f(R,T)$ theory.

The results of this chapter were published in Ref. [17].

2.1. $f(R,T)$ gravity

The modified model of gravity introduced by Harko et al. [12], known as $f(R,T)$ gravity, is described by the following action,

$$S=\int\left(\frac{f(R,T)}{2\kappa}+\mathcal{L}_m\right)\sqrt{-g}\,\mathrm{d}^4x\,, \tag{2.1}$$

[1]Do not confuse with $f(\mathbb{T})$ modified teleparallel gravity [44], [45].

where $f(R,T)$ is an arbitrary function of the scalar curvature, R, and the trace of the energy-momentum tensor, T, and where $\mathcal{L}_m$ is the matter lagrangian, such that $T_{\mu\nu}$ is defined as in the equation (1.22). By varying the action (2.1) with respect to the metric, we obtain the $f(R,T)$ gravity field equations,

$$\frac{\partial f}{\partial R}R_{\mu\nu} - \frac{1}{2}f(R,T)g_{\mu\nu} + (g_{\mu\nu}\Box - \nabla_\mu\nabla_\nu)\frac{\partial f}{\partial R} = \kappa T_{\mu\nu} - \frac{\partial f}{\partial T}(T_{\mu\nu} + \Theta_{\mu\nu}), \tag{2.2}$$

where $\Box \equiv \nabla^\mu\nabla_\mu$, while ∇_μ is the covariant derivative, and $\Theta_{\mu\nu}$ is defined as

$$\Theta_{\mu\nu} \equiv g^{\alpha\beta}\frac{\delta T_{\alpha\beta}}{\delta g^{\mu\nu}} = -2T_{\mu\nu} + g_{\mu\nu}\mathcal{L}_m - 2g^{\alpha\beta}\frac{\delta^2\mathcal{L}_m}{\delta g^{\mu\nu}\delta g^{\alpha\beta}}. \tag{2.3}$$

Note that when $f(R,T)$ does not depend on T, the equations of motion (2.2) reduce to the well–known $f(R)$ gravity. In this work we will assume that $f(R,T) = R + 2\kappa\alpha T$, where α is a real constant. This is the most studied model of $f(R,T)$ gravity and its viability has been investigated in numerous works [57]–[70]. In this particular model, the action of gravity reads,

$$S = \int\left(\frac{R}{2\kappa} + \alpha T\right)\sqrt{-g}\,\mathrm{d}^4x + \int\mathcal{L}_m\sqrt{-g}\,\mathrm{d}^4x\,, \tag{2.4}$$

and from (2.2), the equations of motion can take the following form,

$$R_{\mu\nu} - \frac{1}{2}g_{\mu\nu}R = \kappa T^{(\text{eff})}_{\mu\nu}, \tag{2.5}$$

where we have defined an effective energy-momentum tensor as,

$$T^{(\text{eff})}_{\mu\nu} \equiv T_{\mu\nu} - 2\alpha\left(T_{\mu\nu} - \frac{1}{2}Tg_{\mu\nu} + \Theta_{\mu\nu}\right). \tag{2.6}$$

It is clear from the last expression that when $\alpha \to 0$, we completely recover GR.

2.2. Slow–Roll inflation in $f(R,T)$ gravity

Now we will focus our study on the case in which $\mathcal{L}_m$ is given by (1.78), i.e. a scalar field minimally coupled to $f(R,T)$ gravity. Similar approaches were studied in [56] and [71]. However, unlike these works, we want to analyze the slow-roll approximation exhaustively and use it in different inflationary models. For a single and spatially homogeneous scalar field we have,

$$\Theta_{\mu\nu}^{(\varphi)} = -2T_{\mu\nu}^{(\varphi)} + g_{\mu\nu}\mathcal{L}_m^{(\varphi)} = -2\partial_\mu\varphi\partial_\nu\varphi - g_{\mu\nu}\Big(\frac{1}{2}\dot{\varphi}^2 - V(\varphi)\Big), \tag{2.7}$$

with,

$$\Theta_{00}^{(\varphi)} = -T_{00}^{(\varphi)} - \dot{\varphi}^2, \quad \Theta_{ij}^{(\varphi)} = -T_{ij}^{(\varphi)}, \tag{2.8}$$

where $T_{\mu\nu}^{(\varphi)}$ is given by (1.80). Thus, the trace of $\Theta_{\mu\nu}^{(\varphi)}$ can be easily computed,

$$\Theta^{(\varphi)} = g^{\mu\nu}\Theta_{\mu\nu}^{(\varphi)} = 4V(\varphi). \tag{2.9}$$

Now we can compute the components of the effective energy-momentum tensor defined in (2.6). For a homogeneous inflaton field, the energy-momentum tensor takes a diagonal form, from where we can define an effective energy density and pressure,

$$T_{00}^{(\text{eff})} = \frac{1}{2}\dot{\varphi}^2(1+2\alpha) + V(\varphi)(1+4\alpha) \equiv \rho_\varphi^{(\text{eff})} \tag{2.10}$$

$$T_{ij}^{(\text{eff})} = \Big(\frac{1}{2}\dot{\varphi}^2(1+2\alpha) - V(\varphi)(1+4\alpha)\Big)g_{ij} \equiv p_\varphi^{(\text{eff})}g_{ij}, \tag{2.11}$$

and $T_{\mu\nu}^{(\text{eff})} = 0$ for $\mu \neq \nu$. From these expressions, we can define an effective equation of state as the ratio of the pressure and the energy density,

$$w^{(\text{eff})} \equiv \frac{p_\varphi^{(\text{eff})}}{\rho_\varphi^{(\text{eff})}} = \frac{\dot{\varphi}^2(1+2\alpha) - 2V(\varphi)(1+4\alpha)}{\dot{\varphi}^2(1+2\alpha) + 2V(\varphi)(1+4\alpha)}. \tag{2.12}$$

Additionally, the trace of $T_{\mu\nu}^{(\text{eff})}$ can also be computed,

$$T^{(\text{eff})} = g^{\mu\nu}T_{\mu\nu}^{(\text{eff})} = \dot{\varphi}^2(1+2\alpha) - 4V(\varphi)(1+4\alpha) = 3p_\varphi^{(\text{eff})} - \rho_\varphi^{(\text{eff})} = (3w^{(\text{eff})}-1)\rho_\varphi^{(\text{eff})}. \tag{2.13}$$

By using the above expressions, in addition to (2.5), we can obtain the generalized Friedmann equations for our particular model of $f(R,T)$ gravity. From them, we can also get an expression for $\dot{H}$. The resulting equations read,

$$H^2 = \frac{8\pi G}{3}\rho_\varphi^{(\text{eff})} = \frac{8\pi G}{3}\left(\frac{\dot{\varphi}^2}{2}(1+2\alpha) + V(\varphi)(1+4\alpha)\right), \tag{2.14a}$$

$$\frac{\ddot{a}}{a} = -\frac{8\pi G}{6}(3p_\varphi^{(\text{eff})} + \rho_\varphi^{(\text{eff})}) = -\frac{8\pi G}{3}\Big(\dot{\varphi}^2(1+2\alpha) - V(\varphi)(1+4\alpha)\Big) \tag{2.14b}$$

$$\dot{H} = \frac{\ddot{a}}{a} - H^2 = -\frac{8\pi G}{2}(p_\varphi^{(\text{eff})} + \rho_\varphi^{(\text{eff})}) = -4\pi G\dot{\phi}^2(1+2\alpha). \tag{2.14c}$$

Furthermore, we can find a continuity equation for $\rho_\varphi^{(\text{eff})}$ and $p_\varphi^{(\text{eff})}$ through a similar procedure that gave us equation (1.84). By taking a time derivative on (2.14a) and replacing (2.14c), we obtain the modified Klein–Gordon equation,

$$\ddot{\varphi}(1+2\alpha) + 3H\dot{\varphi}(1+2\alpha) + V_{,\varphi}(1+4\alpha) = 0. \tag{2.15}$$

From the previous analysis we observe that the structure of the cosmological equations in this particular model of $f(R,T)$ gravity is conserved as we replace $p_\varphi \to p_\varphi^{(\text{eff})}$ and $\rho_\varphi \to \rho_\varphi^{(\text{eff})}$. Therefore, the corrections to the inflationary dynamics are enclosed within the corrections to energy density and pressure due to $f(R,T)$ gravity. These corrections seem to show that the conserved energy–momentum tensor is actually $T_{\mu\nu}^{(\text{eff})}$, as it can be noted from (2.5). Taking into account this idea, we will proceed to specify the slow–roll condition according to this model and, then, to compute the corrections to the slow-roll parameters $\tilde{\epsilon}_{\text{V}}$ and $\tilde{\eta}_{\text{V}}$, where we will denote with a tilde the parameters within the framework of $f(R,T)$ gravity. The first slow–roll parameter is given by,

$$\tilde{\epsilon} = -\frac{\dot{H}}{H^2} = \frac{3}{2}\frac{\dot{\varphi}^2(1+2\alpha)}{\left(\frac{\dot{\varphi}^2}{2}(1+2\alpha) + V(\varphi)(1+4\alpha)\right)}. \tag{2.16}$$

An inflationary evolution of the Universe requires that $|\tilde{\epsilon}| \ll 1$. Hence, the slow-roll condition for this model becomes,

$$\dot{\varphi}^2(1+2\alpha) \ll V(\varphi)(1+4\alpha). \tag{2.17}$$

On the other hand, we can show that the second slow-roll parameter is not corrected,

$$\dot{\tilde{\epsilon}} = 2H\tilde{\epsilon}^2 + \frac{8\pi G\dot{\varphi}\ddot{\varphi}(1+2\alpha)}{H^2} = 2H\tilde{\epsilon}^2 + 2\tilde{\epsilon}\frac{\ddot{\varphi}}{\dot{\varphi}} = 2H\tilde{\epsilon}(\tilde{\epsilon}-\tilde{\eta}), \quad \tilde{\eta} = -\frac{1}{H}\frac{\ddot{\varphi}}{\dot{\varphi}}. \tag{2.18}$$

Thus, the conditions $|\tilde{\epsilon}| \ll 1$ and $|\tilde{\eta}| \ll 1$ imply that we can neglect the second order derivative in (2.15), such that the Klein-Gordon equation becomes,

$$3H\dot{\varphi}(1+2\alpha) \approx -V_{,\varphi}(1+4\alpha). \tag{2.19}$$

By using this expression, and by applying the slow-roll condition (2.17) into (2.14a), we can find the correction to the first potential slow-roll parameter due to $f(R,T)$ gravity, which we denote as $\tilde{\epsilon}_{\text{V}}$

$$\tilde{\epsilon} \approx \frac{3\dot{\varphi}^2(1+2\alpha)}{2V(\varphi)(1+4\alpha)} = \frac{3}{2}\frac{1+2\alpha}{V(1+4\alpha)}\left(\frac{V_{,\varphi}}{3H}\left(\frac{1+4\alpha}{1+2\alpha}\right)\right)^2 = \frac{1}{16\pi G}\left(\frac{V_{,\varphi}}{V}\right)^2\left(\frac{1}{1+2\alpha}\right) \equiv \tilde{\epsilon}_{\text{V}}. \tag{2.20}$$

Additionally, if we take a time derivative on (2.19), the term $\ddot{\varphi}$ can be expressed in terms of $V_{,\varphi\varphi}$, by using the chain rule such that $\dot{V} = V_{\varphi}\dot{\varphi}$. Therefore, the second slow–roll parameter is given by,

$$\tilde{\eta} = -\frac{1}{H}\frac{\ddot{\varphi}}{\dot{\varphi}} = \frac{1}{3H^2}\frac{V_{,\varphi\varphi}(1+4\alpha)}{1+2\alpha} + \frac{\dot{H}}{H^2}, \tag{2.21}$$

and by using (2.14a), we can obtain the corrected expression for $\tilde{\eta}_V$ in the slow-roll approximation, which reads

$$\tilde{\eta}_{\text{V}} \equiv \tilde{\epsilon} + \tilde{\eta} \approx \frac{1}{8\pi G}\left(\frac{V_{,\varphi\varphi}}{V}\right)\left(\frac{1}{1+2\alpha}\right). \tag{2.22}$$

The number of e-folds are also modified in this model. The value can be computed from its definition in equation (1.91), also with (2.19) and (2.14a), such that we get,

$$\tilde{N} = \int \frac{H}{\dot{\varphi}}\,\mathrm{d}\varphi \approx 8\pi G(1+2\alpha)\int_{\varphi_{\text{end}}}^{\varphi} \frac{V}{V_{,\varphi}}\,\mathrm{d}\varphi\,. \tag{2.23}$$

It is noteworthy that these expressions are independent of the form of the potential $V(\varphi)$, and hence, the results presented can be interpreted as a generalization of the slow-roll approximation for the model $f(R,T) = R + 2\kappa\alpha T$ of gravity. It should also be noted that certain values for α are problematic since choosing them would cause the slow-roll parameters to blow up or become zero. In general, we will consider that $\alpha > -1/2$ as a minimum requirement to have well-defined parameters.

Another essential feature that we can infer from these results is that this model is entirely equivalent to a particular case of a scalar-tensor model of gravity. For instance, the most general action of scalar-tensor gravity is given by [72],

$$S = \int \left(f(\phi) R - \frac{\omega(\phi)}{\phi} \partial^\alpha \phi \partial_\alpha \phi - v(\phi) \right) \sqrt{-g}\, \mathrm{d}^4 x \,. \tag{2.24}$$

Hence, it can be seen that the action (2.1) is equivalent to the above action (2.24) if $f(\phi) = 1$, $\omega(\phi) = (1+2\alpha)(\phi/2)$ and $v(\phi) = (1+4\alpha)V(\phi)$, where $V(\phi)$ is the original potential. In fact, a further equivalence can be deduced from the above analysis. The action (2.4) can be recast as a scalar field minimally coupled to General Relativity, i.e. the Einstein frame [73],

$$S = \int \left(\frac{R}{2\kappa} - \frac{1}{2} \partial^\alpha \bar{\varphi} \partial_\alpha \bar{\varphi} - \bar{V}_{\text{eff}}(\bar{\varphi}) \right) \sqrt{-g}\, \mathrm{d}^4 x \,,$$

if we perform the following transformations over the field and the potential,

$$\bar{\varphi} \to \sqrt{1+2\alpha}\, \varphi, \quad \bar{V}_{\text{eff}}(\bar{\varphi}) \to (1+4\alpha) V\left(\frac{\bar{\varphi}}{\sqrt{1+2\alpha}} \right), \tag{2.25}$$

where V is the potential initially considered in the original lagrangian (1.78).

2.3. Inflationary models in $f(R,T)$ gravity

2.3.1. Power Law Potentials

As the first example of an inflationary scenario, we will take one of the simplest models by taking a power-law potential of the form,

$$V(\varphi) = \lambda \varphi^n, \tag{2.26}$$

where λ is a coupling constant. From the definitions of $\epsilon_{\rm V}$ and $\eta_{\rm V}$, in equations (1.88) and (1.90) respectively, we obtain the following slow–roll parameters,

$$\epsilon_{\rm V} = \frac{n^2}{16\pi G\varphi^2}, \quad \eta_{\rm V} = \frac{n(n-1)}{8\pi G\varphi^2}. \tag{2.27}$$

As inflation ends when $\epsilon_{\rm V}(\varphi_{\rm end}) = 1$, we have, $\varphi_{\rm end} = \frac{n}{\sqrt{16\pi G}}$. Therefore, the number of e–folds can be computed from (1.91),

$$N = \frac{4\pi G}{n}\left(\varphi^2 - \frac{n^2}{16\pi G}\right) \tag{2.28}$$

Thus, the slow-roll parameters can be expressed in terms of the number of e-folds as follows,

$$\epsilon_{\rm V} = \frac{n}{4N+n}, \quad \eta_{\rm V} = \frac{2(n-1)}{4N+n}. \tag{2.29}$$

The spectral indices for this model can be found from (1.150),

$$n_{\rm S} - 1 \approx 2\eta_{\rm V} - 6\epsilon_{\rm V} = -\frac{2(n+2)}{4N+n} \tag{2.30a}$$

$$n_{\rm T} \approx -2\epsilon_{\rm V} = -\frac{2n}{4N+n} \tag{2.30b}$$

$$r \approx 16\epsilon_{\rm V} = \frac{16n}{4N+n} \tag{2.30c}$$

Now we turn out to compute the corrections to the slow-roll parameters. From (2.20) and (2.22), we obtain,

$$\tilde{\epsilon}_{\rm V} = \left(\frac{1}{1+2\alpha}\right)\frac{n^2}{16\pi G\varphi^2} \tag{2.31}$$

$$\tilde{\eta}_{\rm V} = \left(\frac{1}{1+2\alpha}\right)\frac{n(n-1)}{8\pi G\varphi^2}. \tag{2.32}$$

Inflation ends when the slow-roll condition is no longer valid, i.e. $\bar{\epsilon}_{\rm V} \approx 1$. Thus, we have

$$\varphi^2_{\rm end} = \frac{n^2}{16\pi G(1+2\alpha)}. \tag{2.33}$$

Therefore, from (2.23), the number of e–folds, $\tilde{N}$, is given by the expression,

$$\tilde{N} = (1+2\alpha)8\pi G\int_{\varphi_{\rm end}}^{\varphi}\frac{V(\varphi)}{V_{,\varphi}(\varphi)}\,{\rm d}\varphi = \frac{(1+2\alpha)4\pi G}{n}\left(\varphi^2 - \frac{n^2}{2\kappa(1+2\alpha)}\right). \tag{2.34}$$

With this, we can express the slow-roll parameters $\tilde{\epsilon}_{\mathrm{V}}$ and $\tilde{\eta}_{\mathrm{V}}$ as,

$$\tilde{\epsilon}_{\mathrm{V}} = \frac{n}{4\tilde{N}+n} \tag{2.35a}$$

$$\tilde{\eta}_{\mathrm{V}} = \frac{2(n-1)}{4\tilde{N}+n} \tag{2.35b}$$

Therefore, the spectral indices read from (1.150),

$$n_{\mathrm{S}} - 1 = 2\tilde{\eta}_{\mathrm{V}} - 6\tilde{\epsilon}_{\mathrm{V}} = -\frac{2(n+2)}{4\tilde{N}+n} \tag{2.36a}$$

$$n_{\mathrm{T}} = -2\tilde{\epsilon}_{\mathrm{V}} = -\frac{2n}{4\tilde{N}+n} \tag{2.36b}$$

$$r = 16\tilde{\epsilon}_{\mathrm{V}} = \frac{16n}{4\tilde{N}+n} = \frac{8n(1-n_{\mathrm{S}})}{n+2} \tag{2.36c}$$

It is clear that no corrections from $f(R,T)$ gravity are induced to monomial power-law potentials, as the structure of the slow-roll parameters and the spectral indices remain unaltered. The above results seem to differ from the conclusions of [56], which indicates that $f(R,T)$ gravity modifies the slow-roll parameters for a quadratic potential in a non-trivial way. We can explain the lack of dependence on α in equations (2.36) from the idea of the effective potential of equation (2.25). For a monomial term, for instance, the potential in (2.26), we have,

$$\bar{V}_{\text{eff}}(\bar{\varphi}) = (1+4\alpha)\lambda\left(\frac{\bar{\varphi}}{\sqrt{1+2\alpha}}\right)^{n} = \bar{\lambda}\bar{\varphi}^{n}. \tag{2.37}$$

Thus, the coefficients related to α can be incorporated into a single coupling constant, which determines the strength of the potential, but that does not affect the values of the slow-roll parameters or the spectral indices since they are fixed by the measurements of the CMB amplitudes. This fact implies that α almost have no incidence on the dynamics of an inflationary model triggered by a simple power-law potential and cannot improve the tension between the predictions of power-law potentials and the constraints of the spectral indices measured by Planck 2018 for $50 < \tilde{N} < 60$ [37]. The last assertion does not mean that a different functional form of $f(R,T)$ gravity cannot generate a distinguishable effect for power-law potentials; however, the analysis of these different approaches goes beyond the scope of this work.

2.3.2. Natural & Hilltop Inflation

Now let us apply our results to other types of potentials. To start, we consider Natural inflation [74], [75], a model whose inflaton field is a pseudo-Nambu-Goldstone boson produced by a spontaneous symmetry breaking in addition to an explicit symmetry breaking, such that the dynamics of a single field is governed by a potential of the form,

$$V(\varphi) = \Lambda^4 \left[1 + \cos\left(\frac{\varphi}{f}\right) \right], \tag{2.38}$$

where f and Λ are mass scales. It has been shown that this potential can drive inflation if $\Lambda \sim M_{\text{GUT}} \sim 10^{16}$ GeV and $f \sim M_{\text{Pl}} = \kappa^{-1/2}$. Following a similar procedure as before, we can express the slow-roll parameters in terms of the number of e-folds N, such that,

$$\epsilon_{\text{V}} = \frac{M_{\text{Pl}}^2}{2f^2} \frac{\sin^2(\varphi/f)}{[1+\cos(\varphi/f)]^2} = \frac{M_{\text{Pl}}^2}{2f^2} \frac{1}{e^{NM_{\text{Pl}}^2/f^2} - 1} \tag{2.39}$$

$$\eta_{\text{V}} = -\frac{M_{\text{Pl}}^2}{f^2} \frac{\cos(\varphi/f)}{1+\cos(\varphi/f)} = -\frac{M_{\text{Pl}}^2}{2f^2} \frac{e^{NM_{\text{Pl}}^2/f^2} - 2}{e^{NM_{\text{Pl}}^2/f^2} - 1} \tag{2.40}$$

Thus, the scalar spectral index and the tensor-to-scalar ratio, in the slow-roll approximation, read from (1.150),

$$n_{\text{S}} - 1 \approx -\frac{M_{\text{Pl}}^2}{f^2} \left(\frac{e^{NM_{\text{Pl}}^2/f^2} + 1}{e^{NM_{\text{Pl}}^2/f^2} - 1} \right) \tag{2.41a}$$

$$n_{\text{T}} \approx -\frac{M_{\text{Pl}}^2}{f^2} \left(\frac{1}{e^{NM_{\text{Pl}}^2/f^2} - 1} \right) \tag{2.41b}$$

$$r \approx \frac{8M_{\text{Pl}}^2}{f^2} \left(\frac{1}{e^{NM_{\text{Pl}}^2/f^2} - 1} \right). \tag{2.41c}$$

Moreover, we can rewrite r in terms of n_s, in order to have the representation in the (r, n_s) plane,

$$r(n_s) \approx 4 \left(1 - n_s - \frac{M_{\text{Pl}}^2}{f^2} \right). \tag{2.42}$$

Let us analyze if any change is induced by $f(R,T)$ gravity to this model. The corrected slow–roll parameters can be computed following the same recipe as before, which gives

$$\tilde{\epsilon}_{\rm V} = \frac{M_{\rm Pl}^2}{2(1+2\alpha)f^2}\frac{\sin^2(\varphi/f)}{[1+\cos(\varphi/f)]^2} = \frac{M_{\rm Pl}^2}{2(1+2\alpha)f^2}\frac{1}{e^{\frac{\tilde{N}M_{\rm Pl}^2}{(1+2\alpha)f^2}}-1} \tag{2.43}$$

$$\tilde{\eta}_{\rm V} = -\frac{M_{\rm Pl}^2}{(1+2\alpha)f^2}\frac{\cos(\varphi/f)}{1+\cos(\varphi/f)} = -\frac{M_{\rm Pl}^2}{2(1+2\alpha)f^2}\frac{e^{\frac{\tilde{N}M_{\rm Pl}^2}{(1+2\alpha)f^2}}-2}{e^{\frac{\tilde{N}M_{\rm Pl}^2}{(1+2\alpha)f^2}}-1} \tag{2.44}$$

With this, the spectral indices read,

$$n_{\rm S}-1 \approx -\frac{M_{\rm Pl}^2}{(1+2\alpha)f^2}\left(\frac{e^{\frac{\tilde{N}M_{\rm Pl}^2}{(1+2\alpha)f^2}}+1}{e^{\frac{\tilde{N}M_{\rm Pl}^2}{(1+2\alpha)f^2}}-1}\right) \tag{2.45a}$$

$$n_{\rm T} \approx -\frac{M_{\rm Pl}^2}{(1+2\alpha)f^2}\left(\frac{1}{e^{\frac{\tilde{N}M_{\rm Pl}^2}{(1+2\alpha)f^2}}-1}\right) \tag{2.45b}$$

$$r \approx \frac{8M_{\rm Pl}^2}{(1+2\alpha)f^2}\left(\frac{1}{e^{\frac{\tilde{N}M_{\rm Pl}^2}{(1+2\alpha)f^2}}-1}\right). \tag{2.45c}$$

From the above expressions we can solve $\tilde{N}$ in terms of $n_{\rm S}$ and obtain the representation in the $(r, n_{\rm S})$ plane, which reads,

$$r(n_{\rm S}) = 4\left(1-n_{\rm S}-\frac{M_{\rm Pl}^2}{(1+2\alpha)f^2}\right). \tag{2.46}$$

It is evident that in Natural inflation there is a non-trivial modification to the values of the inflationary quantities due to the action of $f(R,T)$ gravity. We can summarize all the α contribution to the spectral indices and slow–roll parameters as a correction to the mass scale f, i.e., $f \to \sqrt{1+2\alpha}f$, which could change the constraints on the value of f from CMB measurements. This modification can also be understood, as in the previous subsection, from the argument of the effective potential (2.25). This type of shift in the mass scale due to $f(R,T)$ gravity will appear in many other similar inflation theories. For instance, the quartic Hilltop inflationary model, presented in [76], considers a potential of the form,

$$V(\varphi) = \Lambda^4\left[1 - \left(\frac{\varphi}{\mu_4}\right)^4 + \ldots\right] \tag{2.47}$$

where the dots indicate higher-order terms that can be neglected during inflation, and μ_4 is the mass scale that characterizes the inflaton vacuum expectation value, i.e., $\mu_4 \sim \langle\varphi\rangle$. From the previous analysis of Natural inflation, it is straightforward to show that the action of $f(R,T)$ can be summarized as a correction to the mass scale given by $\mu_4 \to \sqrt{1+2\alpha}\mu_4$.

The scalar spectral index and the tensor-to-scalar ratio for the quartic Hilltop model are given, according to [77], by the following expressions

$$n_S - 1 \approx -\frac{3}{N_t}\left[\frac{Z}{Z-1}\right] \tag{2.48a}$$

$$r \approx \frac{128M_{\rm Pl}^8[4N_tP(Z)]^3}{\mu_4^8[2(1-ZP(Z))]^2} = \frac{8}{3}(1-n_S)P(Z), \tag{2.48b}$$

where N_t is the total number of e-folds during inflation, such that

$$N_t = N + \frac{\mu_4^2}{4M_{\rm Pl}^2} \tag{2.49}$$

where N is the number of e-folds after the cosmological scales exit the horizon until the end of inflation, and also

$$Z = 16N_t^2\frac{M_{\rm Pl}^4}{\mu_4^4}, \quad P(Z) = 1 - \sqrt{1-\frac{1}{Z}}. \tag{2.50}$$

By applying the same reasoning as in the previous cases, it is not difficult to prove that when $f(R,T)$ gravity is considered, the induced changes to (2.48) can be expressed as a modification to Z,

$$Z \to \tilde{Z} = \frac{16\tilde{N}_t^2}{(1+2\alpha)^2}\frac{M_{\rm Pl}^4}{\mu_4^4}, \tag{2.51}$$

where $\tilde{N}_t = \tilde{N} + [(1+2\alpha)(\mu_4^2)]/(4M_{\rm Pl}^2)$. Thus, in quartic Hilltop inflation, the action of $f(R,T)$ gravity reduces to a modification of the parameter μ_4, as expected from the analysis of the effective potential defined in (2.25). In practice, these corrections to f and μ_4 do not modify the shape of the curves in the (n_S, r) plane, as it can be seen from Fig. 2.3.

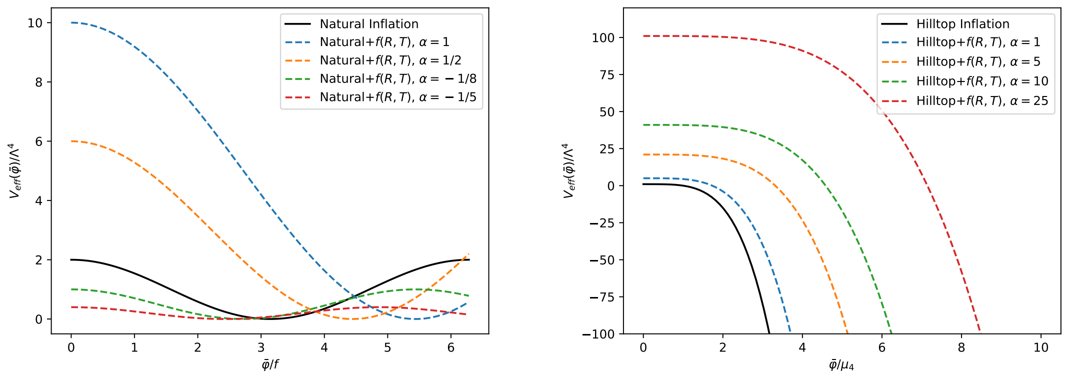

FIGURE 2.1. The solid black lines show the potential of the original Natural/quartic Hilltop inflationary models. In dotted colored lines we have the effective potential, i.e. (2.25), for different values of α.

However, the values of f and μ_4 needed to span some region within the (n_S, r) plane will be different for a non-zero value of α. As an example, we show in Table 2.1 a comparison between the parameters range considered in the analysis of inflationary models done by the Planck collaboration [37], and how they change as we increase the value of α. In order to span some fixed region in the (n_S, r) plane, the accepted range for μ_4 changes as we modify the value of α.

α	Natural Inflation	Quartic Hilltop Inflation
0	$0.30 < \log_{10}(f/M_{Pl}) < 2.50$	$-2.00 < \log_{10}(\mu_4/M_{Pl}) < 2.00$
1	$0.06 < \log_{10}(f/M_{Pl}) < 2.26$	$-2.24 < \log_{10}(\mu_4/M_{Pl}) < 1.76$
5	$-0.22 < \log_{10}(f/M_{Pl}) < 1.97$	$-2.52 < \log_{10}(\mu_4/M_{Pl}) < 1.48$
10	$-0.36 < \log_{10}(f/M_{Pl}) < 1.84$	$-2.66 < \log_{10}(\mu_4/M_{Pl}) < 1.34$
20	$-0.51 < \log_{10}(f/M_{Pl}) < 1.69$	$-2.81 < \log_{10}(\mu_4/M_{Pl}) < 1.19$

TABLE 2.1. Some examples for the parameter range of Natural/quartic Hilltop inflationary models considering different values of α. The $\alpha = 0$ cases are the ranges provided in Planck 2018 results [37] to successfully span the (n_S, r) plane within the intervals $r \in [0, 0.2]$ and $n_S \in [0.93, 1.00]$. Natural inflation is strongly disfavored by the data. However, for quartic Hilltop inflation, the corrected constraint of μ_4 to be within the 95% CL region is given by (2.52).

In particular, Natural inflation is strongly disfavored by the Planck 2018 data, and we reach the same conclusion with the contribution of $f(R,T)$ gravity. On the contrary, quartic

Hilltop inflation provides a good fit with the data as long as the value of μ_4 is constrained to $\log_{10}(\mu_4/M_{\rm Pl}) > 1$ at 95% CL. Therefore, the contribution of $f(R,T)$ gravity provides the following constraint for μ_4 and α in order to fit the data of Planck 2018,

$$\log_{10}(\mu_4/M_{\rm Pl}) > 1 - \frac{1}{2}\log_{10}(1+2\alpha). \tag{2.52}$$

In general, a higher value of α will decrease the constraint on μ_4. This fact could have some important consequences for the interpretation of μ_4. As it can be seen from equation (2.52) and as it has been established in previous works, the inflaton *vev* in the quartic Hilltop model should be super–Planckian, i.e. $\mu_4 > 10M_{\rm Pl}$, to fit the cosmological data. Nevertheless, for values of $\alpha > 50$, this is no longer a requirement and actually arises the possibility that $\mu_4 \sim M_{\rm Pl}$ or even $\mu_4 \leq M_{\rm Pl}$. For instance, if $\tilde{N} \sim 55$, $\mu_4 \sim M_{\rm Pl}$ and $\alpha \sim 100$, we have $n_{\rm S} \sim 0.9631$ and $r \sim 0.012$, which are in good agreement with the Planck constraints. This kind of corrections could modify the interpretation of the Hilltop model and improve its behavior at the quantum level since it is known that super-Planckian values for the inflaton are problematic from the point of view of particle physics and effective field theory [78], [79].

In Fig. 2.1 it can be seen how the shape of effective potential for Natural and Quartic Hilltop Inflation is modified depending on different values of the parameter α. In the case of Natural Inflation, the position of the minimum of the potential is shifted to greater values of $\bar{\varphi}/f$ as the value of α increases. Additionally, the height of the plateau in the Hilltop inflationary model is also shifted by changing the value of α.

2.3.3. Starobinsky Inflation

The last example we are going to address will be the Starobinsky inflation. The origin lies in Starobinsky's seminal investigations in the early eighties [3]. In this model, the standard Einstein–Hilbert action includes a R^2 term,

$$S = \frac{1}{2\kappa}\int\left(R + \frac{R^2}{6M^2}\right)\sqrt{-g}\,\mathrm{d}^4x\,, \tag{2.53}$$

where M is a constant. It is well-known that this model can be recast, by a conformal transformation to the Einstein frame, into a scalar field minimally coupled to gravity [80], [81], i.e., the standard Einstein gravity with a canonically normalized scalar field, χ, and a potential of the form [40]

$$V(\chi) = \frac{3M^2 M_{\rm Pl}^2}{4}\left(1 - e^{-\sqrt{2/3}\frac{\chi}{M_{\rm Pl}}}\right)^2. \tag{2.54}$$

Therefore, interpreting the field χ as our inflaton (also known as a scalaron), we can compute the slow-roll parameters from (1.88) and (1.90),

$$\epsilon_{\rm V} = \frac{4}{3}\frac{e^{2y}}{(1-e^y)^2}, \quad \eta_{\rm V} = \frac{4}{3}\frac{(e^y - 2e^{2y})}{(1-e^y)^2}, \quad y = -\sqrt{\frac{2}{3}}\frac{\chi}{M_{\rm Pl}}.$$

The number of e–folds can be approximated by calculating the integral (1.91), such that

$$N \approx \frac{3}{4}e^{-y} = \frac{3}{4}e^{\sqrt{\frac{2}{3}}\frac{\chi}{M_{\rm Pl}}} \tag{2.55}$$

Thus, the slow–roll parameters can be written as,

$$\epsilon_{\rm V} = \frac{12}{(3-4N)^2} \approx \frac{3}{4N^2} \tag{2.56a}$$

$$\eta_{\rm V} = -\frac{8(2N-3)}{(3-4N)^2} \approx -\frac{1}{N}, \tag{2.56b}$$

wherein each approximation we kept the dominant contributions for large N. Considering the last expressions, we obtain the well-known predictions of the scalar spectral index and the tensor-to-scalar ratio from the Starobinsky model [40],

$$n_{\rm S} \approx 1 - \frac{2}{N} \tag{2.57a}$$

$$r \approx \frac{12}{N^2} = 3(1-n_{\rm S})^2 \tag{2.57b}$$

where we used that $|\epsilon_{\rm V}| \ll |\eta_{\rm V}|$ for large N. The Starobinsky model has regained interest in recent years since its predictions seem to be in good agreement with the last CMB measurements from the Planck collaboration [37], but also because it was found a connection between this model and inflation triggered by a Higgs boson non–minimally coupled to gravity [82], [83]. As a consequence, many extensions of the Starobinsky model, like non-local modifications or the inclusion of higher order terms, are currently investigated [84]–[88].

A simple question immediately arises: Is it possible to apply $f(R,T)$ gravity to Starobinsky inflation? At first glance, in the Jordan frame, i.e., the action (2.53), the model does not consider any matter field, so the trace T is identically zero. Nevertheless, once we are in the Einstein frame, we could apply the prescription of $f(R,T)$ gravity and add a term proportional to the trace of the energy-momentum tensor formed by the inflaton/scalaron. With this procedure, we can follow the previous analysis and compute the corrections to the cosmological parameters due to the additional contribution coming from α.

To start, we can analyze the corresponding effective potential for the Starobinsky model, which is illustrated in Fig. 2.2. From the plot, we can observe that the value of α modifies the height of the potential plateau, which can be interpreted as the vacuum energy V_0 that dominates the inflation dynamics (for $\chi \gg 1$),

$$V_0 = \frac{3}{4} M_{\text{Pl}}^2 M^2 (1 + 4\alpha). \tag{2.58}$$

The slow-roll parameters can be obtained following the standard procedure, and they read

$$\tilde{\epsilon}_{\text{V}} = \frac{4}{3} \frac{e^{2y}}{(1+2\alpha)(1-e^y)^2} = \frac{12(1+2\alpha)}{[3(1+2\alpha) - 4\tilde{N}]^2} \approx \frac{3(1+2\alpha)}{4\tilde{N}^2} \tag{2.59a}$$

$$\tilde{\eta}_{\text{V}} = \frac{4}{3} \frac{(e^y - 2e^{2y})}{(1+2\alpha)(1-e^y)^2} = -\frac{8[2\tilde{N} - 3(1+2\alpha)]}{[3(1+2\alpha) - 4\tilde{N}]^2} \approx -\frac{1}{\tilde{N}}, \tag{2.59b}$$

where $\tilde{N}$ is the number of e–folds till the end of inflation, and we kept the contributions from large N as long as $\alpha \ll N$. Therefore, using these slow-roll parameters, we can

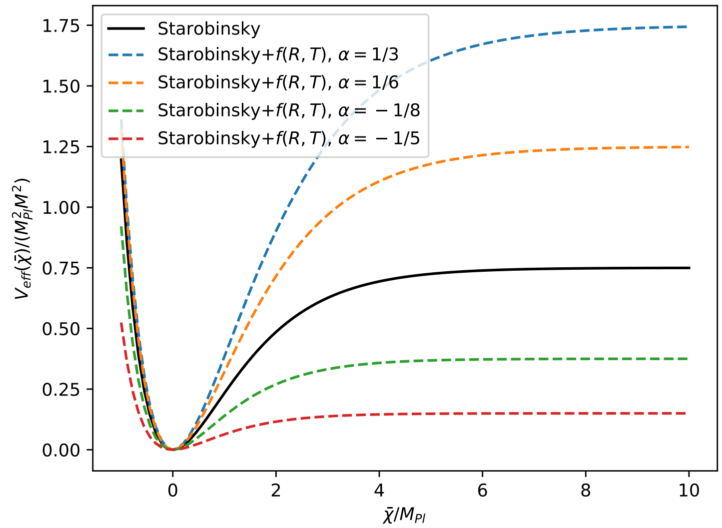

FIGURE 2.2. The solid black line shows the original potential in the Einstein frame for Starobinsky inflation. The dotted colored lines illustrate the effective potential for different values of α.

compute the corrected spectral indices and the tensor-to-scalar ratio,

$$n_\mathrm{S} \approx 1 - \frac{2}{\tilde{N}} \tag{2.60a}$$

$$n_\mathrm{T} \approx -\frac{3(1+2\alpha)}{2\tilde{N}^2} \tag{2.60b}$$

$$r \approx \frac{12(1+2\alpha)}{\tilde{N}^2} = 3(1+2\alpha)(1-n_\mathrm{S})^2. \tag{2.60c}$$

For example, $\tilde{N} = 55$ and $\alpha = 1$ we have $n_\mathrm{S} = 0.9636$, $n_\mathrm{T} = -0.0015$ and $r = 0.012$ (if $\alpha = 0$, $n_\mathrm{T} = -0.0004$ and $r = 0.004$). To understand how α modifies the trajectories, we plot some examples on the (n_S, r) plane, including other models, as is illustrated in Fig. 2.3.

Thus, in general, the contribution from $f(R,T)$ gravity will only modify the tensor spectral index's value and the tensor-to-scalar ratio when comparing it to the standard Starobinsky inflation. For positive values of α, the amount of primordial gravitational waves produced during inflation will increase. Hence, if future measurements of the B-modes of the CMB constrain r or n_T to values quite different than the predictions of the Starobinsky model,

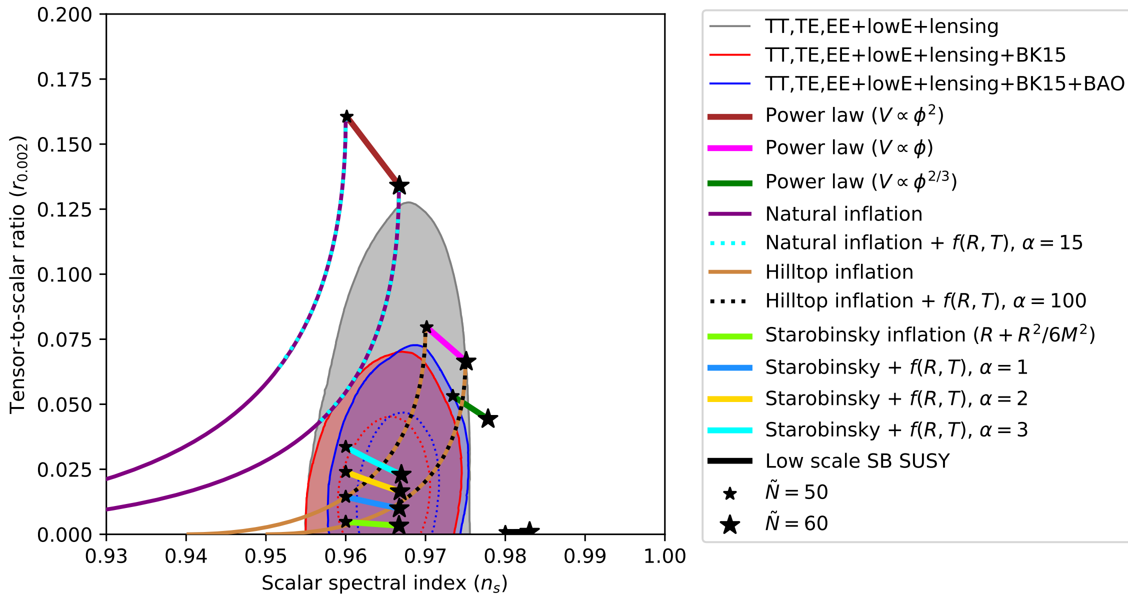

FIGURE 2.3. Marginalized joint 68% (dotted) and 95% (solid) CL regions for n_S and r at $k = 0.002$ Mpc^{-1} from Planck 2018 data release [37]. We shown the prediction of some selected models and in some cases also the corrections due to $f(R,T)$ gravity are included. We consider that $\tilde{N}$ is the number of e–folds until the end of inflation, according to the modified model, i.e. $\alpha \neq 0$.

these modifications due to $f(R,T)$ gravity could stand as a viable model. Conversely, for negative values of α, the magnitude of r will decrease with respect to the standard prediction. Considering the previous example, for $n_S = 0.9636$ and $\alpha = -1/3$, we have $r = 0.001$ (compared with $r = 0.004$ if $\alpha = 0$). It should be noted, however, that the negative values of α are bounded from below in order to ensure a well behavior of the physical parameters, i.e. $-1/2 < \alpha$. Thus, we can set a bound on the allowed values of α such that the resulting r and n_S are in good agreement with the measurement of Planck, and it is given by

$$-0.5 < \alpha < 5.54. \tag{2.61}$$

These are some of the simplest and most popular models, but they are not the only ones. For a comprehensive and extensive compendium of different inflationary models, see [89].

2.4. A brief analysis on models with higher order powers of T

In this thesis we have considered, the simplest minimal coupling between matter and gravity, i.e., $f(R,T) = R + 2\kappa\alpha T$. However, it is worth wondering how difficult it is to address a more complex interaction. For instance, let us consider a function of the form $f_*(R,T) = R + 2\kappa(\alpha T + \beta T^2)$. Using (2.4), the equations of motion for this model can be expressed as in (2.6), with an effective energy–momentum tensor given by,

$$T_{\mu\nu}^{(\text{eff*})} = T_{\mu\nu} - 2(\alpha + 2\beta T)(T_{\mu\nu} + \Theta_{\mu\nu}) + (\alpha T + \beta T^2)g_{\mu\nu}. \tag{2.62}$$

This is, again, a diagonal tensor, but now with the following components,

$$\begin{aligned} T_{00}^{(\text{eff*})} &= \frac{\dot{\varphi}^2}{2}(1 + 2\alpha + 6\beta\dot{\varphi}^2 - 16\beta V) + V(1 + 4\alpha - 16\beta V) \\ &\equiv \rho_\varphi^{(\text{eff*})}, \end{aligned} \tag{2.63}$$

$$\begin{aligned} T_{ij}^{(\text{eff*})} &= \left(\frac{\dot{\varphi}^2}{2}(1 + 2\alpha + 2\beta\dot{\varphi}^2 - 16\beta V) - V(1 + 4\alpha - 16\beta V)\right)g_{ij} \\ &\equiv p_\varphi^{(\text{eff*})}. \end{aligned} \tag{2.64}$$

We can notice that in this example a cross term appears, e.g., $\dot{\varphi}^2 V$, in addition to higher order terms like $\dot{\varphi}^4$ or V^2. Following a similar procedure as we did with the simplest case, we can write the Friedmann equations in their standard fashion, e.g., (2.14a), (2.14a), (2.14c), by doing $\rho_\varphi \to \rho_\varphi^{(\text{eff*})}$ and $p_\varphi \to p_\varphi^{(\text{eff*})}$. Hence, we can define the first slow-roll parameter,

$$\begin{aligned} \tilde{\epsilon}_* &= -\frac{\dot{H}}{H^2} \\ &= \frac{3\dot{\varphi}^2[1 + 2\alpha + 4\beta(\dot{\varphi}^2 - 4V)]}{2V(1 + 4\alpha - 16\beta V) + (1 + 2\alpha - 16\beta V)\dot{\varphi}^2 + 6\beta\dot{\varphi}^4}. \end{aligned} \tag{2.65}$$

If we impose the slow-roll condition as $\tilde{\epsilon}_* \ll 1$, it would reduce to something of the form,

$$\dot{\varphi}^2(1 + 2\alpha - 16\beta V + 3\beta\dot{\varphi}^2) \ll V(1 + 4\alpha - 16\beta V). \tag{2.66}$$

Furthermore, by following the same treatment as before, we can obtain the modified Klein-Gordon equation, which reads

$$\ddot{\varphi}[1+2\alpha-16\beta V+12\beta\dot{\varphi}^2]+V_{,\varphi}[1+4\alpha-32\beta V+8\beta\dot{\varphi}^2]$$
$$+3H\dot{\varphi}[1+2\alpha-16\beta V+4\beta\dot{\varphi}^2]=0. \tag{2.67}$$

As we can observe, all the contributions proportional to β have crossed or higher order terms, and more important, the coefficients of these crossed terms are different at each stage, e.g., the terms $3\beta\dot{\varphi}^4$ and $\beta\dot{\varphi}^4$ in (2.63),(2.64), respectively. Another difficulty can be noticed when we try to define the second slow-roll parameter, because when we derive $\tilde{\epsilon}_*$ we obtain,

$$\dot{\tilde{\epsilon}}_* = 2H\tilde{\epsilon}_*\left(\tilde{\epsilon}_* + \frac{\ddot{\varphi}}{H\dot{\varphi}}\right) - \frac{4\dot{\varphi}^2\beta(2V_{,\varphi}-\dot{\varphi}\ddot{\varphi})}{H^2}. \tag{2.68}$$

Then, the second slow-roll parameter is not of the form $\eta \sim \frac{\ddot{\varphi}}{H\dot{\varphi}}$, and the condition $\eta \ll 1$ cannot be used to simplify the expression of $\tilde{\epsilon}_*$ in order to construct a simpler slow-roll parameter that depends only on the potential and its derivative, i.e., $\tilde{\epsilon}_{V*}$. As a consequence, the slow-roll analysis becomes much more difficult to do in these kind of models, as we cannot easily neglect terms to define more tractable parameters.

In summary, since the inclusion of higher order terms of T introduces major corrections on the definition of cosmological parameters, and therefore on the predictions of inflationary models, the study of this type of theories is quite well motivated. However, as it is beyond the scope of this work, we expect to address these issues in future research.

3. Two-field Inflation from a bosonic 0-form

We studied in the last chapter how General Relativity can be modified by adding additional terms to the Einstein-Hilbert action. However, this is not the only kind of modification that we can have. One of the first generalizations of GR was developed by Élie Cartan [13], who added the contributions from affine torsion to the gravitational interaction, extending the entire Riemannian geometry. Here, we found how a bosonic object can be a source of torsion and be considered the source of inflation.

3.1. Introduction to Einstein-Cartan Gravity

3.1.1. The concept of Vielbien

According to the Equivalence Principle, we can always choose a coordinate system where the spacetime looks locally as Minkowski. In general, we can implement this choice by specifying the vielbein $e^a{}_\mu(x)$ as,

$$g_{\mu\nu}(x) = e^a{}_\mu(x)\eta_{ab}e^b{}_\nu(x), \tag{3.1}$$

where η_{ab} is the Minkowski metric. Latin characters will denote Lorentz indices and greek characters will denote spacetime indices. Given a metric in D dimensions, the choice of the vielbein is not unique: All the equivalent choices are related as

$$e'^a_\mu(x) = \Lambda^a_b(x)e^b_\mu(x), \tag{3.2}$$

where $\Lambda^a_b(x) \in SO(1, D-1)$. Additionally, the vielbein field transform as a 1-form under general coordinate transformations,

$$e'^a_\mu(x') = \frac{\partial x^\nu}{\partial x'^\mu} e^a{}_\nu(x). \tag{3.3}$$

If $\det\left(e^a{}_\mu\right) \neq 0$, there exist an inverse vielbein field E^μ_a such that $E^\mu{}_a e^b{}_\mu = \delta^a_b$ and $E^\mu{}_a e^a_\nu = \delta^\mu{}_\nu$. The inverse vielbein transforms in a similar way,

$$E'^\mu_a(x) = \Lambda^b{}_a(x)E^\mu_b, \qquad E'^\mu_a(x') = \frac{\partial x'^\mu}{\partial x^\nu} E^\nu{}_a(x). \tag{3.4}$$

By using the inverse vielbein, we can invert the relationship between $g_{\mu\nu}$ and η_{ab},

$$E^{\mu}_{\ a}(x) g_{\mu\nu}(x) E^{\nu}_{\ b}(x) = \eta_{ab}. \tag{3.5}$$

The components of the vielbein and the inverse vielbein can be used to construct a new basis for the vector space $\Omega^p(\mathcal{M})$ of differential forms and its tangent space, respectively, as follows,

$$e^a = e^a_{\ \mu}\, \mathrm{d}x^\mu\,, \qquad E_a = E^{\mu}_{\ a}\partial_\mu. \tag{3.6}$$

3.1.2. p-forms and connections

It will be useful to define the concept of a differential p-form, which is a completely $(0,p)$ anti-symmetric tensor which lies on the p-th exterior power of the cotangent space of a manifold $\mathcal{M}$. We can construct a basis of p-forms using the wedge product $\wedge$, defined as $\mathrm{d}x^{\mu_1} \wedge \ldots \wedge \mathrm{d}x^{\mu_p} = \sum_\sigma (-1)^{|\sigma|}\, \mathrm{d}x^{\sigma(\mu_1)} \otimes \ldots \otimes \mathrm{d}x^{\sigma(\mu_p)}$ with σ denoting the permutation of indices. Hence, the wedge product defines a basis of the vector space of the differential p-forms over $\mathcal{M}$, denoted by $\Omega^p(\mathcal{M})$, in such a way that any element of this vector space, i.e., $\alpha \in \Omega^p(\mathcal{M})$, can be written as $\alpha = (p!)^{-1}\alpha_{\mu_1\ldots\mu_p}\, \mathrm{d}x^{\mu_1} \wedge \ldots \wedge \mathrm{d}x^{\mu_p}$.

In order to define covariant derivatives under local Lorentz transformations, we can introduce a gauge connection, called the *Lorentz connection 1-form*, denoted by $\omega^a_{\ b}(x) = \omega^a_{\ b\mu}(x)\, \mathrm{d}x^\mu$, which transforms under $SO(1, D-1)$ as

$$\omega^a_{\ b} \to \omega'^a_{\ b} = \Lambda^a_{\ c}\omega^c_{\ d}\Lambda^d_{\ b} + \Lambda^a_{\ b}\, \mathrm{d}(\Lambda^c_{\ d})\,, \tag{3.7}$$

where the the exterior derivative is defined as $\mathrm{d}\alpha = (p!)^{-1}\partial_\rho\alpha_{\mu_1\ldots\mu_p}\, \mathrm{d}x^\rho \wedge \mathrm{d}x^{\mu_1} \wedge \ldots \wedge \mathrm{d}x^{\mu_p}$ when acting on a p-form α. Therefore, we can define the exterior covariant derivative with respect to the Lorentz connection 1-form as a map $\nabla : \Omega^p(\mathcal{M}) \to \Omega^{p+1}(\mathcal{M})$ acting on a $(p,q)-$rank Lorentz tensor $A^{a_1\ldots a_p}{}_{b_1\ldots b_q} \in \Omega^p(\mathcal{M})$, as follows

$$\begin{aligned} \nabla A^{a_1\ldots a_p}{}_{b_1\ldots b_q} = \mathrm{d}A^{a_1\ldots a_p}{}_{b_1\ldots b_q} + \omega^{a_1}_{\ c_1} \wedge A^{c_1\ldots a_p}{}_{b_1\ldots b_q} + \ldots + \omega^{a_p}_{\ c_p} \wedge A^{a_1\ldots c_p}{}_{b_1\ldots b_q} \\ - \omega^{c_1}_{\ b_1} \wedge A^{a_1\ldots a_p}{}_{c_1\ldots b_q} - \ldots - \omega^{c_q}_{\ b_q} \wedge A^{a_1\ldots a_p}{}_{b_1\ldots c_q}, \end{aligned} \tag{3.8}$$

3.1.3. Curvature and Torsion 2-forms

Thus, the exterior covariant derivative transforms covariantly under local Lorentz transformations. Cartan noticed that the vielbein and the Lorentz connection 1-form could be used to define two essential objects in the context of gravitation: The curvature ($R^a_{\ b}$) and torsion (T^a) 2-forms, which can be expressed in terms of e^a and $\omega^a_{\ b}$ through the Cartan's structure equations,

$$R^a_{\ b} = \mathrm{d}\omega^a_{\ b} + \omega^a_{\ c} \wedge \omega^c_{\ b} = \frac{1}{2} R^a_{\ bcd} e^c \wedge e^d = \frac{1}{2} R^a_{\ b\mu\nu} \, \mathrm{d}x^\mu \wedge \mathrm{d}x^\nu \,, \tag{3.9}$$

$$T^a = \nabla e^a = \mathrm{d}e^a + \omega^a_{\ b} \wedge e^b = \frac{1}{2} T^a_{\ bc} e^b \wedge e^c = \frac{1}{2} T^a_{\ \mu\nu} \, \mathrm{d}x^\mu \wedge \mathrm{d}x^\nu \,. \tag{3.10}$$

By using the definition of the covariant derivative, it can be shown that these objects satisfy the following Bianchi identities,

$$\nabla R^a_{\ b} = 0, \qquad \nabla T^a = R^a_{\ b} \wedge e^b. \tag{3.11}$$

These two objects, the curvature and torsion, are essential within the framework of Cartan's theory of gravity as they encode the dynamics of the fundamental fields e^a and $\omega^a_{\ b}$. Furthermore, from (3.9) we can obtain an expression for the Riemann curvature tensor, $R^\alpha_{\ \beta\mu\nu} = E_a^{\ \alpha} e^b_{\ \beta} R^a_{\ b\mu\nu}$ and from (3.10) we can define the torsion tensor as $T^\alpha_{\ \mu\nu} = E_a^{\ \alpha} T^a_{\ \mu\nu}$. It is well known that the difference between two connections is a tensor, as we discussed during the derivation of the Einstein field equations ($\delta\Gamma^\alpha_{\ \beta\gamma}$ transform as a tensor). Therefore, we can define the *Levi-Civita* connection, denoted by $\tilde{\omega}^a_{\ b}$, as a torsionless connection,

$$\mathrm{d}e^a + \tilde{\omega}^a_{\ b} \wedge e^b = 0. \tag{3.12}$$

Then, we can construct the contorsion 1-form $K^a_{\ b}$ as the difference between the Lorentz and the Levi-Civita connections,

$$K^a_{\ b} = \omega^a_{\ b} - \tilde{\omega}^a_{\ b}. \tag{3.13}$$

Hence, we can decompose the curvature 2-form in a torsionless part plus a torsionful contribution,

$$R^a_{\ b} = \tilde{R}^a_{\ b} + \tilde{\nabla} K^a_{\ b} + K^a_{\ c} \wedge K^c_{\ b}, \tag{3.14}$$

where $\tilde{R}^a_{\ b} = \mathrm{d}\omega^a_{\ b} + \tilde{\omega}^a_{\ b} \wedge \tilde{\omega}^c_{\ b}$ and $\tilde{\nabla} K^a_{\ b} = \mathrm{d}K^a_{\ b} + \tilde{\omega}^a_{\ c} \wedge K^c_{\ b} - \tilde{\omega}^c_{\ b} \wedge K^a_{\ c}$. Moreover, we can also rewrite the torsion 2-form as $T^a = K^a_{\ b} \wedge e^b$. The Levi-Civita connection is determined by two conditions: The metricity condition (that implies $\omega_{ab} = -\omega_{ba}$) and the absence of torsion ($T^a = 0$). As a consequence of the latter, the torsion tensor becomes $T^{\mu}_{\ \alpha\beta} = (1/2)(\Gamma^{\mu}_{\ \alpha\beta} - \Gamma^{\mu}_{\ \beta\alpha}) = 0$, and then, when torsion vanishes, the Christoffel symbols are symmetric in their lower indices.

3.1.4. Einstein-Cartan Gravity

The 4D full Einstein-Cartan theory of gravity can be described by the action

$$S[e^a, \omega^{ab}, \Psi] = \frac{1}{2\kappa} \int \star(e_a \wedge e_a) \wedge \left(R^{ab} - \frac{\Lambda}{6} e^a \wedge e^b \right) + \int \mathcal{L}_{\text{matter}}[e^a, \omega^{ab}, \Psi] \tag{3.15}$$

where the Hodge dual is $\star(e^{a_1} \wedge \ldots \wedge e^{a_p}) = [(D-p)!]^{-1} \epsilon^{a_1 \ldots a_p}{}_{a_{p+1} \ldots a_D} e^{a_{p+1}} \wedge \ldots \wedge e^{a_D}$, Ψ describes matter fields, Λ is a cosmological constant and $R = R^{ab}{}_{ab}$ is the Ricci scalar. The first term is the Einstein-Hilbert action from GR. Thus, we can variate the action with respect to e^a, ω^{ab} and Ψ, obtaining the following field equations, respectively

$$\epsilon_{abcd} \left(R^{bc} - \frac{\Lambda}{3} e^b \wedge e^c \right) \wedge e^d = 2\kappa \tau_a, \tag{3.16a}$$

$$\epsilon_{abcd} T^c \wedge e^d = \kappa \sigma_{ab}, \tag{3.16b}$$

$$\frac{\delta \mathcal{L}_{\text{matter}}}{\delta \Psi} = 0, \tag{3.16c}$$

where $\tau_a \equiv \frac{\delta \mathcal{L}_{\text{matter}}}{\delta e^a}$ is the energy-momentum 3-form (the source of curvature), $\sigma_{ab} \equiv 2 \frac{\delta \mathcal{L}_{\text{matter}}}{\delta \omega^{ab}}$ is the spin density 3-form (the source of torsion) and the last line gives the equation of motion for the matter fields.

3.2. Bosonic 0-form coupled with gravity

According to the work of Alfaro & Riquelme [90], a bosonic field composed by a $(p-1)$-form and coupled to the spin connection of the Einstein-Cartan theory of gravity can become a non-trivial source of spacetime torsion and can provide new insights in the analysis of cosmic inflation. In particular, we will consider the action of gravity in the Einstein-Cartan formalism in the absence of a cosmological constant, given by Eq. (3.15), in the case $p = 1$ and with a matter Lagrangian of the form

$$\mathcal{L}_{\text{matter}} = -\frac{1}{2} \star (\nabla\phi_a) \wedge (\nabla\phi^a), \tag{3.17}$$

where ϕ_a is a SO(1,3)-valued 0-form, and the exterior covariant derivative is $\nabla = \mathrm{d} + [\omega, \ ]$, while d is the exterior derivative operator. The Einstein field equations given by Eq. (3.16a) becomes,

$$\star R^{ab} \wedge e_b = -\kappa \star \tau^a \tag{3.18}$$

where the energy-momentum 3-form, τ^a is given by,

$$\star \tau_i[e, \omega, \phi] = \frac{1}{2} F_{ai} \star F^a - \frac{1}{4} F_{ab} \epsilon^b{}_{fgi} F^a \wedge e^f \wedge e^g \tag{3.19}$$

where we defined $F^a \equiv \nabla\phi^a = \mathrm{d}\phi^a + \omega^a{}_b\phi^b$. Additionally, the matter field has an associated spin-torsion current 3-form, given by

$$\star \sigma_{ab}[e, \omega, \phi] = - \star F_{[a}\phi_{b]} = -\frac{1}{2}\Big(\star (\nabla\phi_a)\phi_b - \star(\nabla\phi_b)\phi_a \Big). \tag{3.20}$$

These both quantities satisfy on-shell conservation laws according to,

$$\delta_{\text{sym}} S[e, \omega, \phi] = \int \Big(\star \tau_a \wedge \delta e^a + \star\sigma_{ab} \wedge \delta\omega^{ab} \Big) = 0 \tag{3.21}$$

such that δ_{sym} could correspond to the Euclidean symmetry, i.e., $\delta_E e_a = \delta\epsilon_a{}^b e_b$, $\delta_E \omega^{ab} = -\nabla\delta\epsilon^{ab}$; or to the diffeomorphism symmetry, i.e., $\delta_{\text{diff}} e^a = -\mathcal{L}_\xi e^a$ and $\delta_{\text{diff}}\omega^{ab} = -\mathcal{L}_\xi \omega^{ab}$, where $\mathcal{L}_\xi$ stands for the Lie derivative. In the latter case, the conservation laws reduce to,

$$\nabla_\alpha \mathcal{T}^\alpha_\chi + \mathcal{T}^\alpha_\beta T^\beta_{\ \alpha\chi} + S^\lambda{}_{\alpha\beta} R^{\alpha\beta}_{\ \ \lambda\chi} = 0, \tag{3.22}$$

where $T^{\alpha}_{\beta\gamma}$ is the torsion tensor, $R^{\alpha}_{\beta\gamma\delta}$ is the Riemann tensor, $\mathcal{T}^{\alpha\beta}$ and $S^{\lambda}_{\ \alpha\beta}$ are the energy-momentum tensor and the spin tensor, respectively, defined as

$$\mathcal{T}^{i}_{k} = \star(e^i \wedge \star\tau_k) \tag{3.23}$$

$$S^{i}_{\ jk} = \star(e^i \wedge \star\sigma_{jk}) \tag{3.24}$$

The absence of spin and torsion in (3.22) reduces the conservation laws to the standard divergence-free energy-momentum tensor of general relativity. On the other hand, the equation of motion of the field ϕ^a is given by the variation of the action with respect to the field, i.e., (3.16c), and reads

$$\nabla \star F^a = \nabla \star \nabla\phi^a = 0, \tag{3.25}$$

which can be interpreted as a generalization of the Klein-Gordon equation for the 0-form field. By combining Eq. (3.10) with (3.16b), we obtain the following expression,

$$\nabla \star (e_a \wedge e_b) = -2\kappa \star \sigma_{ab}, \tag{3.26}$$

and as we can write the torsion 2-form in terms of the contorsion, i.e., $T^a = K^a_{\ b} \wedge e^b$, Eq. (3.16b) can also be written as,

$$\frac{1}{2}\epsilon_{ab}{}^{cd} K_c{}^f \wedge e_f \wedge e_d = -\kappa \star \sigma_{ab} = -\kappa \star \tilde{\sigma}_{ab} + \frac{\kappa}{2}\Big(\star (K_a{}^f \phi_f)\phi_b - \star(K_b{}^f \phi_f)\phi_a \Big), \tag{3.27}$$

where we defined the torsionless contribution to τ_{ab} as follows,

$$\star\, \tilde{\sigma}_{ab} \equiv -\frac{1}{2}\Big(\star (\tilde{\nabla}\phi_a)\phi_b - \star(\tilde{\nabla}\phi_b)\phi_a \Big), \tag{3.28}$$

and where $\tilde{(\cdot)}$ will stand for Riemannian quantities that depend only on the torsion-free Levi-Civita spin connection $\tilde{\omega}^{ab}$. On the other hand, according to Ref. [90], the matter action can also be decomposed in a torsion-free part and other contribution due to interactions of the ϕ^a field,

$$S_{\text{matter}}[e,\omega,\phi] = -\frac{1}{2}\int \star(\nabla\phi_a)\wedge(\nabla\phi^a) = -\frac{1}{2}\int \star\tilde{F}_a\wedge\tilde{F}^a + \frac{1}{2\kappa}\int \star(e_a\wedge e_b)\wedge K^a{}_d\wedge K^{db}$$
$$+\frac{1}{2}\int \star K_a{}^f\wedge K^a{}_d\,\phi_f\phi^d \tag{3.29}$$

By taking the Hodge dual to Eq. (3.27), such that $\star\star\,\omega_p = (-1)^{p(n-p)}\omega_p$, we get

$$\frac{1}{2}\epsilon_{abcd}K_{clj}\epsilon_{ijld} - \frac{\kappa}{2}\{K_{ali}\phi_b\phi_l - K_{bli}\phi_a\phi_l\} - \kappa\tau_{abi} = 0, \tag{3.30}$$

where $(\star\star\,\tilde{\tau}_{ab})_i e^i \equiv \tau_{abi}e^i$, $K_{abi} = -K_{bai}$ and $\tau_{abi} = -\tau_{bai}$. Let us consider the following notation: Let $A_{ijk\ldots rst}$ be a generic tensor field. From now on we will call it $A_{ijk\ldots rst} \equiv A(i,j,k,\ldots,r,s,t)$. In this manner we will shorten the notation for objects like $A_{ijk\ldots rst}\varphi_i \equiv A(\varphi,j,k,\ldots,r,s,t)$ where $\varphi_i \equiv \varphi(i)$ is a generic vector field. Therefore, the equation (3.30) becomes,

$$\frac{1}{2}K(\phi,a,i)\phi(b)\kappa - \frac{1}{2}K(\phi,b,i)\phi(a)\kappa + \frac{1}{2}K(a,i,b) - \frac{1}{2}K(a,l,l)d(b,i)$$
$$-\frac{1}{2}K(b,i,a) + \frac{1}{2}K(b,l,l)d(a,i) = \kappa\tau(a,b,i), \tag{3.31}$$

where we also denote $d(a,b)\equiv\delta_{ab}$. The explicit solution of the above algebraic equation for the contorsion reads,

$$\begin{aligned}
K(a,b,i) &= \kappa\tau(a,b,i) + \kappa\tau(a,i,b) - \kappa\tau(b,i,a) + \kappa^2\phi(i)\tau(a,b,\phi)\\
&+ \frac{\kappa^2}{[1-\kappa\phi^2]}\Big\{\phi(a)\tau(\phi,b,i) + \phi(a)\tau(\phi,i,b) - \phi(b)\tau(\phi,a,i) - \phi(b)\tau(\phi,i,a)\Big\}\\
&+ \frac{2\kappa}{[2-\kappa\phi^2]}d(b,i)\Big\{\kappa\tau(\phi,a,\phi) - \frac{\kappa[2-\kappa^2\phi^4]}{[1-\kappa\phi^2][2+\kappa\phi^2]}\phi(a)\tau(\phi,l,l) - [1-\kappa\phi^2]\tau(a,l,l)\Big\}\\
&- \frac{2\kappa}{[2-\kappa\phi^2]}d(a,i)\Big\{\kappa\tau(\phi,b,\phi) - \frac{\kappa[2-\kappa^2\phi^4]}{[1-\kappa\phi^2][2+\kappa\phi^2]}\phi(b)\tau(\phi,l,l) - [1-\kappa\phi^2]\tau(b,l,l)\Big\}\\
&+ \frac{\kappa^2}{[2-\kappa\phi^2]}\phi(b)\phi(i)\Big\{\frac{\kappa^2\phi^2}{[1-\kappa\phi^2]}\tau(\phi,a,\phi) - 2\tau(a,l,l)\Big\}\\
&- \frac{\kappa^2}{[2-\kappa\phi^2]}\phi(a)\phi(i)\Big\{\frac{\kappa^2\phi^2}{[1-\kappa\phi^2]}\tau(\phi,b,\phi) - 2\tau(b,l,l)\Big\}.
\end{aligned} \tag{3.32}$$

In summary, the full gravitational action is given by,

$$
\begin{aligned}
S_{\text{total}}[e,\tilde{\omega},\phi] = &-\frac{1}{2\kappa}\int \star(e_a\wedge e_b)\wedge \tilde{R}^{ab} - \frac{1}{2}\int \star\tilde{F}_a\wedge\tilde{F}^a + \frac{1}{2\kappa}\int \star(e_a\wedge e_b)\wedge K^a{}_d\wedge K^{db} \\
&+ \frac{1}{2}\int \star K_a{}^f\wedge K^a{}_d\,\phi_f\phi^d \\
=& \; S_G[e,\tilde{\omega}] + S_{\text{M}}[e,\tilde{\omega},\phi] + S_{\text{int}}[e,\tilde{\omega},\phi],
\end{aligned}
\tag{3.33}
$$

The first two terms are Riemannian. The other two are torsional contributions which depend upon the contorsion one-form and through (3.32) they generate a highly non-trivial (self)-interaction potential for the ϕ^a field. In fact, the interactive part of the action, namely,

$$
S_{\text{int}}[e,\tilde{\omega},\phi] = \frac{1}{2\kappa}\int \star(e_a\wedge e_b)\wedge K^a{}_d\wedge K^{db} + \frac{1}{2}\int \star K_a{}^f\wedge K^a{}_d\,\phi_f\phi^d \tag{3.34}
$$

produces, at least at first order in κ, an interaction lagrangian given by,

$$
\begin{aligned}
\mathcal{L}^{(1)}_{\text{int}} &= \kappa\tau_{ab}{}^b\tau^{ac}{}_c - \frac{1}{2}\kappa\tau_{abc}\tau^{abc} + \kappa\tau_{abc}\tau^{bca} \\
&= -\frac{1}{2}\kappa\phi^\mu\phi^\nu\tilde{D}_\mu\phi_\nu\tilde{D}_\rho\phi^\rho + \frac{1}{2}\kappa\phi^\mu\phi^\nu\tilde{D}_\mu\phi^\rho\tilde{D}_\rho\phi_\nu + \frac{1}{4}\kappa\phi^\mu\phi^\nu\tilde{D}_\rho\phi_\mu\tilde{D}^\rho\phi_\nu \\
&\quad + \frac{1}{4}\kappa\phi^2\tilde{D}_\mu\phi^\mu\tilde{D}_\nu\phi^\nu - \frac{1}{4}\kappa\phi^2\tilde{D}_\mu\phi_\nu\tilde{D}^\mu\phi^\nu - \frac{1}{4}\kappa\phi^2\tilde{D}_\mu\phi_\nu\tilde{D}^\nu\phi^\mu,
\end{aligned}
\tag{3.35}
$$

3.3. A bosonic 0-form as the Inflaton

Let us consider that this bosonic 0-form previously discussed will be the inflaton field at the primordial epoch. The interaction part of the action can be enclosed in a certain potential $V(a,\phi)$. Thus, the action can be written as a combination between the torsion-free gravitational action and the matter action as follows,

$$
S = S_{\text{G}} + S_{\text{matter}}, \tag{3.36}
$$

where all the torsional contributions are enclosed in the potential such that,

$$
S_{\text{matter}} = \int \mathrm{d}^4x\,\sqrt{-g}\mathcal{L}_m = \int \mathrm{d}^4x\,\sqrt{-g}\Big(\frac{1}{2}\tilde{D}_\mu\phi_\nu\tilde{D}^\mu\phi^\nu - V(a,\phi^\mu)\Big). \tag{3.37}
$$

In this action $\tilde{D}_\mu \phi_\nu = \partial_\mu \phi_\nu - \tilde{\Gamma}^\sigma{}_{\mu\nu}\phi_\sigma$, is the covariant derivative, such that $\tilde{\Gamma}^\sigma{}_{\mu\nu}$ are the components of the Christoffel symbols in torsion-less general relativity. We can expand them as,

$$\tilde{D}_\mu \phi_\nu = \partial_\mu \phi_\nu - \tilde{\Gamma}^\sigma{}_{\mu\nu}\phi_\sigma = \partial_\mu \phi_\nu - \tilde{\Gamma}^0{}_{\mu\nu}\phi_0 - \tilde{\Gamma}^i{}_{\mu\nu}\phi_i \tag{3.38}$$

where Greek indices (μ,ν,σ,...) are reserved to 4D spacetime components, while Latin indices (i, j, k,...) refer to 3D spatial components. The non-zero Christoffel symbols for the FLRW metric, i.e., $g_{\mu\nu} = \mathrm{diag}(1, -a^2, -a^2, -a^2)$, are given by

$$\tilde{\Gamma}^i{}_{0j} = H\delta^i{}_j, \qquad \tilde{\Gamma}^0{}_{ij} = a^2 H\delta_{ij}. \tag{3.39}$$

Thus, the matter Lagrangian can be expanded as follows,

$$\begin{aligned}
\mathcal{L}_m &= \frac{1}{2} g^{\mu\alpha} g^{\nu\beta} (\tilde{D}_\mu \phi_\nu)(\tilde{D}_\alpha \phi_\beta) - V(a, \phi^\mu) \\
&= \frac{1}{2} g^{00} g^{\nu\beta} (\tilde{D}_0 \phi_\nu)(\tilde{D}_0 \phi_\beta) + \frac{1}{2} g^{ij} g^{\nu\beta} (\tilde{D}_i \phi_\nu)(\tilde{D}_j \phi_\beta) - V(a, \phi^\mu)
\end{aligned}$$

The temporal and spatial components of the covariant derivatives are decomposed as,

$$\tilde{D}_0 \phi_\nu = \partial_0 \phi_\nu - \tilde{\Gamma}^0{}_{0\nu}\phi_0 - \tilde{\Gamma}^i{}_{0\nu}\phi_i = \partial_0 \phi_\nu - \tilde{\Gamma}^i{}_{0\nu}\phi_i \tag{3.40}$$

$$\tilde{D}_i \phi_\nu = \partial_i \phi_\nu - \tilde{\Gamma}^0{}_{i\nu}\phi_0 - \tilde{\Gamma}^j{}_{i\nu}\phi_j = -\tilde{\Gamma}^0{}_{i\nu}\phi_0 - \tilde{\Gamma}^j{}_{i\nu}\phi_j \tag{3.41}$$

Therefore, inserting these expressions into the Lagrangian reads,

$$
\begin{aligned}
\mathcal{L}_m &= \frac{1}{2}g^{\nu\beta}(\partial_0\phi_\nu - \tilde{\Gamma}^i{}_{0\nu}\phi_i)(\partial_0\phi_\beta - \tilde{\Gamma}^i{}_{0\beta}\phi_i) - \frac{1}{2a^2}\delta^{ij}g^{\nu\beta}(\tilde{\Gamma}^0{}_{i\nu}\phi_0 + \tilde{\Gamma}^l{}_{i\nu}\phi_l)(\tilde{\Gamma}^0{}_{j\beta}\phi_0 + \tilde{\Gamma}^l{}_{j\beta}\phi_l) - V \\
&= \frac{1}{2}g^{00}(\partial_0\phi_0 - \tilde{\Gamma}^i{}_{00}\phi_i)(\partial_0\phi_0 - \tilde{\Gamma}^i{}_{00}\phi_i) - \frac{1}{2a^2}\delta^{mn}(\partial_0\phi_m - \tilde{\Gamma}^i{}_{0m}\phi_i)(\partial_0\phi_n - \tilde{\Gamma}^i{}_{0n}\phi_i) \\
&\quad - \frac{1}{2a^2}\delta^{ij}g^{00}(\tilde{\Gamma}^0{}_{i0}\phi_0 + \tilde{\Gamma}^l{}_{i0}\phi_l)(\tilde{\Gamma}^0{}_{j0}\phi_0 + \tilde{\Gamma}^l{}_{j0}\phi_l) \\
&\quad + \frac{1}{2a^4}\delta^{ij}\delta^{mn}(\tilde{\Gamma}^0{}_{im}\phi_0 + \tilde{\Gamma}^l{}_{im}\phi_l)(\tilde{\Gamma}^0{}_{jn}\phi_0 + \tilde{\Gamma}^l{}_{jn}\phi_l) - V \\
&= \frac{\dot{\phi}_0^2}{2} - \frac{1}{2a^2}\delta^{mn}\Big[\dot{\phi}_m\dot{\phi}_n - \tilde{\Gamma}^i{}_{0n}\phi_i\dot{\phi}_m - \tilde{\Gamma}^i{}_{0m}\phi_i\dot{\phi}_n + \tilde{\Gamma}^i{}_{0m}\tilde{\Gamma}^k{}_{0n}\phi_i\phi_k\Big] \\
&\quad - \frac{1}{2a^2}\delta^{ij}\Big[\tilde{\Gamma}^l{}_{i0}\phi_l\tilde{\Gamma}^k{}_{j0}\phi_k\Big] + \frac{1}{2a^4}\delta^{ij}\delta^{mn}\Big[\tilde{\Gamma}^0{}_{im}\phi_0\tilde{\Gamma}^0{}_{jn}\phi_0\Big] - V \\
&= \frac{\dot{\phi}_0^2}{2} - \frac{1}{2a^2}\delta^{mn}\Big[\dot{\phi}_m\dot{\phi}_n - H\delta^i{}_n\phi_i\dot{\phi}_m - H\delta^i{}_m\phi_i\dot{\phi}_n + H^2\delta^i{}_m\delta^k{}_n\phi_i\phi_k\Big] \\
&\quad - \frac{1}{2a^2}\delta^{ij}[H^2\delta^l{}_i\phi_l\delta^k{}_j\phi_k] + \frac{1}{2a^4}\delta^{ij}\delta^{mn}\Big[a^4H^2\phi_0^2\delta_{im}\delta_{jn}\Big] - V \\
&= \frac{\dot{\phi}_0^2}{2} - \frac{1}{2a^2}\delta^{mn}\Big[\dot{\phi}_m\dot{\phi}_n - H\phi_n\dot{\phi}_m - H\phi_m\dot{\phi}_n + 2H^2\phi_m\phi_n\Big] + \frac{3}{2a^4}\Big[a^4H^2\phi_0^2\Big] - V \\
&= \frac{1}{2}\left[\dot{\phi}_0^2 - \frac{\dot{\phi}_i\dot{\phi}^i}{a^2}\right] + \frac{H}{a^2}\dot{\phi}_i\phi^i + \frac{H^2}{2}\left[3\phi_0^2 - 2\frac{\phi_i\phi^i}{a^2}\right] - V \\
\mathcal{L}_m &= \frac{1}{2}\left[\dot{\phi}_0^2 - \frac{\dot{\phi}_i\dot{\phi}^i}{a^2}\right] + \frac{\dot{a}}{a^3}\dot{\phi}_i\phi^i + \frac{\dot{a}^2}{2a^2}\left[3\phi_0^2 - 2\frac{\phi_i\phi^i}{a^2}\right] - V
\end{aligned}
$$

where we denoted $\phi_i\phi^i = \delta^{ij}\phi_i\phi_j = \sum_{i=1}^3 \phi_i^2$, and similarly for $\dot{\phi}_i\dot{\phi}^i$. We will consider that the entire contribution to the potential V comes from $\mathcal{L}_{\text{int}}$. By developing a similar expansion in Eq. (3.35), we can show that

$$
\mathcal{L}_{\text{int}} = \kappa H^2\left(3\phi_0^2\frac{\phi_i\phi^i}{a^2} - \frac{9}{2}\phi_0^4 - \frac{(\phi_i\phi^i)^2}{4a^4}\right) + \mathcal{O}\Big(\phi_a\dot{\phi}^a H, \dots\Big) = -V, \tag{3.42}
$$

where we neglected mixed terms that coupled derivatives of fields with fields for simplicity. As the Lagrangian is explicitly invariant under rotations of the ϕ^i field, we can introduce the following expansion,

$$\phi_1 = \phi_r a \sin(\theta)\cos(\varphi) \tag{3.43}$$

$$\phi_2 = \phi_r a \sin(\theta)\sin(\varphi) \tag{3.44}$$

$$\phi_3 = \phi_r a \cos(\theta) \tag{3.45}$$

such that,

$$\phi_r^2 \equiv \frac{\phi_i \phi^i}{a^2}. \tag{3.46}$$

Thus, the kinetic term becomes,

$$\frac{\dot{\phi}_i \dot{\phi}^i}{a^2} = \dot{\phi}_r^2 + \phi_r^2[\dot{\theta}^2 + \dot{\varphi}^2 \sin^2(\theta) - H^2] + 2H\frac{\dot{\phi}_i \phi^i}{a^2} \tag{3.47}$$

Therefore, the Lagrangian acquire the following form,

$$\mathcal{L}_m = \frac{1}{2}\Big[\dot{\phi}_0^2 - \dot{\phi}_r^2 - \phi_r^2(\dot{\theta}^2 + \dot{\varphi}^2 \sin^2(\theta) + H^2) + 3H^2\phi_0^2\Big] - V \tag{3.48}$$

Since φ is a cyclical coordinate, the canonical momenta related to the φ variable is conserved,

$$p_\varphi = \frac{\partial \mathcal{L}_m}{\partial \dot{\varphi}} = -\phi_r^2 \dot{\varphi} \equiv \ell = \text{constant} \tag{3.49}$$

Thus, due to the explicit spherical symmetry, and without loss of generality, we can set the coordinates in such a way that $\theta = \pi/2$. Hence, the Lagrangian reduces to,

$$\mathcal{L}_m = \frac{1}{2}\Big[\dot{\phi}_0^2 - \dot{\phi}_r^2\Big] - v = \frac{1}{2}G_{ab}\dot{\Phi}^a\dot{\Phi}^b - v(H, \Phi^a), \tag{3.50}$$

where

$$v = \frac{\ell^2}{2\phi_r^2} - \frac{1}{4}\left(\frac{H}{M_{\rm Pl}}\right)^2\Big[12\phi_0^2\phi_r^2 - 18\phi_0^4 - \phi_r^4\Big] - \frac{H^2}{2}(3\phi_0^2 - \phi_r^2) \tag{3.51}$$

$$\Phi^a = (\phi^0, \phi^r), \tag{3.52}$$

and the components of field-space metric are given by,

$$[G_{ab}] = \begin{pmatrix} 1 & 0 \\ 0 & -1 \end{pmatrix} \tag{3.53}$$

Here, we can notice two critical features of this model: The first is that the field-space metric is flat (actually is a 2D version of the Minkowski metric). The second feature is that the potential v depends not only on the fields Φ^a, but the interaction terms also depend on the Hubble parameter H. This coupling comes from the torsionful contribution of the action and is the main consequence of considering the bosonic 0-form as the inflaton.

On the other hand, the components of the energy-momentum tensor can be computed in the standard way, i.e., from Eq. (1.22),

$$T_{\mu\nu} = -\frac{2}{\sqrt{-g}}\frac{\delta(\sqrt{-g}\mathcal{L}_m)}{\delta g^{\mu\nu}} = G_{ab}\partial_\mu\Phi^a\partial_\nu\Phi^b - g_{\mu\nu}\left[\frac{1}{2}G_{ab}g^{\rho\sigma}\partial_\rho\Phi^a\partial_\sigma\Phi^b - v\right] \tag{3.54}$$

We define the energy density, ρ, as the 00 component of $T_{\mu\nu}$,

$$T_{00} = \frac{1}{2}G_{ab}\dot{\Phi}^a\dot{\Phi}^b + v \equiv \rho \tag{3.55}$$

and the isotropic pressure, P, as following,

$$T_{ij} = -g_{ij}\left[\frac{1}{2}G_{ab}\dot{\Phi}^a\dot{\Phi}^b - v\right] \equiv -g_{ij}P \tag{3.56}$$

The background equations of motion for the scalar fields can be obtained from the continuity equation, i.e, the $\nu = 0$ component of the energy-momentum tensor conservation $T^{\mu\nu}_{\ ;\mu} = 0$,

$$D_t\dot{\Phi}^a + 3H\dot{\Phi}^a + G^{ab}v_{,b} = 0 \tag{3.57}$$

where we define D_t as,

$$D_t\dot{\Phi}^a = \frac{\mathrm{d}\dot{\phi}^a}{\mathrm{d}t} + \bar{\Gamma}^a_{\ bc}\dot{\Phi}^b\dot{\Phi}^c. \tag{3.58}$$

Since G_{ab} is constant, the Christoffel symbols of the field-space metric, i.e., $\bar{\Gamma}^a{}_{bc}$, are identically zero, and the EoM becomes

$$\ddot{\Phi}_a + 3H\dot{\Phi}_a + v_{,a} = 0, \tag{3.59}$$

which is fully consistent with the Klein-Gordon equation for the matter fields Φ^a that comes from the Euler-Lagrange procedure in curved spacetime,

$$\frac{\partial \mathcal{L}_m}{\partial \Phi^a} = \frac{1}{\sqrt{-g}}\partial_\mu\left(\sqrt{-g}\frac{\partial \mathcal{L}_m}{\partial(\partial_\mu \Phi^a)}\right). \tag{3.60}$$

3.4. Two-Field Inflation and the Slow-Roll Approximation

3.4.1. Slow-Roll Conditions

Since the curvature contribution in Einstein-Cartan gravity reduces to the Einstein-Hilbert action of GR, see Eq. (3.33), we can write the full action of the inflationary model as follows,

$$S = \int \mathrm{d}^4x\,\sqrt{-g}\left(\frac{R}{2\kappa} + \mathcal{L}_m\right) \tag{3.61}$$

The variation of this action with respect to the metric $g^{\mu\nu}$ reduces to the Standard Einstein Field equations,

$$R_{\mu\nu} - \frac{1}{2}g_{\mu\nu}R = \kappa T_{\mu\nu}, \tag{3.62}$$

where $T_{\mu\nu}$ is given by equation (3.54). We can combine the 00 and ij components of the Field equations to find the Friedmann equations,

$$H^2 = \frac{8\pi G}{3}\left[\frac{1}{2}\dot{\Phi}^2 + v(H,\Phi^a)\right] \tag{3.63}$$

$$\dot{H} = -4\pi G\dot{\Phi}^2 \tag{3.64}$$

where $\dot{\Phi}^2 = G_{ab}\dot{\Phi}^a\dot{\Phi}^b = \dot{\phi}_0^2 - \dot{\phi}_r^2$. Replacing the expression of the effective potential, the first Friedmann equation becomes,

$$H^2 = \frac{8\pi G}{3}\left[\frac{\frac{1}{2}\dot{\Phi}^2 + \frac{\ell^2}{2\phi_r^2}}{1 + M_{\mathrm{Pl}}^{-4}\left(\phi_0^2\phi_r^2 - \frac{3}{2}\phi_0^4 - \frac{1}{3}\phi_r^4\right) + M_{\mathrm{Pl}}^{-2}\left(\frac{\phi_0^2}{2} - \frac{\phi_r^2}{6}\right)}\right] \tag{3.65}$$

In order to generalize the slow-roll approximation, we can define the first slow-roll parameter and, as usual, using the Friedmann and the Klein-Gordon equations,

$$\epsilon \equiv -\frac{\dot{H}}{H^2} = \frac{\frac{8\pi G}{2}\dot{\Phi}^2}{\frac{8\pi G}{3}\left[\frac{\frac{1}{2}\dot{\Phi}^2+\frac{\ell^2}{2\phi_r^2}}{1+M_{\rm Pl}^{-4}\left(\phi_0^2\phi_r^2-\frac{3}{2}\phi_0^4-\frac{1}{3}\phi_r^4\right)+M_{\rm Pl}^{-2}\left(\frac{\phi_0^2}{2}-\frac{\phi_r^2}{6}\right)}\right]} \tag{3.66}$$

Therefore, the slow-roll condition necessary for inflation to occur, i.e., $\epsilon \ll 1$, becomes

$$\dot{\Phi}^2 \ll \frac{\ell^2}{\phi_r^2}\frac{1}{3f-1} \sim \frac{\ell^2}{\phi_r^2}\frac{1}{f}, \tag{3.67}$$

where $f \equiv 1 + M_{\rm Pl}^{-4}\left(\phi_0^2\phi_r^2 - \frac{3}{2}\phi_0^4 - \frac{1}{3}\phi_r^4\right) + M_{\rm Pl}^{-2}\left(\frac{\phi_0^2}{2} - \frac{\phi_r^2}{6}\right)$. Thus, H^2 reduces to

$$H^2 \approx \frac{8\pi G}{3}\left[\frac{\frac{\ell^2}{2\phi_r^2}}{1 + M_{\rm Pl}^{-4}\left(\phi_0^2\phi_r^2 - \frac{3}{2}\phi_0^4 - \frac{1}{3}\phi_r^4\right) + M_{\rm Pl}^{-2}\left(\frac{\phi_0^2}{2} - \frac{\phi_r^2}{6}\right)}\right] = \frac{8\pi G}{3}V_{\rm eff} \tag{3.68}$$

The slow-roll condition becomes $\dot{\Phi}^2 \ll V_{\rm eff}$ when in the above equation we defined the effective potential, sketched in Fig. 3.1, as

$$V_{\rm eff} \approx \frac{\frac{\ell^2}{2\phi_r^2}}{1 + M_{\rm Pl}^{-4}\left(\phi_0^2\phi_r^2 - \frac{3}{2}\phi_0^4 - \frac{1}{3}\phi_r^4\right) + M_{\rm Pl}^{-2}\left(\frac{\phi_0^2}{2} - \frac{\phi_r^2}{6}\right)} \tag{3.69}$$

3.4.2. Multifield Inflation Formalism

In order to analyze the second slow-roll parameter, we will use the geometrical convention of Refs. [91] and [92] from now on. In this interpretation, we can consider the scalar fields Φ^a as a coordinate of a real manifold $\mathcal{M}$ on which the metric G_{ab} is defined. Thus, we define a vector $\mathbf{A} = A^a$ in the tangent space $T_p\mathcal{M}$ at a point $p \in \mathcal{M}$ if it transforms as $A^a \to \bar{A}^a = X^a{}_{,b}A^b$, where the comma denotes differentiation with respect to the coordinates. On the other hand, the cotangent space is the dual of the tangent space an its elements are linear operators on the tangent space: ${}^*\mathbf{C} : T_p\mathcal{M} \to \mathbb{R}$, so C_aA^a is a scalar object. We can use G_{ab} to construct a cotangent vector from a tangent vector $\mathbf{A}$, i.e., $(\mathbf{A}^\dagger) = A^bG_{ba}$. Besides, with the metric we can introduce an inner product of two vectors and the corresponding

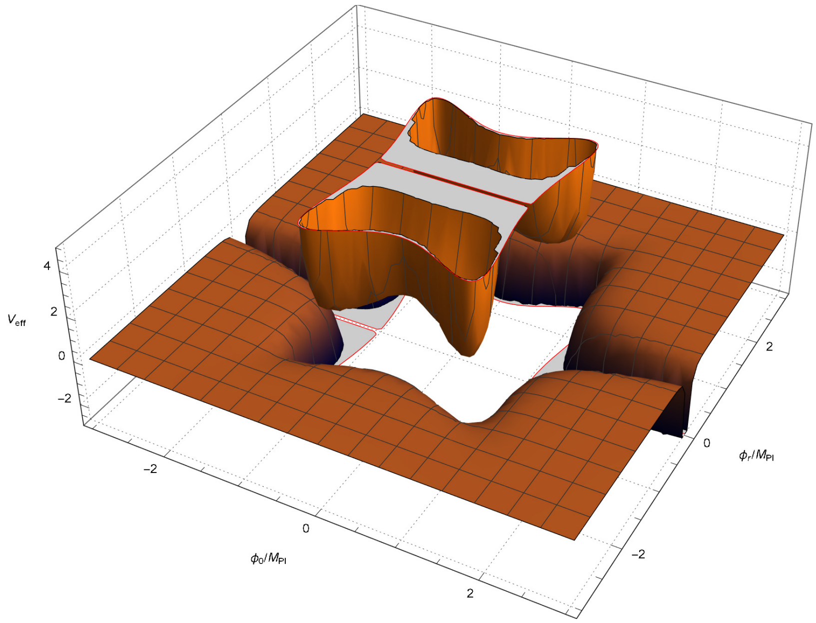

FIGURE 3.1. Tridimensional plot of the effective potential V_{eff} in terms of ϕ_0 and ϕ_r, and normalized by M_{Pl}.

norm,

$$\mathbf{A}\cdot\mathbf{B} = \mathbf{A}^{\dagger}\mathbf{B} = \mathbf{A}^{T}\mathbf{G}\mathbf{B} = A^{a}G_{ab}B^{b}, \qquad |\mathbf{A}| = \sqrt{\mathbf{A}\cdot\mathbf{A}}, \tag{3.70}$$

while the Hermitian conjugate of a linear operator $\mathbf{L} : T_p\mathcal{M} \to T_p\mathcal{M}$ is defined by satisfying $\mathbf{L}^{\dagger} = \mathbf{G}^{-1}\mathbf{L}^{T}\mathbf{G}$. Thus, an Hermitian operator satisfies $\mathbf{H}^{\dagger} = \mathbf{H}$.

We can also define two different types of derivatives. The first one is the covariant derivative on the manifold, that we will denote by $\nabla_b A^a = A^a{}_{,b} + \Gamma^a{}_{bc}A^c$ when it is acting on a vector, and $\nabla V = V_{,a}$ when acting on a scalar. Conversely, we will define the covariant derivative on spacetime dependent tangent vectors as $\mathcal{D}_\mu A^a = \partial_\mu A^a + \Gamma^a{}_{bc}\partial_\mu\phi^b A^c$. Then, since Φ is the time-dependent scalar field background, we will denote the derivatives of $\mathbf{\Phi}$ as,

$$\mathbf{\Phi}^{(1)} = \dot{\mathbf{\Phi}} = \frac{\mathrm{d}\mathbf{\Phi}}{\mathrm{d}t}, \qquad \mathbf{\Phi}^{(n)} = \mathcal{D}_t^{(n-1)}\dot{\mathbf{\Phi}} \quad \text{for } n \leq 2. \tag{3.71}$$

As the vectors $\mathbf{\Phi}^{(1)}$ (the velocity) and $\mathbf{\Phi}^{(2)}$ (the acceleration) do not point in the same direction, we can generate a set of orthonormal unit vectors $\mathbf{e}_1, \ldots, \mathbf{e}_n$ through a Gram-Schmidt procedure from a vector $\mathbf{\Phi}^{(n)}$. By taking the projector $\mathbf{P}_0^{\perp} = \mathbb{I}$, then,

$$\Phi_n^{(n)} = \left|\mathbf{P}_{n-1}^{\perp}\mathbf{\Phi}^{(n)}\right|, \quad \mathbf{e}_n = \frac{\mathbf{P}_{n-1}^{\perp}\mathbf{\Phi}^{(n)}}{\Phi_n^{(n)}}, \quad \mathbf{P}_n = \mathbf{e}_n\mathbf{e}_n^{\dagger}, \qquad \mathbf{P}_n^{\perp} = \mathbb{I} - \sum_{q=1}^{n}\mathbf{P}_q. \tag{3.72}$$

With all these considerations, we can write the slow-roll parameters as follows,

$$\epsilon(\mathbf{\Phi}) \equiv -\frac{\dot{H}}{H^2}, \quad \boldsymbol{\eta}(\mathbf{\Phi}) \equiv \frac{\mathbf{\Phi}^{(2)}}{H\left|\dot{\mathbf{\Phi}}\right|}. \tag{3.73}$$

Consequently, we specify the components of the second slow-roll parameter in terms of the unit vectors $\mathbf{e}_1$ and $\mathbf{e}_1$,

$$\eta^{\parallel} = \mathbf{e}_1 \cdot \boldsymbol{\eta} = \frac{(\mathcal{D}_t\dot{\mathbf{\Phi}}) \cdot \dot{\mathbf{\Phi}}}{H\left|\dot{\mathbf{\Phi}}\right|^2} = \frac{\ddot{\Phi}_a\dot{\Phi}^a}{H\dot{\Phi}^2}, \qquad \eta^{\perp} = \mathbf{e}_2 \cdot \boldsymbol{\eta} = \frac{\left|(\mathcal{D}_t\dot{\mathbf{\Phi}})^{\perp}\right|}{H\left|\dot{\mathbf{\Phi}}\right|} = \frac{\left|\ddot{\Phi}^{\perp}\right|}{H\left|\dot{\Phi}\right|}, \tag{3.74}$$

where in the last equalities we used that in our case G_{ab} is a constant metric, so $\mathcal{D}_t = \mathrm{d}/\mathrm{d}t$. In order to simplify the numerical analysis, we introduce the number of e-folds N as a new time variable, i.e, $\mathrm{d}N = H\,\mathrm{d}t$, following the formalism developed in Ref. [93]. We will denote $(\cdot)'$ as the derivative with respect to N. Hence, the exact form of the first slow-roll parameter can be written as,

$$\epsilon = -\frac{\dot{H}}{H^2} \;\rightarrow\; \epsilon(N) = -[\ln(H)]'. \tag{3.75}$$

As the time derivative of ϵ can be expressed as,

$$\dot{\epsilon} = \frac{\mathrm{d}}{\mathrm{d}t}\left(-\frac{\dot{H}}{H^2}\right) = 2\frac{\dot{H}^2}{H^3} - \frac{\ddot{H}}{H^2} = 2\epsilon^2 H + 8\pi G\frac{\dot{\Phi}_a\ddot{\Phi}^a}{H^2} = 2\epsilon H(\epsilon + \eta^{\parallel}), \tag{3.76}$$

we can write $\eta^{\parallel}$ in terms of N as follows,

$$\eta^{\parallel}(N) = \frac{\epsilon'(N)}{2\epsilon(N)} - \epsilon(N). \tag{3.77}$$

Furthermore, if we define $\boldsymbol{\eta}_N \equiv \boldsymbol{\Phi}'' = \boldsymbol{\eta} - \epsilon\, \mathrm{e}_1$, the equation of motion (3.57) becomes

$$\boldsymbol{\Phi}' + \boldsymbol{\nabla}^\dagger \ln(V_{\text{eff}}) = -\frac{\boldsymbol{\eta}_N}{3-\epsilon}. \tag{3.78}$$

Therefore, the slow-roll condition now takes the form $\epsilon \ll 1$ and $\left|\eta^{\parallel}\right| \ll 1$, and since in our case we will naturally have $\left|\eta^{\perp}\right| \sim 0$, the above equation reduces to,

$$\boldsymbol{\Phi}' = -\boldsymbol{\nabla}^\dagger \ln(V_{\text{eff}}). \tag{3.79}$$

Consequently, by solving the differential equation (3.79) for certain initial conditions, we can find $\Phi^a(N)$. Thus, we can evaluate $H(N) = \sqrt{V_{\text{eff}}/3M_{\text{Pl}}^2}$ and directly compute $\epsilon(N)$ from Eq. (3.75), and then, $\eta^{\parallel}(N)$ from Eq. (3.77).

3.4.3. Numerical Analysis

To start, we will consider a well-known model to have a proper comparison with known results. Let us consider the double quadratic potential $V(\chi_1, \chi_2) = m^2(\chi_1^2/2 + \chi_2^2/2)$ with canonical kinetical terms, i.e., $G^{\chi}_{ab} = \delta_{ab}$. By considering an initial condition such that $\chi_1(60) = \chi_2(60)$, we can solve the differential equation (3.79), reproducing the results of Ref. [93], and obtaining the plot of Fig. 3.2. The value of N in the next plots represents the number of e-folds before the end of inflation.

We observe that the slow-roll parameters for the double quadratic potential have a good behavior during 50+ e-folds before the end of inflation, and the slow-roll conditions $\epsilon \ll 1$ and $\left|\eta^{\parallel}\right| \ll 1$ break precisely at the end of the inflationary epoch, just as we discussed in previous models of inflation.

Now, we turn on the discussion of our inflationary model, described by an effective potential given by (3.69) and a space-field metric $G_{ab} = \mathrm{diag}(1, -1)$. It is important to state that the dynamics of the fields are highly dependent on the value of the initial conditions. In fact, for several different combinations, the evolution of the fields and the inflationary parameters are quite unstable and, in some cases, give negative or imaginary values for the quantities. We found a special combination of initial conditions that bring well-behaved dynamics to the fields, as we show in Fig. 3.4a. Both fields have an almost constant but

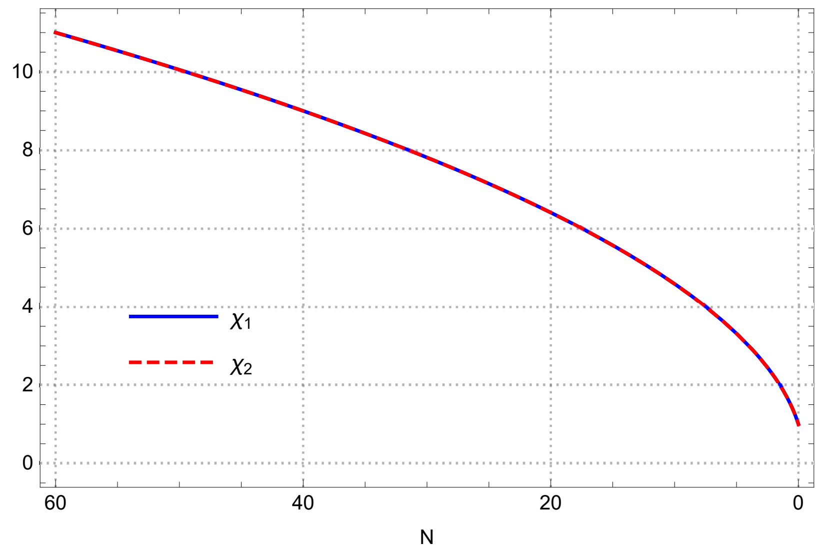

FIGURE 3.2. The numerical solution for $\chi_{1,2}$ for the double quadratic potential in the slow-roll approximation. Both fields have the same solution over 60 e-folds of inflation.

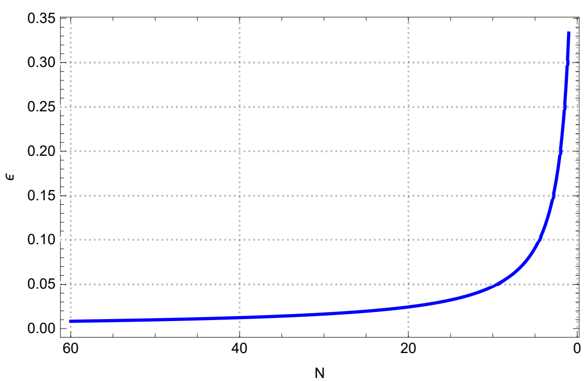

(A)

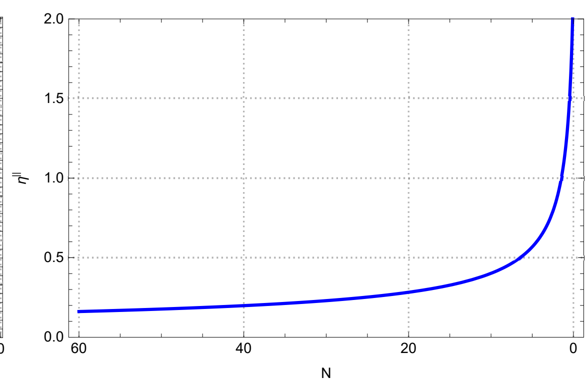

(B)

FIGURE 3.3. (A) The first slow-roll parameter for the double quadratic potential. 60 e-folds before the end of inflation the value of ϵ is quite small, increasing its value at the final e-folds of inflation. (B) The second slow-roll parameter, which has a similar behavior as ϵ, but the condition $\left|\eta^{\parallel}\right| \ll 1$ breaks earlier.

different value for several e-folds, and during the end of inflation, their values get closer to each other. Moreover, due to this time evolution, we can guarantee the validity of the first slow-roll condition for at least 55 e-folds, as it is shown in Fig. 3.4b.

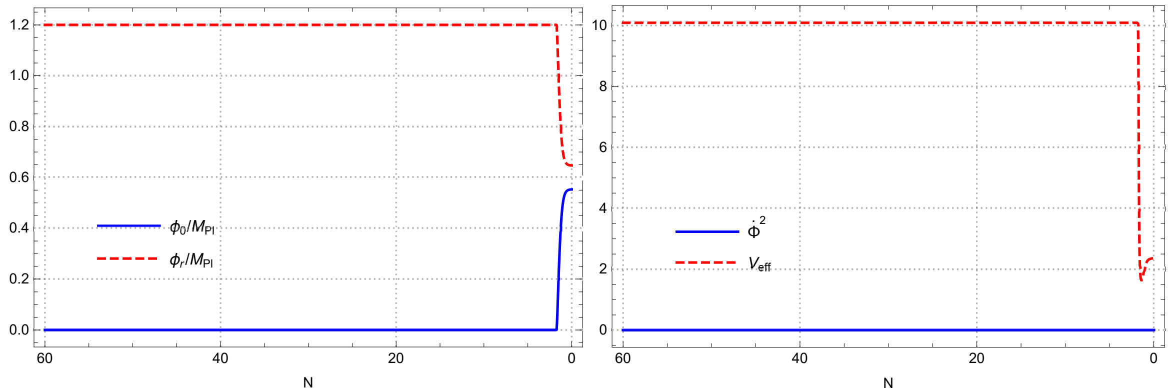

(A) (B)

FIGURE 3.4. (A) Numerical solution for ϕ_0 and ϕ_r, with initial conditions $\phi_0(1) = 0.5M_{\rm Pl}$ and $\phi_r = 0.7M_{\rm Pl}$. (B) The evolution of the slow-roll condition $\dot{\Phi}^2 \ll V_{\rm eff}$. As both fields basically do not vary over time, the kinetic part is almost negligible at all times, except fo the final e-folds, when the value of the effective potential plunges and the slow-roll condition tends to break.

Additionally, we can study the evolution of the slow-roll parameters. As it is shown in Fig. 3.5a, the value of ϵ is almost close to zero for several e-folds, except for the final period of inflation, when the parameter breaks the condition $\epsilon \ll 1$. On the other hand, in Fig. 3.5b, it can be seen how $\eta^{\parallel}$ follows a similar evolution as ϵ, but with a higher value (0.3 over more than 55 e-folds). This model provides a strange behavior at the end of inflation, similar to a phase transition between the extremely slow-roll epoch and the end of inflation.

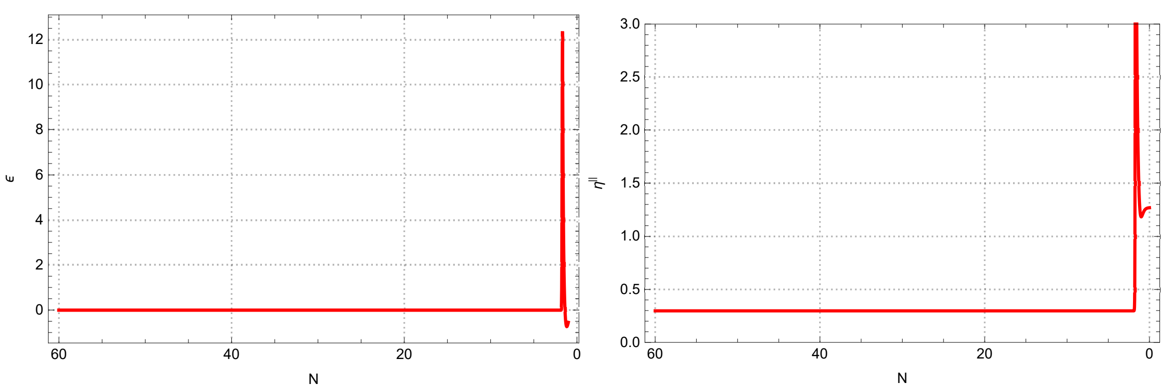

(A) (B)

FIGURE 3.5. (A) The first slow-roll parameter for the bosonic 0-form inflaton model. (B) The same plot for the second slow-roll parameter, which has a similar behavior as ϵ.

Finally, in order to compare the results with the double quadratic potential with equal masses, we show in Fig. 3.6a the trajectories of the fields on the manifold defined by the metric G_{ab}. Both trajectories are perfectly straight lines, which implies that $\eta^{\perp} \sim 0$ in both cases. Therefore, as it is well studied in the literature, this kind of inflationary model produces only adiabatic scalar perturbations, and the multiple field effects are negligible. On the other hand, in Fig. (3.6b), we show the evolution of the Hubble parameter in both models. It is interesting that in our model, the value of H is practically constant for more than 55 e-folds, in contrast to the double quadratic potential, where H changes in a logarithmic way over time. Another way to understand this effect is by proposing that the torsionful contributions of a bosonic 0-form coupled to Einstein-Cartan gravity provide an almost perfectly de Sitter evolution of the Universe during tens of e-folds.

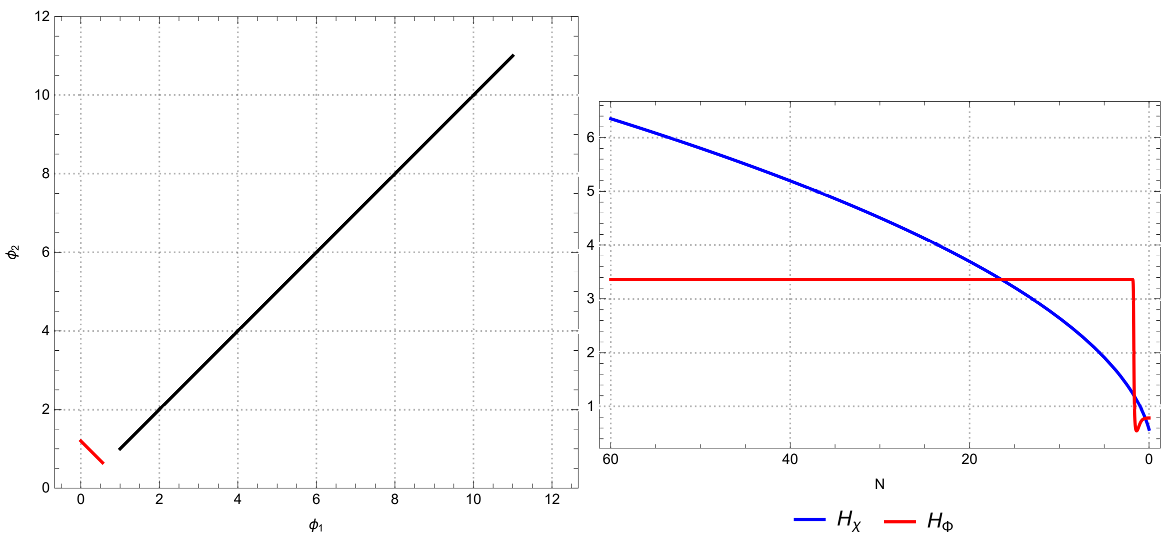

(A) (B)

FIGURE 3.6. (A) Trajectories of fields $\phi_{1,2}$ on the space-field. In black, the double quadratic potential ($\phi_{1,2} = \chi_{1,2}$), and in red the bosonic 0-form coupled to EC gravity ($\phi_{1,2} = \phi_{0,r}$). (B) Evolution of the Hubble parameter for both models (in blue the double quadratic potential and in red our model).

3.5. Some remarks

In this section, we discussed certain cosmological properties of a mathematical object called bosonic 0-form. In Ref. [90], some toy models were developed to understand how this object can be considered as the source of torsion in the framework of Einstein-Cartan gravity. Moreover, it was proposed the idea of considering this object as the inflaton field. Here, in this thesis, we delve into this proposal by analyzing the properties of the bosonic 0-form in the inflationary context. It is clear, from Eq. (3.69), that this model provides a specific effective potential for the inflaton field naturally, without any other requirements rather than the minimal coupling with curvature in EC gravity, and it has a resemblance to the Mexican hat potential of spontaneously symmetry breaking.

We studied the conditions to generate slow-roll inflation with this multi-field model by solving the equations of motion numerically and computing the inflationary parameters ϵ and η. We observed that the solutions are quite sensitive to the initial conditions provided, and there are not physically realistic solutions for many combinations of them. However, we found some combination of the initial conditions that give an almost perfect de Sitter solution for H for more than 55 e-folds, e.g., see Fig. 3.6b. In this case, the slow-roll conditions also hold for more than 55 e-folds, and the fields behave like a straight line in the induced field manifold, which implies that effects like non-gaussianities are suppressed [94].

Considering that this is preliminary work, it is clear that this line of research requires more analysis to assert that the bosonic 0-form can provide a viable model of inflation. In particular, we believe that a more detailed study about the primordial perturbations could share light on the observational predictions this model could give to contrast these predictions with the measurements of the Planck Collaboration. We expect to keep working on the challenges of this model in the near future.

4. Gravitational Waves in an expanding Universe

In the previous chapters, we discussed how fluctuations of the primordial Universe produced the seeds of the large-scale structure and primordial gravitational waves during the inflationary epoch. Then, we studied the dynamics of inflation in modified models of gravity. Now let us change the subject a little. The perturbations of spacetime can also be generated in the late Universe. In fact, the mergers of neutron stars or black holes were responsible for the gravitational waves observed by LIGO a couple of years ago. However, as we discussed in the introduction, the evolution of GWs is well studied in a flat background.

Considering the previous facts, in Ref. [95] it is discussed the effects produced by a non-zero cosmological constant Λ on the propagation of gravitational waves, which includes corrections of order $\sim \sqrt{\Lambda}$ to the phase and the amplitude. Later, it was found [96], [97] that certain modifications to the frequency (i.e., the usual redshift) and a non-trivial correction to the wave number can be found. Furthermore, in those papers, it was proposed that the magnitude of residual time in a PTA experiment could change due to the action of the cosmological constant. A comprehensive explanation and a review of this phenomenon can be found in Ref. [98], where the action of the non-relativistic matter was included in the phenomenon, showing that Dark Matter increases the effect of Λ on the propagation of gravitational waves. In that sense, we expect that each cosmological component of the Universe affects the propagation of GWs similar to the case of Λ, which is why we follow the idea of using the Hubble constant as the main control parameter. The results of this chapter were published in Ref. [16].

4.1. Appropriate coordinate systems

The simplest and standard way to study GW is using the coordinates that emerge from the GW source (i.e., t, r) in a vacuum. It is important to note that the coordinates $x^\mu = (t, r, \theta, \phi)$ corresponds to the spherically symmetric geometry, and they will represent the coordinates with an origin placed at the –usually spherical shaped– source of gravitational waves. If the source is located at an intermediate cosmological distance, a solution of (1.30) will be described approximately by a spherical harmonic wave,

$$h_{ij}^{\mathrm{TT}}(x^\mu) = \frac{A_{ij}}{r}\sin[k_\mu x^\mu] = \frac{A_{ij}}{r}\sin[-\Omega t + kr], \tag{4.1}$$

where $A_{ij} = \{h_{++}, h_{\times\times}\}$ are the components of the polarization tensor, k_μ are the covariant components of the 4–wavevector of a spherical and monochromatic gravitational wave, such that $k_\mu k^\mu = 0$. We will denote $\Omega = ck_0$ as the emitted angular frequency and $k = k_r = \Omega/c$ as the emitted wavenumber.

Let us consider the following situation: Two remote galaxies are merging, so their central supermassive black holes are orbiting around a common center of mass and slowly approaching each other. This is a Keplerian problem with –approximate– spherical symmetry. For this reason, near the source of gravitational waves, the set of coordinates $x^\mu = (t, r, \theta, \phi)$ with spherical symmetry is very useful in order to describe spacetime and its perturbations. A very detailed discussion about these considerations are given in [98], where also it is established that GWs in their simplest form and expressed in these source-centered coordinates will have the form of the equation (4.1).

However, these coordinates are not useful in cosmology because the cosmological measurements are described in comoving coordinates, i.e., $X^\mu = (T, R, \theta, \phi)$. Thus, the main objective of this research is to find the coordinate transformation between x^μ and X^μ. With this transformation, and by taking advantage of the principle of covariance and relativity, we will describe the propagation of gravitational waves as seen by a cosmological observer. The most straightforward example that we can give to illustrate the situation is showing the de Sitter case, where only the action of the cosmological constant is taken into account. We note that an approximately spherical source of GWs would produce a Schwarzschild metric in a vacuum background. Thus, if we take $\Lambda \neq 0$, then when we are far from the source (i.e., neglecting the mass term at the cosmological horizon, where $\Lambda r^3 \gg 6M$), the geometry of spacetime will be described approximately by a de Sitter (dS) metric,

$$\mathrm{d}s^2 = -\left(1 - \frac{\Lambda}{3}r^2\right)\mathrm{d}t^2 + \frac{\mathrm{d}r^2}{1 - \frac{\Lambda}{3}r^2} + r^2\Big(\mathrm{d}\theta^2 + \sin^2(\theta)\,\mathrm{d}\phi^2\Big). \tag{4.2}$$

For a detailed analysis and a derivation of the dS metric, see Appendix C. On the other hand, the FLRW metric –expressed in comoving coordinates– is given by (1.45) and the scale factor is of the form $a(T) = \exp\Big(\sqrt{\Lambda/3}\Delta T\Big)$, where $\Delta T = T - T_0$. The main idea is to express the coordinates of the SdS metric in terms of the comoving coordinates of the FLRW metric, as they are two equivalent representations of the same spacetime. It was found that the coordinate transformation is given by,

$$r(T,R) = a(T)R \tag{4.3}$$

$$t(T,R) = T - \sqrt{\frac{\Lambda}{3}}\ln\sqrt{1 - \frac{\Lambda}{3}a(T)^2R^2}. \tag{4.4}$$

If we expand them at order $\sqrt{\Lambda}$, we get,

$$r(T,R) = R\left[1 + \Delta T\sqrt{\frac{\Lambda}{3}}\right] + \mathcal{O}(\Lambda) \tag{4.5}$$

$$t(T,R) = T + \left(\frac{R^2}{2}\sqrt{\frac{\Lambda}{3}}\right) + \mathcal{O}(\Lambda). \tag{4.6}$$

These expressions show us how comoving coordinates are related to the coordinates in the dS metric, and replacing the coordinates in (4.1) would show how GWs are seen by a cosmological observer. That is the main idea and it is what we are going to exploit next.

In order to develop a more general discussion of the phenomenon, we will first consider a Universe filled by a single fluid with an arbitrary equation of state, i.e. $p_i = \chi_i\rho_i$. The methodology to be used is basically build a diagonal, spherically symmetric and asymptotically flat metric (that we will denote by $SS\chi$), described by the coordinates x^μ, that recovers the corresponding FLRW metric in comoving coordinates, then find the coordinate transformation between both frames and, finally, replace the coordinates in (4.1), showing how it affects on the propagation of gravitational radiation.

In Appendix D is available the full derivation of the exact expression of the SSχ metric, which is of the form

$$\begin{aligned}\mathrm{d}s^2 &= g'_{\mu\nu}\,\mathrm{d}x^\mu\,\mathrm{d}x^\nu \\ &= -\frac{\mathrm{d}t^2}{\left(1-\dfrac{\kappa\rho_i r^2}{3}\right)\left(1+\dfrac{\kappa\rho_i r^2(3\chi_i+1)}{6}\right)^{\dfrac{1-3\chi_i}{1+3\chi_i}}} + \frac{\mathrm{d}r^2}{1-\dfrac{\kappa\rho_i r^2}{3}} \\ &\quad + r^2\Big(\mathrm{d}\theta^2+\sin^2(\theta)\,\mathrm{d}\phi^2\Big),\end{aligned} \tag{4.7}$$

and the transformation between x^μ and X^μ in terms of ρ_i and $\rho_{i0}=\rho_i(T_0)$ (for any fluid of type i), given by

$$t = \frac{\left[c+R^2(\kappa\rho_{i0})^{\frac{2}{3(\chi_i+1)}}(\kappa\rho_i)^{\frac{3\chi_i+1}{3(\chi_i+1)}}\right]^{\frac{1}{2n}}}{\left(A^{\frac{1}{2n}}\right)\sqrt{\kappa\rho_i}} \tag{4.8a}$$

$$r = a(T)R = R\left(\frac{\rho_{i0}}{\rho_i}\right)^{\frac{1}{3(\chi_i+1)}}, \tag{4.8b}$$

where n and A are constants that depends on χ_i, given by (D.13) and (D.20) respectively (see appendix D for more details). The expansion of (4.8a) and (4.8b) in terms of the energy density of the fluid at the present day, i.e. ρ_{i0}, becomes

$$t = T + \frac{R^2}{2}\sqrt{\frac{\kappa\rho_{i0}}{3}} + \frac{R^2}{12}(1-3\chi_i)\kappa\rho_{i0}\Delta T + \mathcal{O}\Big(\kappa^2{\rho_{i0}}^2\Big) \tag{4.9a}$$

$$r = R\left(1+\Delta T\sqrt{\frac{\kappa\rho_{i0}}{3}} - \frac{\kappa\rho_{i0}\Delta T^2}{12}(1+3\chi_i)\right) + \mathcal{O}\Big(\kappa^2{\rho_{i0}}^2\Big). \tag{4.9b}$$

These results agree with Ref. [98], and they show that, regardless the equation of state, the first term in the expansion is always at order $\sqrt{\rho_{i0}}$. Using this fact, we can expand the First Friedmann equation at first order in $H_0\Delta T$,

$$a(T) = 1 + H_0\Delta T + \mathcal{O}\Big(H_0^2T_0^2\Big), \tag{4.10}$$

where $\Delta T = T - T_0$ and H_0 is the *Hubble constant*, which can be written in terms of the energy densities as,

$$H_0 = \sqrt{\frac{\kappa\rho_{\text{eff}}(T_0)}{3}} = \sqrt{\frac{\Lambda}{3} + \frac{\kappa\rho_{d0}}{3} + \frac{\kappa\rho_{r0}}{3}}. \tag{4.11}$$

In order to use a dimensionless expansion parameter and, to simplify the notation, we recall the definition of cosmological redshift, denoted by z, such that the scale factor reads,

$$a(T) = \frac{1}{1+z} = 1 - z + \mathcal{O}\left(z^2\right). \tag{4.12}$$

Therefore, we can use that $RH_0/c \sim z$, as we are working at the first order. On the other hand, as the r coordinate has to transform as $r \to a(T)R$ to preserve spherical symmetry, a comparison between (4.9a), (4.9b) and (4.10) shows that the cosmological components are added inside the square root, as was discussed in Ref. [98] in the case of non-relativistic matter. Thus, in order to obtain the correct limits for the previous models, the most general linearized coordinate transformations must be of the form,

$$t = T + \frac{R^2}{2}H_0 + \mathcal{O}\left(z^2\right) \tag{4.13a}$$

$$r = R\left(1 + \Delta T H_0\right) + \mathcal{O}\left(z^2\right). \tag{4.13b}$$

The fact that only linear terms of H_0 appear (or, equivalently, the act of neglecting quadratic terms of redshift and beyond) implies that our framework is approximately valid at a local scale, which means that we can consider only sources of GWs at cosmological distances within the condition $z \ll 1$. The coordinate transformation and the effects studied in this work do not apply for sources at redshift $z \sim 1$ or greater. By replacing (4.13a) and (4.13b) into (4.1), we obtain an expression in terms of the comoving coordinates,

$$h'^{\text{TT}}_{ij} = \frac{1}{R}\left(1 + \frac{RH_0}{c}\right) A'_{ij} \sin\left[-\Omega_{\text{eff}}T + k_{\text{eff}}R\right] + \mathcal{O}\left(z^2\right), \tag{4.14}$$

where A'_{ij} are the transformed components of the polarization tensor, and the effective angular frequency and wave number are given by

$$\Omega_{\text{eff}} \equiv \Omega\left(1 - \frac{RH_0}{c}\right), \quad k_{\text{eff}} \equiv \frac{\Omega}{c}\left(1 - \frac{RH_0}{2c}\right). \tag{4.15}$$

From the last two expressions, we can infer how the Hubble constant affects the propagation of GWs when a cosmological observer (e.g., laboratories on the Earth's surface or local celestial bodies as pulsars) is measuring them using comoving coordinates. These results show that the previous works were particular cases and, therefore, incomplete. At the same time, it is partially discarded the possibility of measuring the cosmological constant Λ separately from the other components of the Universe, since all of them are coupled within H_0. It is important to note that the expression for the effective frequency Ω_{eff} in the equation (4.15) reproduces the usual cosmological redshift (for small values of z), i.e. $\Omega_{\text{observed}} \sim \Omega_{\text{emitted}}/(1+z) \sim \Omega_{\text{emitted}}(1-z)$, expected from the expansion of the Universe. However, the effect on the wavenumber k_{eff} cannot be derived from other simpler considerations, e.g., time dilation or redshift, and represents an additional feature of this framework. On the other hand, as it is discussed by [98], even when the phase velocity of the GW is not exactly 1 (in natural units), if it is computed with respect to the ruler distance traveled, it can be shown that its value is exactly equal to 1.

4.1.1. The effect of the cosmological expansion on the waveform of low–frequency GWs

Using the expression for the metric perturbation of gravitational radiation, given by the equations (4.14) and (4.15), some quantitative effects due to the expansion of the Universe on the waveform of gravitational waves can be analyzed. We will choose, in particular, low–frequency GWs since the most common sources at cosmological distances are Supermassive Black Holes (SMBHs) and a Stochastic Background, both sources of low and very low-frequency gravitational waves, which are expected to be measured by Pulsar Timing Arrays (PTAs) experiments in the following years [99], [100]. We are more interested in the SMBHs sources because our framework can describe how the expansion of spacetime

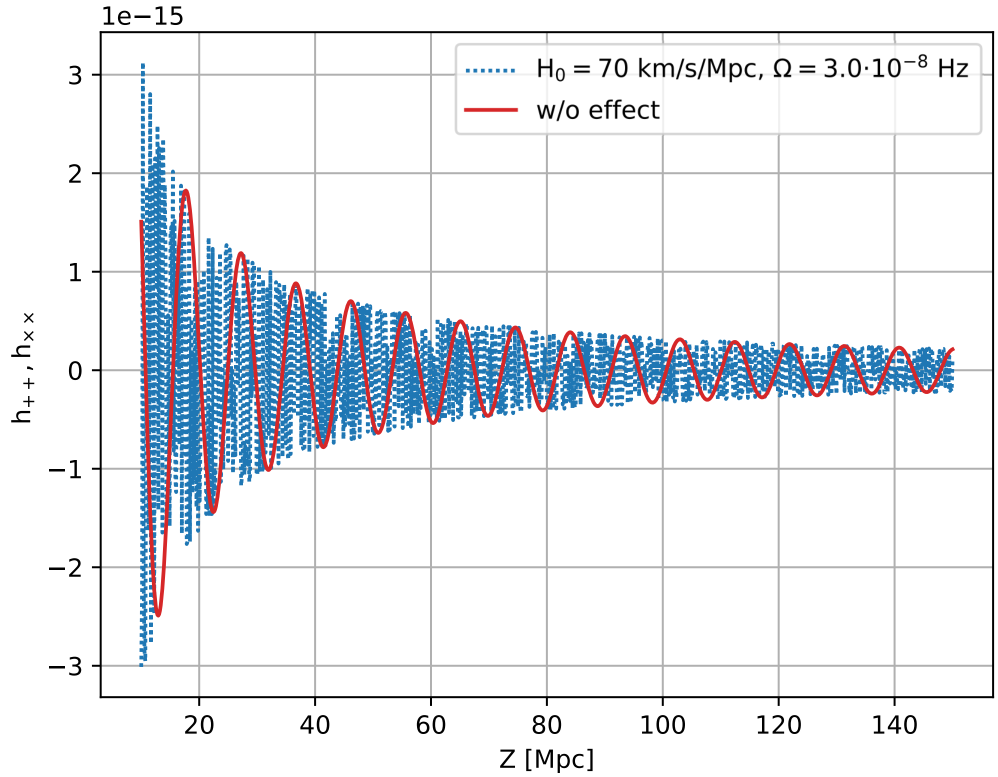

FIGURE 4.1. Dimensionless strain of a GW. The time was fixed at $T \sim 100$ Myr. In solid red, the signal observed neglecting the cosmological expansion. In dotted blue, the waveform expected when the effect is taken into account.

affects the properties of gravitational radiation coming from this kind of origin.

To start, we fix the waveform in time to observe the distribution of the waveform over distance. Moreover, the values of the cosmological constant and the emitted angular frequency of the gravitational wave must be specified in order to compute the waveform. In Fig. 4.1 the blue dotted line shows the dimensionless strain of a monochromatic GW for a fixed time with an emitted angular frequency $\Omega = 3.0 \cdot 10^{-8}$ rad/s and taking $H_0 = 70$ km/s/Mpc, while the red line is the perturbation without considering any cosmological effect. As we expected, the amplitude decreases over distance as $1/R$ in both cases, but the

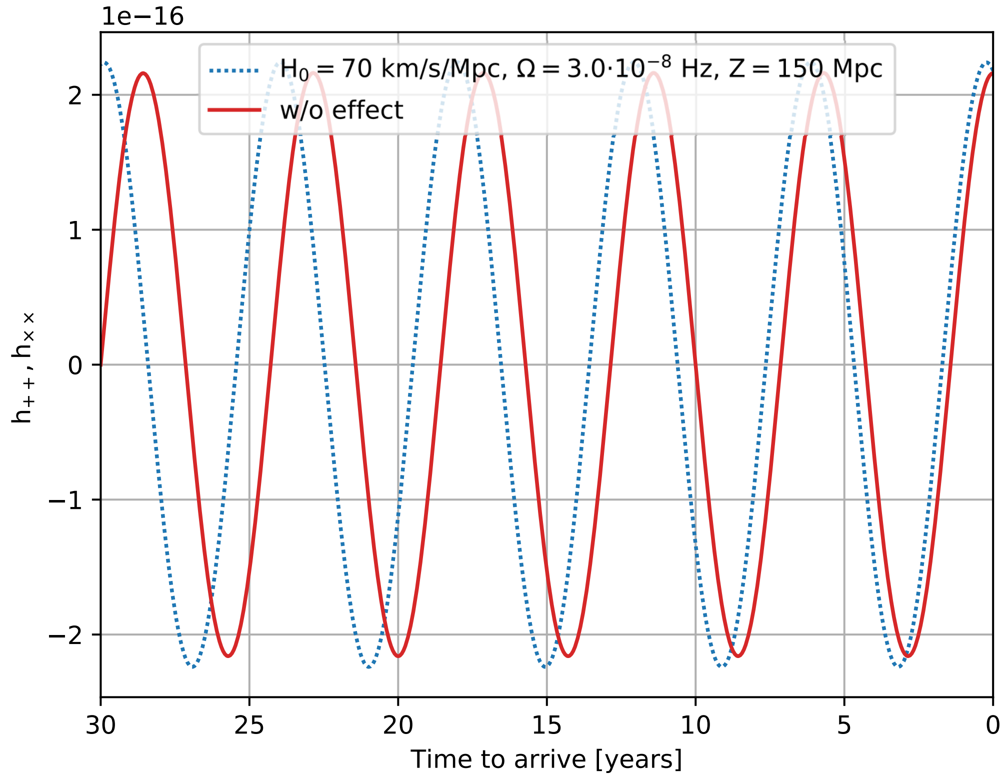

FIGURE 4.2. The same plot but now fixing the position of the source at $R = Z \sim 150$ Mpc. In solid red the wave without cosmological effects and in dotted blue the signal expected when the effect is considered. The time axis was inverted, in order to show the waveform during the last 30 years before reaching the observer at $T = 0$. In both cases we take $H_0 = 70$ km/s/Mpc and $\Omega = 3.0 \cdot 10^{-8}$ rad·Hz.

main difference is related to the considerable shrinking of the wavelength over cosmological distances. This effect, due to the H_0 extra term in the k_{eff} in equation (4.15), will be significant when the waveform is integrated over a trajectory, as we will see in section 4.2.

Conversely, we can also fix the R coordinate, i.e., the position of the observer in space, and compute the waveform of the perturbation in the time domain. The result for a wave that has traveled 150 Mpc from its source with an emitted frequency $\Omega = 3.0 \cdot 10^{-8}$ rad/s appears in Fig. 4.2, where the last 30 years of the wave propagation before reaching the Earth are plotted. It is clear from the picture that the effective frequency of the gravitational wave is different depending on whether our effect is considered or not. In this way, our framework reproduces the standard cosmological redshift of the frequency expected for electromagnetic and gravitational waves when they travel through spacetime.

However, it should be noted that this phenomenon could be detected only by observing the waveform for long periods. This is not the case for detectors like LIGO or LISA because they measure GWs from the merger of black holes or neutron stars that last seconds or minutes, but it could be the case for PTA experiments because they have been observing pulsars for decades. Furthermore, we can anticipate that as the observation time span increases, the magnitude of cosmological effects should rise. In the next section, we develop a framework using our results to analyze how this effect can affect the measurements of PTA, and in the final section, we estimate the feasibility of detection by the computation of signal-to-noise ratios.

4.2. Pulsar Timing Arrays and Timing Residual

4.2.1. Timing residual of pulsars

The results obtained in the last section, e.g., equations (4.14) and (4.15), show that the Hubble constant should influence the propagation of gravitational waves. Now we will set an experimental framework in which this effect can be taken into account. We will use the light coming from a local pulsar and the shift in the time of arrival of the electromagnetic (EM) pulse due to the pass of GWs. In Fig. 4.3 we show a source of continuous gravitational waves at low–frequency ($\Omega_{\rm GW} \sim 10^{-8}$ rad/s), e.g., a pair of orbiting Supermassive Black Holes (SMBHs), at a distance Z from Earth. In general, we can separate different regions far from the GW source: The Strong Field Zone (SFZ), where spacetime is strongly curved due to full relativistic effects; the Local Wave Zone (LWZ), which starts approximately at a distance $d \sim \lambda_{\rm GW} = c/(\Omega_{\rm GW}/2\pi) \sim 20$ ly from the source, where we will consider the plane wave approximation, i.e., the propagation of monochromatic and spherical GWs from the position of the source. These waves will be measured by a distant cosmological observer, e.g., the Earth, and our goal is to estimate how the cosmological expansion of the Universe affects the propagation and observation of these low-frequency gravitational waves.

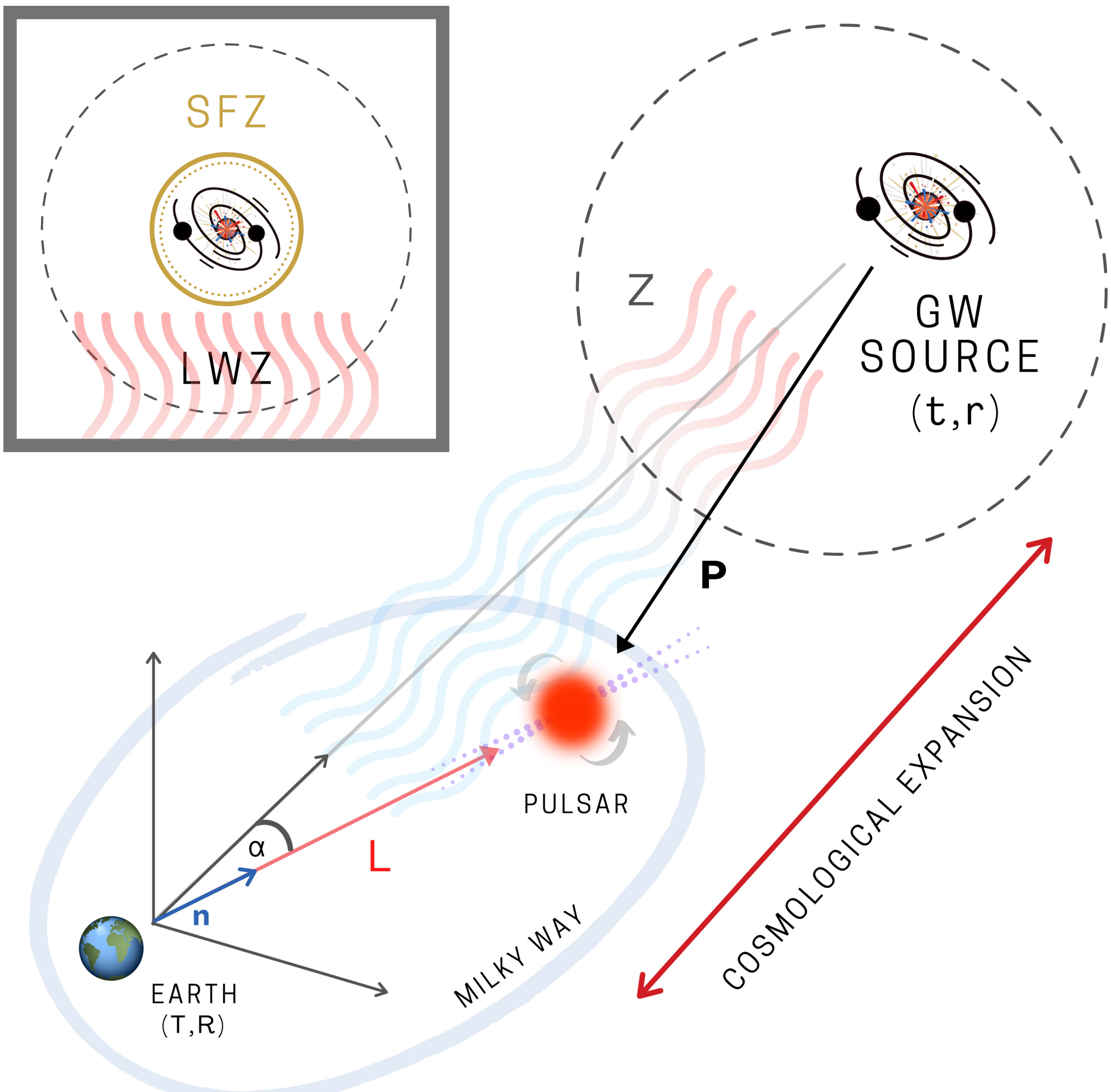

FIGURE 4.3. Setup of the configuration analyzed in this work: A source of gravitational waves at distance Z from the Earth and a nearby Pulsar located at a position $\mathbf{P}$ referred to the source. The only relevant angle will be α, i.e. the angle between the source and the pulsar with respect to us. We can obtain α from the galactic coordinates of those objects with equation (4.16).

In this sense, the main goal of Pulsar Timing Arrays (PTAs) experiments is to measure low–frequency gravitational radiation that reaches the Earth and nearby pulsars, which are typically located at galactic distances and are not affected by cosmological effects. However, the natural sources of low-frequency GWs, e.g., SMBHs, are usually observed at local cosmological distances ($z \lesssim 0.5$) and, hence, the discussion and results of the previous chapter could apply. To start, we will compute the timing residual due to the pass of a monochromatic gravitational wave over a single pulsar. If this object has a galactic longitude ℓ_p and a galactic latitude b_p; and if we consider a source of gravitational waves with galactic longitude ℓ_s and galactic latitude b_s, the cosine of the angle α between the line of sight of the pulsar and the one of the source, with respect to us, is given by the expression,

$$\cos(\alpha) = \cos(b_s)\cos(b_p)\cos(\ell_s - \ell_p) + \sin(b_s)\sin(b_p). \tag{4.16}$$

In Fig 4.3 we have a pulsar at a distance L from Earth, which emits EM pulses with a certain time-dependent phase ϕ_0 measured at the pulsar. Thus, the phase of the EM pulse measured at Earth reads,

$$\phi(T) = \phi_0 \left[T - \frac{L}{c} - \tau_0(T) - \tau_{\text{GW}}(T) \right] \tag{4.17}$$

where c the speed of light, $\tau_0(T)$ is the timing correction associated with the motion of the Earth with respect to the Solar system and $\tau_{\text{GW}}(T)$ is the timing correction due to the action of GWs passing through the system. According to Refs. [98], [101], [102], the correction to the EM phase due to the pass of monochromatic gravitational waves, is given by

$$\tau_{\text{GW}}(T) = -\frac{1}{2}\hat{\mathbf{n}}^i\hat{\mathbf{n}}^j H_{ij}(T), \tag{4.18}$$

where $\hat{\mathbf{n}}$ is a unit vector pointing from Earth to the pulsar and H_{ij} is the integral of the metric perturbation along the null geodesic in the path pulsar–Earth, which could be parameterized by $\mathbf{R}(x) = \mathbf{P} - L(1+x)\hat{\mathbf{n}}$ with $x \in [-1, 0]$, such that from $x = -1$ to $x = 0$ we follow the geodesic from pulsars to Earth. Using this path, $H_{ij}(T)$ becomes,

$$H_{ij}(T) = \frac{L}{c}\int_{-1}^{0} h'^{\text{TT}}_{ij}\left(T + \frac{L}{c}x, |\mathbf{R}(x)|\right) \mathrm{d}x. \tag{4.19}$$

From the equation (4.17) we can infer the consequences of a non-zero value of the timing residual. In general, the pass of gravitational waves will distort spacetime and induce on a pulsar a change in the time of arrival of the electromagnetic pulse. For instance, $\tau_{\text{GW}} > 0$ implies a delay on the signal with respect to the expected time of arrival (which is equivalent to consider that the distance between Earth and the pulsar, L, increased). If $\tau_{\text{GW}} < 0$, the signal will arrive earlier than expected (equivalently to consider that L decreased). Nevertheless, for all the practical purposes of this thesis, e.g., the computation of statistical significance, the signal-to-noise ratio, or the qualitative analysis of the timing residual, the significant quantity involved will be the total amount of the temporal shift, i.e., the absolute value of τ_{GW}.

4.2.2. Including the ΛCDM model

According to Ref. [102], the plane wave approximation is valid only when $L/Z \ll 1$. If this condition is imposed, we can show that $|\mathbf{R}(x)| = R(x) \approx Z + xL\cos\alpha$. Thus, the equation (4.18) follows, using (4.19). But first, as we imposed the TT-Lorenz gauge, for a GW propagating through the Z axis the only non-zero values of the components of A'_{ij} are in the X,Y components (the polarizations h_{++} and $h_{\times\times}$). We can also additionally assume, in order to simplify the computation of the integral, that $\left|A'_{ij}\right| \equiv \varepsilon\ \forall i, j$. Therefore, the full timing residual in the arrival time of the pulsar due to the pass of GWs in the ΛCDM model reads,

$$\tau_{\text{GW}}(\alpha, H_0, T, L, Z, \Omega, \varepsilon) = -\frac{L\varepsilon}{2c}\sin^2(\alpha)\int_{-1}^{0}\frac{1 + H_0\left[T + \frac{xL}{c}\right]}{Z + xL\cos\alpha}\left[\cos\Theta + \sin\Theta\right]\,\mathrm{d}x, \tag{4.20}$$

where the phase Θ is given by the expression,

$$\begin{aligned}\Theta = {} & \Omega\left(1 - \frac{Z + xL\cos\alpha}{c}H_0\right)\left(T + \frac{xL}{c}\right) \\ & - \frac{\Omega}{c}\left(1 - \frac{Z + xL\cos\alpha}{2c}H_0\right)\left(\frac{Z + xL\cos\alpha}{c}\right).\end{aligned} \tag{4.21}$$

4.3. Effects of the Hubble constant on the timing residual

4.3.1. Simulation of the timing residual of an individual pulsar

As we discussed before, the geometrical parameters involved in $\tau_{\rm GW}$ are the angle α between the pulsar and the GW-Source, the distance Earth-Pulsar, L, and the distance Earth–GW-source, Z. In order to perform a numerical analysis, we can choose some reasonable values of the parameters that appear in the equation (4.20) and fix them to visualize the behavior of the timing residual $\tau_{\rm GW}$. Thus, the setup described in Fig. 4.3 can be approximately modeled with the values that appear in the Table 4.1.

Parameter	SI value	
Z	$3 \cdot 10^{24}$ m	~ 100 Mpc
T	$Z/c = 10^{16}$s	~ 300 Myr
L	10^{19}m	~ 1000 ly
Ω	10^{-8} rad$/s$	
ε	1.2×10^{9} m	

TABLE 4.1. List of values considered for the parameters in the numerical integration of the timing residual $\tau_{\rm GW}$ in (4.20), according to current accuracy of Pulsar Timing Arrays.

For the source of GWs, we choose a typical distance Z where supermassive black holes are present, and although it is large, it is not a cosmological distance near the Big Bang. On the other hand, the distance between Earth and the pulsar is within the margin of a local galactic scale. It can be seen, from Table 4.1, that $L \ll Z$, as required from the previous considerations. The angular frequency is of the expected order for future PTA projects and the same argument is used to fix ε, due to that it satisfies $|h_{++}| \sim |h_{\times\times}| \sim \varepsilon/Z \sim 10^{-15}$, where $|h|$ and Ω are within the expected accuracy of PTA projects, e.g. the EPTA [103] or the NANOGrav collaboration [104]. Employing these parameters, the numerical integration of $\tau_{\rm GW}$ gives the results that are shown in figure 4.4a. As we can see, the value of the timing residual can be positive or negative. Since the meaningful physical magnitude is the amount of time, rather than the direction of the shift, we can also plot the absolute value of $\tau_{\rm GW}$, but now changing the value of H_0 within a region of parameters, obtaining the plot in Fig. 4.4b.

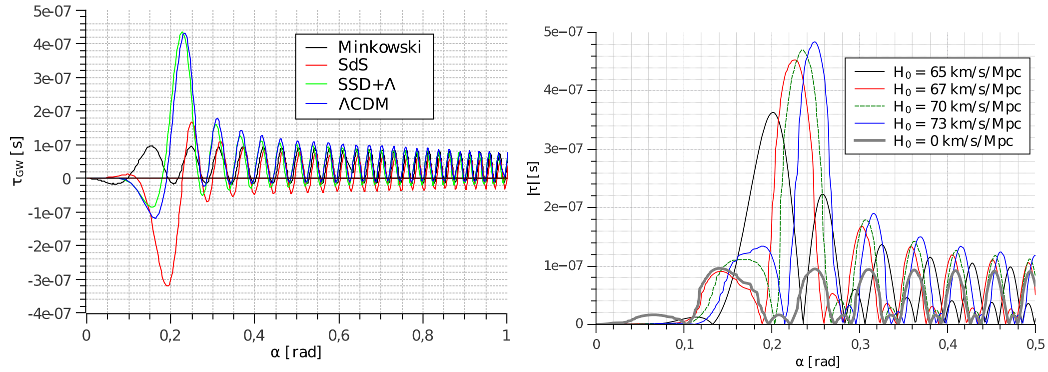

(A) (B)

FIGURE 4.4. (a) Comparison between different material contents of the Universe. SdS is the de Sitter case (only Λ), SDS+Λ is where Dark Energy and Dark Matter (dust+Λ) are taken account. The ΛCDM case also includes radiation. Note that in the Minkowski spacetime no peak is observed. This graphic also agrees with the results obtained by [98]. (b) Numerical analysis of the absolute value of timing residual in terms of α, varying the value of H_0. For a non–zero H_0, a dominant peak is present, whose angular position (i.e. at an angle α_m) in the α–axis increases as the value of H_0 also increases.

First, in order to understand the role of the angle α_m, in which the maximum of $\tau_{\rm GW}$ is reached, we analyze the dependency on the original angular frequency of the incoming gravitational wave, namely Ω, e.g. see equation (4.21). From figure 4.5a we note that for the region 10^{-6} rad/s $< \Omega < 10^2$ rad/s, the value of $|\tau_{\rm GW}|$ is practically zero. However, in the region 10^{-8} rad/s $< \Omega < 10^{-6}$ rad/s the value starts to rise. This is the main reason why the other type of detectors as LISA or LIGO are useless in this context: Only PTA works in the proper range of the frequency spectrum [105]–[107]. On the other hand, in Fig. 4.5b we note a lack of angular dependence on the maximum values of $\tau_{\rm GW}$, and moreover, the same behavior is observed for the distance L, in Fig. 4.6a.

However, in Fig. 4.6b it is clear that for different values of the distance Earth–GW-Source, the angle α_m changes dramatically, and therefore it depends on the distance Z in an explicit but unknown way. For the Hubble constant, Fig. 4.7a shows a similar situation. In fact, it represents how the dependency on H_0 is quite similar to the case of Z in Fig. 4.6b.

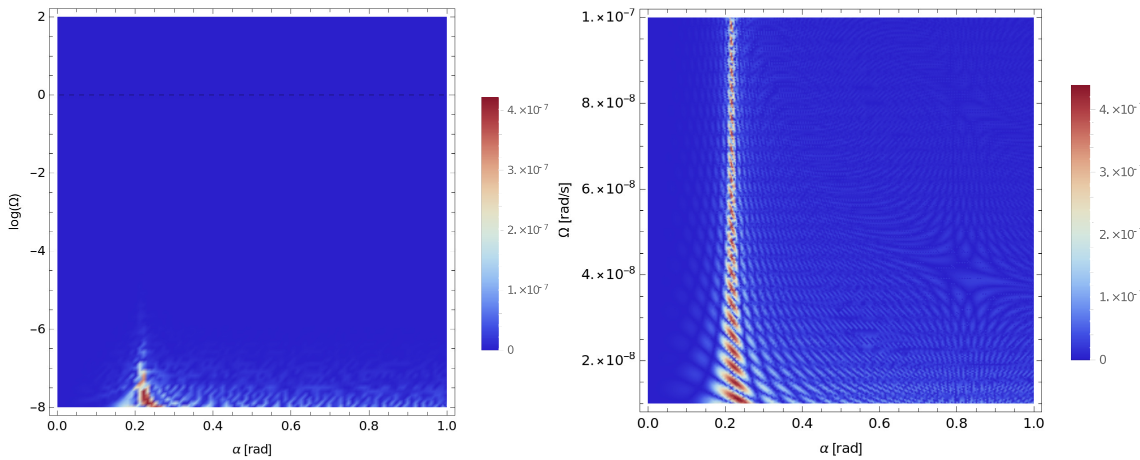

(A) (B)

FIGURE 4.5. (a) Density plot of $|\tau_{\rm GW}|$ in terms of the common logarithm of angular frequency Ω and the angle α. This graphic shows why PTAs are so important to measure this effect. Other values given by table 4.1, with $H_0 = 70$ km/s/Mpc. (b) The same plot but focused in the range 10^{-8} rad/s $< \Omega < 10^{-7}$ rad/s. We can note the lack of dependence on Ω.

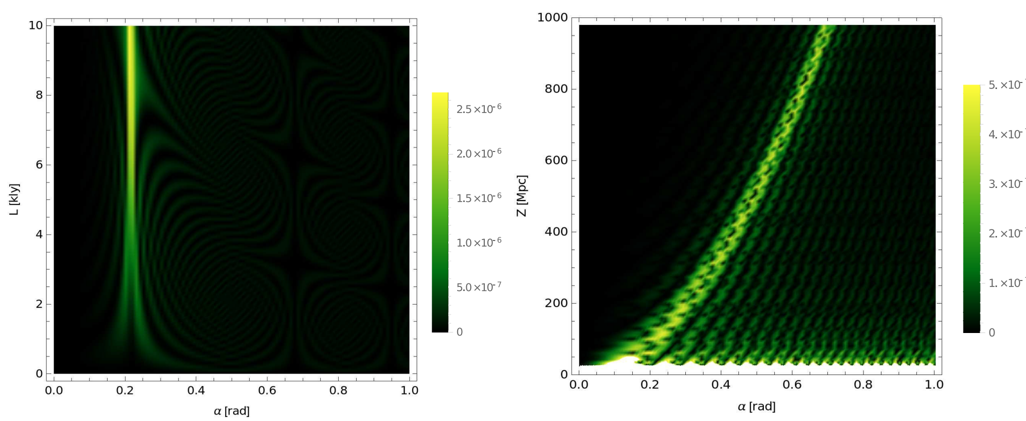

(A) (B)

FIGURE 4.6. (a) Density plot of $|\tau_{\rm GW}|$ in terms of the distance L (in kilolight-years), and the angle α. The rest of parameters are given by Table 4.1, with $H_0 =$ 70 km/s/Mpc. Again, there is almost no dependence on L. (b) Density plot of $|\tau_{\rm GW}|$ in terms of the distance Z (in megaparsecs), and the angle α. The rest of parameters are given by Table 4.1, with $H_0 = 70$ km/s/Mpc. Unlike the previous cases, we do see an angular dependency on Z.

From this behavior, we can speculate about a possible relationship between these parameters. Zooming up, we obtain the Fig. 4.7b, where we can see that the maximum value of the timing residual τ_{GW} (i.e., the white spots) has a slightly oscillatory structure around a characteristic maximal angle α_m. It can be noticed that the whole white stripe has a slight slope, showing a slow variation of the angular position, in agreement with the Fig. 4.4b.

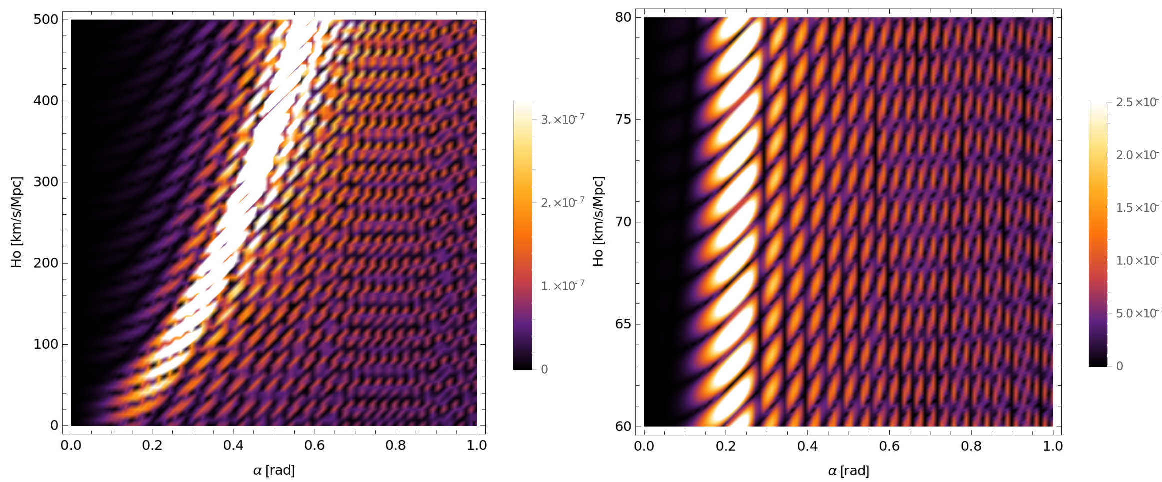

(A) (B)

FIGURE 4.7. (a) Density plot of $|\tau_{\text{GW}}|$ in terms of H_0, and the angle α. The rest of parameters are given by Table 4.1. (b) The same plot but zoomed to the suitable range 60 km/s/Mpc $< H_0 <$ 80 km/s/Mpc. We note a slight slope in angular position, in accordance with Fig. 4.4b.

We can summarize the previous analysis as follows: The numerical integration of the equation (4.20), with the parameters given by the Table 4.1, gives the density plots shown above. From Fig. 4.5a we can also establish the crucial role of PTAs in the eventual measurement of the effects caused by the cosmological components of the Universe on the propagation of gravitational waves: The effect that Dark Matter, Dark Energy, and other cosmological fluids induce to the propagation of GWs, is sensitive to the frequency spectrum of current Pulsar Timing Arrays experiments.

Furthermore, the figures 4.6b and 4.7a support the hypothesis of the existence of an implicit relationship between the H_0, Z, and α_m. From the figures, 4.4a and 4.4b we note that it could be difficult to find the best value of H_0 that fit the data unequivocally due to the complicated dependencies of the parameters within the equation (4.20) and because of the background (i.e., the null test for H_0, the flat Minkowski spacetime) has a not negligible amplitude for a large part of the angular values of α. However, this situation does not happen within the vicinity of the characteristic peak of $\tau_{\rm GW}$ when $H_0 \neq 0$, which occurs at a certain angle α_m, where the difference with the background is considerable. In that sense, if this tiny effect is ever observed, it is very likely that must be the case of a pulsar located in the vicinity of the angle α_m, in such a way that the value of its timing residual is maximized, and that the signal is strong enough to rule out the experimental noise. Thus, the relationship between H_0, α_m, and Z will be clarified, and we could state its importance.

4.3.2. A relationship between PTA observables and the Hubble constant

Using the stationary phase approximation for $\tau_{\rm GW}$ and considering reasonable asymptotic expansions, we obtain the following expression,

$$H_0 \cong \frac{2c}{Z} \sin^2\left(\frac{\alpha_m}{2}\right). \tag{4.22}$$

A derivation of this equation can be found in Appendix E. The expression in (4.22) provides a precise relationship between H_0 and the observables α_m and Z. Under ideal assumptions, this formula can be used to estimate the local value of the Hubble constant knowing the two main observables: Z and α_m. In Fig. 4.8 we show the behavior of the approximation formula with respect to the numerical analysis, including some values of current observations.

However, there are some experimental obstacles when we want to measure H_0 using this framework, in particular, because we need to determine the value of Z by independent astrophysical methods. Nevertheless, a PTA experiment could determine, considering the experimental uncertainties, the value of the timing residual $|\tau_{\rm GW}|$, the value of the emitted frequency of the source Ω and the direction of the incoming Gravitational Wave (and therefore, the value of α). In the ongoing PTA experiments, several pulsars are observed at once. Each of them will be located at different angular positions. If a GW is passing through the set of pulsars, then each of them will have, according to our model, a different

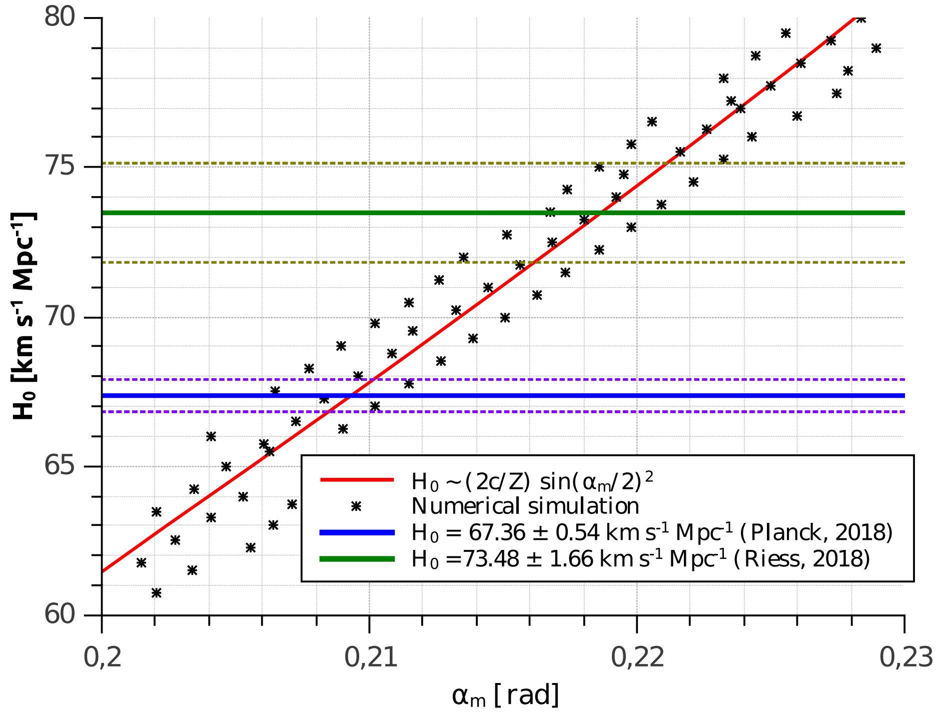

FIGURE 4.8. The value of H_0 using the formula (4.22) and the numerical maximum of $|\tau_{\rm GW}|$. The average error in the approximation is of the 1.5% from numerical simulation.

associated $|\tau_{\rm GW}|$. Evidently, it is more likely that the pulsars have a relative angular position with the source in which the $|\tau_{\rm GW}|$ is not maximum (i.e., $\alpha \neq \alpha_m$). Clearly, these cases are challenging to measure experimentally because the value of $|\tau_{\rm GW}|$ for these cases is indistinguishable from the background. However, there is a tiny possibility that one or some of these pulsars are located just at an angular position where the value of $|\tau_{\rm GW}|$ is distinguishable with respect to the background (i.e., $\alpha \approx \alpha_m$). If that were the case, then the value of $|\tau_{\rm GW}|$ should be large enough to be measured by the expected accuracy for PTA detectors.

Furthermore, in light of the standard cosmological model, for a small redshift, i.e., $z \ll 1$, it holds that $z \sim (Z/c)H_0$ [108]. Thus, equation (4.22), we obtain an expression that could be interpreted as the redshift of the source of GWs, denoted by z_s, in terms of the maximal angle α_m,

$$z_s \cong 2\sin^2\left(\frac{\alpha_m}{2}\right), \tag{4.23}$$

if, and only if, the source has a redshift $z_s \ll 1$, according to the previous discussion about the local validity of this work. Consequently, the maximal angle is restricted to the condition $\alpha_m \ll \pi/2$, to assure the redshift condition. The relationship between the redshift of the source and α_m was not identified in the previous results of Ref. [98], hence it represents a new and interesting insight in this line. This result implies that the ΛCDM model predicts large timing residuals for pulsars located approximately at the same direction of the (local) sources of gravitational waves. This effect could be useful for PTAs research and the measurement of Continuous Gravitational Waves through this method, a task that is expected to be accomplished in the next years [103], [104], [109]: The angular separation between the sources of GWs and the monitored pulsars is strongly constrained in order to measure distinguishable differences in the timing residual. Therefore, if a PTA experiment seeks to measure a strong signal of gravitational radiation coming from single sources (e.g. mergers of supermassive black holes), only the signal coming from sources located near to the angle α_m with respect to the pulsars observed seem to be measurable. In that sense, this prediction of the standard ΛCDM model represents an alternative way to improve the detection of GWs using PTA experiments by taking advantage of this local cosmological effect on the propagation of gravitational waves within our expanding Universe.

4.4. Statistical significance and Signal–to–Noise Ratios

4.4.1. Estimates of statistical significance in the timing residual analysis

As we have discussed, an essential feature of the cosmological effects on GWs in PTA experiments is the presence of a significant peak in the value of the timing residual for a particular angle α. Moreover, we note that this peak changes its angular position according to the value of the Hubble constant. This is our first clue of the existence of a distinguishable signal coming from the cosmological effects on the propagation of GWs.

In order to study the intensity of the signal shown in the previous figures, we will use some pulsars from the ATNF catalog [110]. As we know, pulsars are stable clocks whose periods are known with great accuracy. Assuming a modest precision of $\sigma_t \approx 10^{-6}s$ which is obtained by averaging the precision achieved of best pulsars in the IPTA collaboration, we can define a *statistical significance* of the timing residual, of the form

$$\sigma = \sqrt{\frac{1}{N_p N_t} \sum_{i,j=1}^{N_p,N_t} \left(\frac{\tau_{\rm GW}}{\sigma_t}\right)^2}, \tag{4.24}$$

where index i running from 1 to N_p (number of pulsars averaged) and j running from 1 to N_t (number of observations). Assuming we perform measurements every 11 days through 3 years, then $N_t = 101$. We considered the clustered pulsars shown in table 4.2.

Pulsar Name	b_i	L_i
J0024-7204E	$-44.89°$	4.69 kpc
J0024-7204D	$-44.88°$	4.69 kpc
J0024-7204M	$-44.89°$	4.69 kpc
J0024-7204G	$-44.89°$	4.69 kpc
J0024-7204I	$-44.88°$	4.69 kpc

TABLE 4.2. List of pulsars averaged for an hypothetical source at angular separation α. It is shown the data given in [110], where b_i is the galactic latitude and L_i the distance between Earth and pulsar. We can note that this set simplify the computation of σ because all pulsars are very close to each other.

We will keep α as a free parameter and suppose that an hypothetical GW source is located at α radians between Earth and pulsars. Thus, the statistical significance is given by

$$\sigma(\alpha) = \sqrt{\frac{1}{5 \cdot 101} \sum_{i=1}^{5} \sum_{j=1}^{101} \left(\frac{\tau_{\rm GW}(b_i)}{\sigma_t}\right)^2} \tag{4.25}$$

The result of the simulation can be observed in Fig. 4.9a, showing the characteristic peak as we expected. However, we can develop a more realistic simulation. In figure 4.9a, only a cluster of 5 pulsars was considered, and all of them were averaged at the same angle α. However, one can expect that all the pulsars are located at different angles (in galactic coordinates) and randomly located. Therefore, we have considered 11 randomly distributed groups of 5 pulsars each (see appendix F), two test clusters of pulsars with a suitable location (65 pulsars in total), and a source of gravitational waves located at galactic coordinates $\ell_S = 20°$ and $b_S = 15°$.

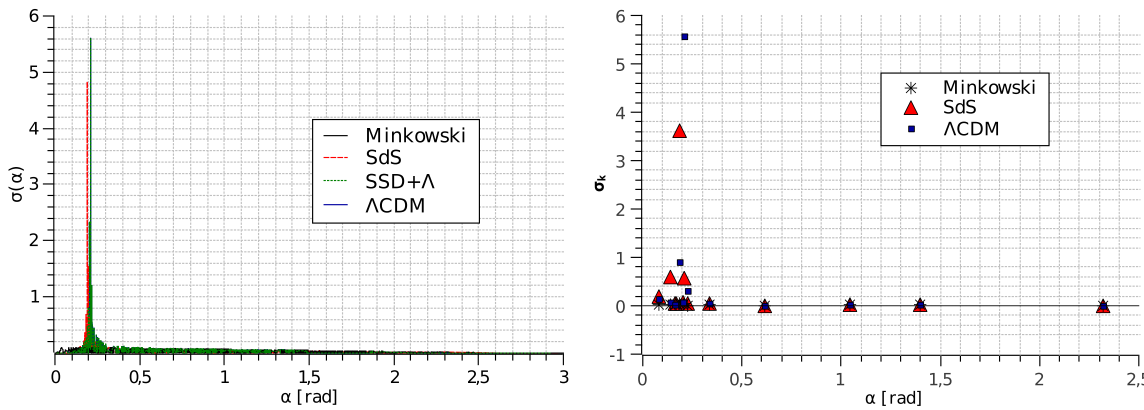

(A) (B)

FIGURE 4.9. (a) Simplified simulation of σ in an hypothetical observation of the peak in $\tau_{\rm GW}$, which is located near 0.2 rad. Green and blue curves overlap due to the similarity of models. (b) Numerical simulation σ in the measurement of $\tau_{\rm GW}$ for three different models. We used 13 sets with 5 pulsars each, and for 11 of them, we took randomly distributed pulsars from the ATNF catalog (see Appendix F), and 2 of them as test groups with suitable parameters. The larger peaks come from the later, showing the difficulty of a successful measurement.

Then, we averaged them using the statistical significance given by

$$\sigma_k = \sqrt{\frac{1}{5\cdot 101}\sum_{i=1}^{5_k}\sum_{j=1}^{101}\left(\frac{\tau_{\rm GW}(L_i,\ell_i,b_i)}{10^{-6}}\right)^2} \tag{4.26}$$

and plot it as a function of the average angle of the group, namely $\bar{\sigma}_k = \sum_{i=1}^{5_k}\alpha_i/5$. From this simulation, we obtained figure 4.9b, where we can note how the randomly distributed pulsars mostly do not show any signal, except for those that are located very close to the maximal angle, namely α_m, where the value of the timing residual is maximized. For a pulsar located within the vicinity of the angle α_m, the effect of the Hubble constant on the propagation of GWs and the capability of measuring them using PTAs is greatly increased.

This fact indicates that only the pulsars placed near the angle α_m with respect to the source of GWs will show the characteristic peak in the timing residual with great statistical significance, which implies a significant obstacle when trying to observe this effect. Nevertheless, as more pulsars are observed and studied, it is more likely to measure the existence of this peak, which could represent a challenge for the future research of PTA experiments.

4.4.2. Computation of the Signal-to-Noise Ratios

A better way to estimate the feasibility of measuring the effect of the cosmological expansion of the Universe on the propagation of low–frequency GWs is by computing signal-to-noise ratios (SNRs). This quantity compares the level of a signal observed by a PTA experiment with the experimental noise. To start, let us consider a source of low-frequency gravitational waves located at a fixed position in the sky, $\ell_s = 0°$ and $b_s = 45°$. According to [111], the Signal-to-Noise Ratio (SNR) for a PTA observation can be obtained from the following expression,

$$\mathrm{SNR}^2 = \sum_{j=1}^{N_p} (\mathrm{SNR})_j^2 = \sum_{j=1}^{N_p} \sum_{i=1}^{N_T^{(j)}} \left(\frac{\tau(\alpha_j, L_j, H_0, \Omega, Z, \varepsilon, T_i)}{w_j^{\mathrm{rms}}} \right)^2, \tag{4.27}$$

where $(\mathrm{SNR})_j$ is the individual signal-to-noise ratio for each pulsar, α_j is the angle between the source and each pulsar, as appears in (4.16), τ is the expected signal to be observed by PTA experiments, w_i^{rms} is the root-mean-squared (rms) noise of each pulsar, and each of them are observed during a time span N_{TS}^j, which we can subdivide, e.g. $1, \ldots, N_T^{(j)}$. As discussed in the introduction, IPTA is a global collaboration, i.e., NANOgrav+EuropeanPTA(EPTA)+ParkesPTA(PPTA), which monitors several pulsars sky to detect continuous low–frequency GWs in the next years. Thus, we will take ten pulsars from the 2019 Second Data Release of IPTA collaboration [100] listed in Table 4.3. We compute the SNRs assuming a Gaussian stationary noise and plot its magnitude for different values of the redshift of the source and the frequency of GWs. The result appears in Fig. 4.10a, where we can observe that the left side of the region of parameters has $1 < \rho < 10$, a weak/moderate signal. However, for values of $\Omega > 10^{-8}$ rad/s and independent of the redshift of the source, the SNR decreases to almost zero. This result shows how this effect only can be observed for very small values of the GW frequency.

	Pulsar Name	ℓ_j	b_j	L_j (kpc)	$w_j^{\rm rms}$ (μs)	$N_{\rm TS}^j$ (years)
#1	J0030+0451	$113.141°$	$-57.611°$	0.34	1.48	15.1
#2	J0613–0200	$210.413°$	$-9.305°$	1.11	1.14	16.0
#3	J1022+1001	$231.795°$	$51.101°$	0.72	1.97	17.5
#4	J1024–0719	$251.702°$	$40.515°$	1.20	1.71	18.2
#5	J1455–3330	$330.722°$	$22.562°$	1.00	4.12	9.7
#6	J1640+2224	$41.051°$	$38.271°$	1.50	0.77	17.2
#7	J1643–1224	$5.699°$	$21.218°$	1.10	2.55	20.1
#8	J1738+0333	$27.721°$	$17.742°$	1.50	1.38	7.3
#9	J1730–2304	$3.137°$	$6.023°$	0.60	1.57	20.3
#10	J1744–1134	$14.794°$	$9.18°$	0.41	0.73	19.9

TABLE 4.3. List of pulsars considered to compute the SNRs of the figures 4.10a and 4.10b. The distances, rms noise and the time span of the observation were obtained from the second data release of IPTA [100], and the location in the sky in galactic coordinates from the ATNF pulsar catalog [110]. Only the pulsars observed by more than one team from IPTA (between EPTA, Nanograv and PPTA) were considered to the computation of the Signal–to–Noise Ratios of figures 4.10a and 4.10b.

Another alternative is fixing the frequency and the distance of the source (or, equivalently, its redshift). This procedure is illustrated in Fig. 4.10b, which shows a fascinating pattern: A ring surrounding some pulsars where the SNR is significantly enhanced. This is not surprising since the ring is the main consequence of the peak in the timing residual due to the cosmological effect discussed in section 4.3. We can use (4.16) and (4.23) to describe the enhancement ring for a pulsar located at ℓ_p and b_p in galactic coordinates, and is approximately the geometrical region that satisfies the following parametric equation,

$$\cos\left(2\arcsin\left(\sqrt{\frac{z_s}{2}}\right)\right) = \cos(b_s)\cos(b_p)\cos(\ell_s-\ell_p)+\sin(b_s)\sin(b_p), \tag{4.28}$$

where $z_s = ZH_0/c$ is the redshift of the source of gravitational waves and (ℓ_s, b_s) its location in galactic coordinates. This phenomenon, i.e., that the signal of gravitational waves enhances enormously in a specific region of the sky depending on the value of H_0 and the distance of the source or, equivalently, the redshift z_s, is the primary footprint of cosmological expansion on the propagation of low–frequency gravitational waves. According to Fig.

4.10b, the sources of GWs observed with PTA experiments that are placed within this characteristic ring would have a much larger SNR, and therefore, they are potentially observable by these GW detectors. Furthermore, if we increase the number of pulsars monitored and the time span for each of them (as IPTA expects it), the SNRs will be surely bigger, raising the feasibility of observing this phenomenon in the future years of PTA measurements.

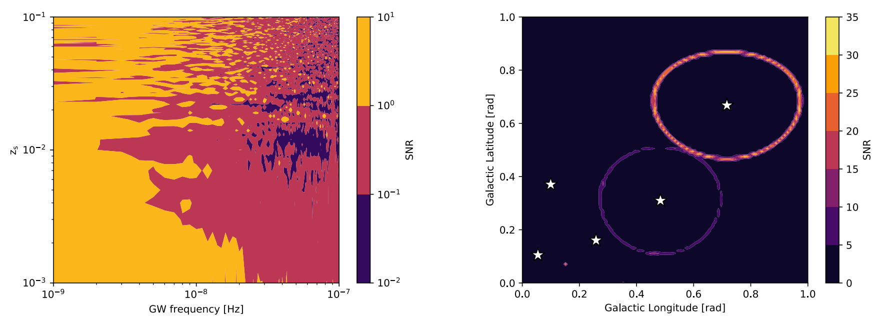

(A) (B)

FIGURE 4.10. (a) Signal-to-noise ratio for a fixed position in the sky of the source at $\ell_s = 0°$ and $b_s = 45°$, and where the contributions to the SNRs of each pulsar from the Table 4.3 were included. In the vertical axis we have the redshift of the source, i.e. $z_s = H_0 Z/c$, and in the horizontal axis we have the emitted frequency of GW, Ω. In the region of parameters suited for PTA observations we obtain, for these conventional values, a SNR between 1 and 10, a weak/moderate signal. (b) Signal-to-noise ratio for different positions of the source in the sky, with $Z = 100$ Mpc and $\Omega = 10^{-8}$ Hz. White stars represent the positions of the pulsars #6, #7, #8, #9 and #10 from Table 4.3. When $H_0 \neq 0$, it appears a ring centered at each pulsar, following the equation (4.28), where the feasibility of a measurement increases $\sim$30 times. The more sensitive pulsar is J1640+2224, with a rms noise of 0.77μs, whose ring is the brighter in the plot. Other rings have much lower SNRs since the noise of the other pulsars is higher. If the action of H_0 is neglected completely, the ring does not appear. In both plots we have considered $H_0 = 70$ km/s/Mpc, and all the parameters involved have the typical values expected for future measurements of PTA experiments, according to the literature [99], [100], [103], [104], [111].

5. Conclusions and Outlook

The models and simulations presented in this thesis result from three different projects developed by the author during his Master's degree. The first project discussed here was the study of cosmic inflation and its slow-roll regime within the framework of the $f(R,T)$ model of modified gravity. We considered the minimal coupling between T and R and added a single inflaton field. Then, we computed the corrections due to this theory to the inflationary observables and applied these results to several well-known models. Regarding the results obtained, we can highlight the following aspects: Power-law potentials' trajectories are not modified. In the case of Natural and Quartic Hilltop inflation, the contribution from $f(R,T)$ gravity can modify the constraints on the only parameter of both models. We also applied the prescription to Starobinsky inflation, where we found that the trajectories in the (n_{S}, r) plane can be strongly modified. Then, we outlined a brief analysis of models with higher powers of T, finding that some crossed terms arise, making the computation of parameters more challenging.

Secondly, we discussed the implications of considering a bosonic 0-form couple to Einstein-Cartan gravity as a source for inflation. After expanding the interacting terms and construct an effective Lagrangian, we reduced the fields to ϕ_0 and ϕ_r, and then we study the formalism of multi-field inflation to analyze the effects of the effective potential. We can highlight the following: Both fields move on a straight line over the space-field manifold, so multi-field effects are negligible. For certain initial conditions, the model can reproduce well-behaved slow-roll inflation for at least 55 e-folds. However, a more detailed analysis is required to confirm the viability of inflation in this model.

Finally, regarding the study of astrophysical sourced gravitational waves propagating through an expanding Universe, we found the following: Due to a coordinate transformation, harmonic gravitational waves become anharmonic when a cosmological observer measures them. By assuming the standard ΛCDM model, we predict a moderate/strong signal in the arrival time of electromagnetic emissions from pulsars, making this effect quite sensitive to PTA experiments.

REFERENCES

[1] C. Rovelli, "Notes for a brief history of quantum gravity," in *9th Marcel Grossmann Meeting on Recent Developments in Theoretical and Experimental General Relativity, Gravitation and Relativistic Field Theories (MG 9)*, Jun. 2000. arXiv: gr-qc/0006061.

[2] N. Aghanim *et al.*, "Planck 2018 results. vi. cosmological parameters," *Astron. Astrophys.*, vol. 641, A6, 2020. arXiv: 1807.06209 [astro-ph.CO].

[3] A. A. Starobinsky, "A new type of isotropic cosmological models without singularity," *Physics Letters B*, vol. 91, no. 1, pp. 99–102, Mar. 1980. DOI: 10.1016/0370-2693(80)90670-X.

[4] A. H. Guth, "Inflationary universe: A possible solution to the horizon and flatness problems," *Phys. Rev. D*, vol. 23, no. 2, pp. 347–356, Jan. 1981. DOI: 10.1103/PhysRevD.23.347.

[5] A. D. Linde, "A new inflationary universe scenario: A possible solution of the horizon, flatness, homogeneity, isotropy and primordial monopole problems," *Physics Letters B*, vol. 108, no. 6, pp. 389–393, Feb. 1982. DOI: 10.1016/0370-2693(82)91219-9.

[6] A. G. Riess, A. V. Filippenko, P. Challis, A. Clocchiatti, A. Diercks, P. M. Garnavich, R. L. Gilliland, C. J. Hogan, S. Jha, R. P. Kirshner, B. Leibundgut, M. M. Phillips, D. Reiss, B. P. Schmidt, R. A. Schommer, R. C. Smith, J. Spyromilio, C. Stubbs, N. B. Suntzeff, and J. Tonry, "Observational evidence from supernovae for an accelerating universe and a cosmological constant," *Astronomical Journal*, vol. 116, pp. 1009–1038, 1998. arXiv: astro-ph/9805201 [astro-ph].

[7] M. Li, Xiao-Dong, S. Wang, and Y. Wang, "Dark Energy: A brief review," *Front. Phys. (Beijing)*, vol. 8, pp. 828–846, 2013. arXiv: 1209.0922 [astro-ph].

[8] V. C. Rubin, N. Thonnard, and W. K. Ford Jr., "Rotational properties of 21 SC galaxies with a large range of luminosities and radii, from NGC 4605 /R = 4kpc/ to

UGC 2885 /R = 122 kpc/," *Astrophys. J.*, vol. 238, p. 471, 1980. DOI: 10.1086/158003.

[9] D. J. E. Marsh, "Axion Cosmology," *Phys. Rept.*, vol. 643, pp. 1–79, 2016. DOI: 10.1016/j.physrep.2016.06.005. arXiv: 1510.07633 [astro-ph.CO].

[10] J. L. Feng, "Dark Matter Candidates from Particle Physics and Methods of Detection," *Ann. Rev. Astron. Astrophys.*, vol. 48, pp. 495–545, 2010. DOI: 10.1146/annurev-astro-082708-101659. arXiv: 1003.0904 [astro-ph.CO].

[11] B. Carr, F. Kuhnel, and M. Sandstad, "Primordial Black Holes as Dark Matter," *Phys. Rev. D*, vol. 94, no. 8, p. 083 504, 2016. DOI: 10.1103/PhysRevD.94.083504. arXiv: 1607.06077 [astro-ph.CO].

[12] T. Harko, F. S. Lobo, S. Nojiri, and S. D. Odintsov, "$f(R,T)$ gravity," *Phys. Rev. D*, vol. 84, p. 024 020, 2011. DOI: 10.1103/PhysRevD.84.024020. arXiv: 1104.2669 [gr-qc].

[13] E. Cartan, "Sur une generalisation de la notion de courbure de riemann et les espaces a torsion," *Comptes rendus de l'Academie des Sciences de Paris*, 1924.

[14] N. J. Popławski, "Cosmology with torsion: An alternative to cosmic inflation," *Phys. Lett. B*, vol. 694, pp. 181–185, 2010, [Erratum: Phys.Lett.B 701, 672–672 (2011)]. DOI: 10.1016/j.physletb.2010.09.056. arXiv: 1007.0587 [astro-ph.CO].

[15] B. Abbott *et al.*, "Observation of Gravitational Waves from a Binary Black Hole Merger," *Phys. Rev. Lett.*, vol. 116, no. 6, p. 061 102, 2016. DOI: 10.1103/PhysRevLett.116.061102. arXiv: 1602.03837 [gr-qc].

[16] J. Alfaro and M. Gamonal, "A nontrivial footprint of standard cosmology in the future observations of low-frequency gravitational waves," *Gen. Rel. Grav.*, vol. 52, no. 12, p. 118, 2020. DOI: 10.1007/s10714-020-02771-2. arXiv: 1902.04550 [astro-ph.CO].

[17] M. Gamonal, "Slow-roll inflation in f(R,T) gravity and a modified Starobinsky-like inflationary model," *Phys. Dark Univ.*, vol. 31, p. 100 768, 2021. DOI: 10.1016/j.dark.2020.100768. arXiv: 2010.03861 [gr-qc].

[18] A. Einstein, “Erklärung der perihelbewegung des Merkur aus der allgemeinen relativitätstheorie,” *Sitzungsberichte der Königlich Preußischen Akademie der Wissenschaften*, pp. 831–839, 1915.

[19] F Dyson, A Eddington, and C Davidson, “A Determination of the deflection of light by the Sun’s Gravitational Field, from observations made at the Total Eclipse of May 29, 1919,” *Philosophical Transactions of the Royal Society of London Series A*, vol. 220, pp. 291–333, 1920.

[20] N Ashby, “Relativity in the Global Positioning System,” *Living Reviews Foundations of Gravitation*, vol. 6, p. 1, 2003.

[21] B Abbott *et al.*, “Observations of Gravitational Waves from a Binary Black Hole Merger,” *Physical Review Letters*, vol. 116, no. 6, p. 061 102, 2016. arXiv: 1602.03837 [gr-qc].

[22] S. Weinberg, *Gravitation and Cosmology: Principles and Applications of the General Theory of Relativity*. Wiley, 1972.

[23] S. Carroll, *Spacetime and Geometry: An Introduction to General Relativity*, 1ra Ed. Addison Wesley, 2004.

[24] A. Einstein, “Die grundlage der allgemeinen relativitätstheorie,” *Annalen der Physik*, vol. 354, pp. 769–822, 1916.

[25] A. Einstein, “Näherungsweise Integration der Feldgleichungen der Gravitation,” *Sitzungsberichte der Königlich Preußischen Akademie der Wissenschaften, Berlin*, pp. 688–696, Jan. 1916.

[26] A. Le Tiec and J. Novak, “Theory of Gravitational Waves,” in *An Overview of Gravitational Waves: Theory, Sources and Detection*, G. Auger and E. Plagnol, Eds. 2017. DOI: 10.1142/9789813141766_0001. arXiv: 1607.04202 [gr-qc].

[27] A. Ashtekar and E. Bianchi, “A short review of loop quantum gravity,” *Rept. Prog. Phys.*, vol. 84, no. 4, p. 042 001, 2021. DOI: 10.1088/1361-6633/abed91. arXiv: 2104.04394 [gr-qc].

[28] O. Aharony, S. S. Gubser, J. M. Maldacena, H. Ooguri, and Y. Oz, "Large N field theories, string theory and gravity," *Phys. Rept.*, vol. 323, pp. 183–386, 2000. DOI: 10.1016/S0370-1573(99)00083-6. arXiv: hep-th/9905111.

[29] J. Ambjorn, J. Jurkiewicz, and R. Loll, "The Universe from scratch," *Contemp. Phys.*, vol. 47, pp. 103–117, 2006. DOI: 10.1080/00107510600603344. arXiv: hep-th/0509010.

[30] M. Fierz and W. Pauli, "On relativistic wave equations for particles of arbitrary spin in an electromagnetic field," *Proc. Roy. Soc. Lond. A*, vol. 173, pp. 211–232, 1939. DOI: 10.1098/rspa.1939.0140.

[31] M. Maggiore, *Gravitational Waves. Vol. 1: Theory and Experiments*, ser. Oxford Master Series in Physics. Oxford University Press, 2007, ISBN: 978-0-19-857074-5, 978-0-19-852074-0.

[32] A. Friedmann, "Über die krümmung des raumes," *Zeitschrift fur Physik*, vol. 10, pp. 377–386, 1922.

[33] G. Lemaître, "Un univers homogène de masse constante et de rayon croissant rendant compte de la vitesse radiale des nébuleuses extra-galactiques," *Annales de la Société Scientifique de Bruxelles*, vol. 47, pp. 47–59, 1927.

[34] H. Robertson, "Kinematics and World-Structure," *Astrophysical Journal*, vol. 82, p. 284, 1935.

[35] A. Walker, "On Milne's Theory of World-Structure," *Proceedings of the London Mathematical Society*, vol. 42, pp. 90–127, 1937.

[36] E. Di Valentino, O. Mena, S. Pan, L. Visinelli, W. Yang, A. Melchiorri, D. F. Mota, A. G. Riess, and J. Silk, "In the Realm of the Hubble tension − a Review of Solutions," Mar. 2021. arXiv: 2103.01183 [astro-ph.CO].

[37] N. Aghanim *et al.*, "Planck 2018 results. VI. Cosmological parameters," *Astron. Astrophys.*, vol. 641, A6, 2020. DOI: 10.1051/0004-6361/201833910. arXiv: 1807.06209 [astro-ph.CO].

[38] A. A. Penzias and R. W. Wilson, "A Measurement of excess antenna temperature at 4080-Mc/s," *Astrophys. J.*, vol. 142, pp. 419–421, 1965. DOI: 10.1086/148307.

[39] D. Baumann, "Primordial Cosmology," *PoS*, vol. TASI2017, p. 009, 2018. DOI: 10.22323/1.305.0009. arXiv: 1807.03098 [hep-th].

[40] O. F. Piattella, *Lecture Notes in Cosmology*, ser. UNITEXT for Physics. Cham: Springer, 2018. DOI: 10.1007/978-3-319-95570-4. arXiv: 1803.00070 [astro-ph.CO].

[41] S. Weinberg, *Cosmology*. 2008, ISBN: 978-0-19-852682-7.

[42] M. Abramowitz and I. Stegun, *Handbook of mathematical functions with formulas, graphs, and mathematical tables*. Dept. of Commerce, National Bureau of Standards., 1972.

[43] C. M. Will, "The Confrontation between general relativity and experiment," *Living Rev. Rel.*, vol. 9, p. 3, 2006. DOI: 10.12942/lrr-2006-3. arXiv: gr-qc/0510072.

[44] R. Ferraro and F. Fiorini, "Modified teleparallel gravity: Inflation without inflaton," *Phys. Rev. D*, vol. 75, p. 084 031, 2007. DOI: 10.1103/PhysRevD.75.084031. arXiv: gr-qc/0610067.

[45] A. Golovnev and M.-J. Guzmán, "Bianchi identities in $f(T)$ gravity: Paving the way to confrontation with astrophysics," *Phys. Lett. B*, vol. 810, p. 135 806, 2020. DOI: 10.1016/j.physletb.2020.135806. arXiv: 2006.08507 [gr-qc].

[46] H. Shabani and M. Farhoudi, "f(R,T) Cosmological Models in Phase Space," *Phys. Rev. D*, vol. 88, p. 044 048, 2013. DOI: 10.1103/PhysRevD.88.044048. arXiv: 1306.3164 [gr-qc].

[47] H. Shabani and M. Farhoudi, "Cosmological and Solar System Consequences of f(R,T) Gravity Models," *Phys. Rev. D*, vol. 90, no. 4, p. 044 031, 2014. DOI: 10.1103/PhysRevD.90.044031. arXiv: 1407.6187 [gr-qc].

[48] F. Alvarenga, A. de la Cruz-Dombriz, M. Houndjo, M. Rodrigues, and D. Sáez-Gómez, "Dynamics of scalar perturbations in $f(R,T)$ gravity," *Phys. Rev. D*, vol. 87, no. 10, p. 103 526, 2013, [Erratum: Phys.Rev.D 87, 129905 (2013)]. DOI: 10.1103/PhysRevD.87.103526. arXiv: 1302.1866 [gr-qc].

[49] M. Sharif and M. Zubair, "Thermodynamics in f(R,T) Theory of Gravity," *JCAP*, vol. 03, p. 028, 2012, [Erratum: JCAP 05, E01 (2012)]. DOI: 10.1088/1475-7516/2012/03/028. arXiv: 1204.0848 [gr-qc].

[50] G. Sun and Y.-C. Huang, "The cosmology in f(R,τ) gravity without dark energy," *Int. J. Mod. Phys. D*, vol. 25, no. 03, p. 1 650 038, 2016. DOI: 10.1142/S0218271816500383. arXiv: 1510.01061 [gr-qc].

[51] R. Zaregonbadi, M. Farhoudi, and N. Riazi, "Dark Matter From f(R,T) Gravity," *Phys. Rev. D*, vol. 94, p. 084 052, 2016. DOI: 10.1103/PhysRevD.94.084052. arXiv: 1608.00469 [gr-qc].

[52] R. Myrzakulov, "FRW Cosmology in F(R,T) gravity," *Eur. Phys. J. C*, vol. 72, p. 2203, 2012. DOI: 10.1140/epjc/s10052-012-2203-y. arXiv: 1207.1039 [gr-qc].

[53] M. Alves, P. Moraes, J. de Araujo, and M. Malheiro, "Gravitational waves in $f(R,T)$ and $f(R,T^\phi)$ theories of gravity," *Phys. Rev. D*, vol. 94, no. 2, p. 024 032, 2016. DOI: 10.1103/PhysRevD.94.024032. arXiv: 1604.03874 [gr-qc].

[54] M. Sharif and A. Siddiqa, "Propagation of polar gravitational waves in $f(R,T)$ scenario," *Gen. Rel. Grav.*, vol. 51, no. 6, p. 74, 2019. DOI: 10.1007/s10714-019-2558-6. arXiv: 1907.05714 [gr-qc].

[55] M.-X. Xu, T. Harko, and S.-D. Liang, "Quantum Cosmology of $f(R,T)$ gravity," *Eur. Phys. J. C*, vol. 76, no. 8, p. 449, 2016. DOI: 10.1140/epjc/s10052-016-4303-6. arXiv: 1608.00113 [gr-qc].

[56] S. Bhattacharjee, J. Santos, P. Moraes, and P. Sahoo, "Inflation in $f(R,T)$ gravity," *Eur. Phys. J. Plus*, vol. 135, no. 7, p. 576, 2020. DOI: 10.1140/epjp/s13360-020-00583-6. arXiv: 2006.04336 [gr-qc].

[57] M. Jamil, D. Momeni, M. Raza, and R. Myrzakulov, "Reconstruction of some cosmological models in f(R,T) gravity," *Eur. Phys. J. C*, vol. 72, p. 1999, 2012. DOI: 10.1140/epjc/s10052-012-1999-9. arXiv: 1107.5807 [physics.gen-ph].

[58] P. Moraes, J. D. Arbañil, and M. Malheiro, "Stellar equilibrium configurations of compact stars in $f(R,T)$ gravity," *JCAP*, vol. 06, p. 005, 2016. DOI: 10.1088/1475-7516/2016/06/005. arXiv: 1511.06282 [gr-qc].

[59] Z. Yousaf, K. Bamba, and M. Z. u. H. Bhatti, "Causes of Irregular Energy Density in $f(R,T)$ Gravity," *Phys. Rev. D*, vol. 93, no. 12, p. 124 048, 2016. DOI: 10.1103/PhysRevD.93.124048. arXiv: 1606.00147 [gr-qc].

[60] P. Moraes and J. Santos, "A complete cosmological scenario from $f(R,T^{\phi})$ gravity theory," *Eur. Phys. J. C*, vol. 76, p. 60, 2016. DOI: 10.1140/epjc/s10052-016-3912-4. arXiv: 1601.02811 [gr-qc].

[61] P. Moraes and P. Sahoo, "Modelling wormholes in $f(R,T)$ gravity," *Phys. Rev. D*, vol. 96, no. 4, p. 044 038, 2017. DOI: 10.1103/PhysRevD.96.044038. arXiv: 1707.06968 [gr-qc].

[62] H. Shabani and A. H. Ziaie, "Bouncing cosmological solutions from $f(\mathsf{R},\mathsf{T})$ gravity," *Eur. Phys. J. C*, vol. 78, no. 5, p. 397, 2018. DOI: 10.1140/epjc/s10052-018-5886-x. arXiv: 1708.07874 [gr-qc].

[63] S. dos Santos, G. Carvalho, P. Moraes, C. Lenzi, and M. Malheiro, "A conservative energy-momentum tensor in the $f(R,T)$ gravity and its implications for the phenomenology of neutron stars," *Eur. Phys. J. Plus*, vol. 134, no. 8, p. 398, 2019. DOI: 10.1140/epjp/i2019-12830-8. arXiv: 1803.07719 [gr-qc].

[64] Z. Yousaf, K. Bamba, M. Bhatti, and U. Ghafoor, "Charged Gravastars in Modified Gravity," *Phys. Rev. D*, vol. 100, no. 2, p. 024 062, 2019. DOI: 10.1103/PhysRevD.100.024062. arXiv: 1907.05233 [gr-qc].

[65] D. Taser, "Conformally symmetric Friedmann–Robertson–Walker metric in $f(R,T)$ gravity," *Mod. Phys. Lett. A*, vol. 35, no. 10, p. 2 050 067, 2020. DOI: 10.1142/S0217732320500674.

[66] S. Maurya, A. Errehymy, K. N. Singh, F. Tello-Ortiz, and M. Daoud, "Gravitational decoupling minimal geometric deformation model in modified $f(R,T)$ gravity theory," *Phys. Dark Univ.*, vol. 30, p. 100 640, 2020. DOI: 10.1016/j.dark.2020.100640. arXiv: 2003.03720 [gr-qc].

[67] A. K. Yadav, L. K. Sharma, B. Singh, and P. Sahoo, "Existence of bulk viscous universe in $f(R,T)$ gravity and confrontation with observational data," *New Astron.*, vol. 78, p. 101 382, 2020. DOI: 10.1016/j.newast.2020.101382. arXiv: 2002.12763 [physics.gen-ph].

[68] S. Bhattacharjee and P. Sahoo, "Comprehensive Analysis of a Non-Singular Bounce in $f(R,T)$ Gravitation," *Phys. Dark Univ.*, vol. 28, p. 100 537, 2020. DOI: 10.1016/j.dark.2020.100537. arXiv: 2003.14211 [gr-qc].

[69] S. Bhattacharjee and P. Sahoo, "Redshift Drift in $f(R,T)$ Gravity," *New Astron.*, vol. 81, p. 101 425, 2020. DOI: 10.1016/j.newast.2020.101425. arXiv: 2005.11163 [gr-qc].

[70] R. K. Tiwari, D. Sofuoğlu, and S. K. Mishra, "Accelerating universe with varying Λ in $f(R,T)$ theory of gravity," *New Astron.*, vol. 83, p. 101 476, 2021. DOI: 10.1016/j.newast.2020.101476.

[71] S. Aygün, C. Aktaş, P. K. Sahoo, and B. K. Bishi, "Scalar Field Cosmology in $f(R,T)$ Gravity with Λ," *Grav. Cosmol.*, vol. 24, no. 3, pp. 302–307, 2018. DOI: 10.1134/S0202289318030039.

[72] V. Faraoni, *Cosmology in scalar tensor gravity*. 2004, vol. 139, ISBN: 978-1-4020-1988-3. DOI: 10.1007/978-1-4020-1989-0.

[73] M. Postma and M. Volponi, "Equivalence of the Einstein and Jordan frames," *Phys. Rev. D*, vol. 90, no. 10, p. 103 516, 2014. DOI: 10.1103/PhysRevD.90.103516. arXiv: 1407.6874 [astro-ph.CO].

[74] K. Freese, J. A. Frieman, and A. V. Olinto, "Natural inflation with pseudo - Nambu-Goldstone bosons," *Phys. Rev. Lett.*, vol. 65, pp. 3233–3236, 1990. DOI: 10.1103/PhysRevLett.65.3233.

[75] F. C. Adams, J. Bond, K. Freese, J. A. Frieman, and A. V. Olinto, "Natural inflation: Particle physics models, power law spectra for large scale structure, and constraints from COBE," *Phys. Rev. D*, vol. 47, pp. 426–455, 1993. DOI: 10.1103/PhysRevD.47.426. arXiv: hep-ph/9207245.

[76] L. Boubekeur and D. H. Lyth, "Hilltop inflation," *JCAP*, vol. 07, p. 010, 2005. DOI: 10.1088/1475-7516/2005/07/010. arXiv: hep-ph/0502047.

[77] K. Dimopoulos, "An analytic treatment of quartic hilltop inflation," *Phys. Lett. B*, vol. 809, p. 135 688, 2020. DOI: 10.1016/j.physletb.2020.135688. arXiv: 2006.06029 [hep-ph].

[78] A. Mazumdar and J. Rocher, "Particle physics models of inflation and curvaton scenarios," *Phys. Rept.*, vol. 497, pp. 85–215, 2011. DOI: 10.1016/j.physrep.2010.08.001. arXiv: 1001.0993 [hep-ph].

[79] D. Chialva and A. Mazumdar, "Cosmological implications of quantum corrections and higher-derivative extension," *Mod. Phys. Lett. A*, vol. 30, no. 03n04, p. 1 540 008, 2015. DOI: 10.1142/S0217732315400088. arXiv: 1405.0513 [hep-th].

[80] S. Kaneda, S. V. Ketov, and N. Watanabe, "Fourth-order gravity as the inflationary model revisited," *Mod. Phys. Lett. A*, vol. 25, pp. 2753–2762, 2010. DOI: 10.1142/S0217732310033918. arXiv: 1001.5118 [hep-th].

[81] L. Sebastiani and R. Myrzakulov, "F(R) gravity and inflation," *Int. J. Geom. Meth. Mod. Phys.*, vol. 12, no. 9, p. 1 530 003, 2015. DOI: 10.1142/S0219887815300032. arXiv: 1506.05330 [gr-qc].

[82] F. L. Bezrukov and M. Shaposhnikov, "The Standard Model Higgs boson as the inflaton," *Phys. Lett. B*, vol. 659, pp. 703–706, 2008. DOI: 10.1016/j.physletb.2007.11.072. arXiv: 0710.3755 [hep-th].

[83] A. Kehagias, A. Moradinezhad Dizgah, and A. Riotto, "Remarks on the Starobinsky model of inflation and its descendants," *Phys. Rev. D*, vol. 89, no. 4, p. 043 527, 2014. DOI: 10.1103/PhysRevD.89.043527. arXiv: 1312.1155 [hep-th].

[84] Y. Aldabergenov, R. Ishikawa, S. V. Ketov, and S. I. Kruglov, "Beyond Starobinsky inflation," *Phys. Rev. D*, vol. 98, no. 8, p. 083 511, 2018. DOI: 10.1103/PhysRevD.98.083511. arXiv: 1807.08394 [hep-th].

[85] R. Cuzinatto, L. Medeiros, and P. Pompeia, "Higher-order modified Starobinsky inflation," *JCAP*, vol. 02, p. 055, 2019. DOI: 10.1088/1475-7516/2019/02/055. arXiv: 1810.08911 [gr-qc].

[86] S. F. King and E. Perdomo, "Starobinsky-like inflation and soft-SUSY breaking," *JHEP*, vol. 05, p. 211, 2019. DOI: 10.1007/JHEP05(2019)211. arXiv: 1903.08448 [hep-ph].

[87] D. Y. Cheong, H. M. Lee, and S. C. Park, "Beyond the Starobinsky model for inflation," *Phys. Lett. B*, vol. 805, p. 135 453, 2020. DOI: 10.1016/j.physletb.2020.135453. arXiv: 2002.07981 [hep-ph].

[88] A. S. Koshelev, K. Sravan Kumar, A. Mazumdar, and A. A. Starobinsky, "Non-Gaussianities and tensor-to-scalar ratio in non-local R^2-like inflation," *JHEP*, vol. 06, p. 152, 2020. DOI: 10.1007/JHEP06(2020)152. arXiv: 2003.00629 [hep-th].

[89] J. Martin, C. Ringeval, and V. Vennin, "Encyclopædia Inflationaris," *Phys. Dark Univ.*, vol. 5-6, pp. 75–235, 2014. DOI: 10.1016/j.dark.2014.01.003. arXiv: 1303.3787 [astro-ph.CO].

[90] J. Alfaro and S. M. Riquelme, "Bosonic (p-1)-forms in Einstein-Cartan theory of gravity," *Phys. Rev. D*, vol. 90, no. 10, p. 104 005, 2014. DOI: 10.1103/PhysRevD.90.104005. arXiv: 1402.0057 [hep-th].

[91] S. Groot Nibbelink and B. J. W. van Tent, "Scalar perturbations during multiple field slow-roll inflation," *Class. Quant. Grav.*, vol. 19, pp. 613–640, 2002. DOI: 10.1088/0264-9381/19/4/302. arXiv: hep-ph/0107272.

[92] S. Groot Nibbelink and B. J. W. van Tent, "Density perturbations arising from multiple field slow roll inflation," Nov. 2000. arXiv: hep-ph/0011325.

[93] C. M. Peterson and M. Tegmark, "Testing Two-Field Inflation," *Phys. Rev. D*, vol. 83, p. 023 522, 2011. DOI: 10.1103/PhysRevD.83.023522. arXiv: 1005.4056 [astro-ph.CO].

[94] A. Achúcarro, G. A. Palma, D.-G. Wang, and Y. Welling, "Origin of ultra-light fields during inflation and their suppressed non-Gaussianity," *JCAP*, vol. 10, p. 018, 2020. DOI: 10.1088/1475-7516/2020/10/018. arXiv: 1908.06956 [hep-th].

[95] J. Bernabeu, D. Espriu, and D. Puigdomenech, "Gravitational waves in the presence of a cosmological constant," *Phys. Rev. D*, vol. 84, p. 063 523, 2011, [Erratum: Phys.Rev.D 86, 069904 (2012)]. DOI: 10.1103/PhysRevD.84.063523. arXiv: 1106.4511 [hep-th].

[96] D. Espriu and D. Puigdomenech, "Local measurement of Λ using pulsar timing arrays," *Astrophys. J.*, vol. 764, p. 163, 2013. DOI: 10.1088/0004-637X/764/2/163. arXiv: 1209.3724 [gr-qc].

[97] D. Espriu, "Pulsar Timing Arrays and the cosmological constant," *AIP Conf. Proc.*, vol. 1606, no. 1, pp. 86–98, 2015. DOI: 10.1063/1.4891120. arXiv: 1401.7925 [astro-ph.CO].

[98] J. Alfaro, D. Espriu, and L. Gabbanelli, "On the propagation of gravitational waves in a ΛCDM universe," *Class. Quant. Grav.*, vol. 36, no. 2, p. 025 006, 2019. DOI: 10.1088/1361-6382/aaf675. arXiv: 1711.08315 [hep-th].

[99] G. Hobbs and S. Dai, "Gravitational wave research using pulsar timing arrays," *Natl. Sci. Rev.*, vol. 4, no. 5, pp. 707–717, 2017. DOI: 10.1093/nsr/nwx126. arXiv: 1707.01615 [astro-ph.IM].

[100] B. Perera *et al.*, "The International Pulsar Timing Array: Second data release," *Mon. Not. Roy. Astron. Soc.*, vol. 490, no. 4, pp. 4666–4687, 2019. DOI: 10.1093/mnras/stz2857. arXiv: 1909.04534 [astro-ph.HE].

[101] L. S. Finn, "The Response of interferometric gravitational wave detectors," *Phys. Rev. D*, vol. 79, p. 022 002, 2009. DOI: 10.1103/PhysRevD.79.022002. arXiv: 0810.4529 [gr-qc].

[102] X. Deng and L. S. Finn, "Pulsar timing array observations of gravitational wave source timing parallax," *Mon. Not. Roy. Astron. Soc.*, vol. 414, pp. 50–58, 2011. DOI: 10.1111/j.1365-2966.2010.17913.x. arXiv: 1008.0320 [astro-ph.CO].

[103] S. Babak *et al.*, "European Pulsar Timing Array Limits on Continuous Gravitational Waves from Individual Supermassive Black Hole Binaries," *Mon. Not. Roy. Astron.*

Soc., vol. 455, no. 2, pp. 1665–1679, 2016. DOI: 10.1093/mnras/stv2092. arXiv: 1509.02165 [astro-ph.CO].

[104] L. Kelley, M. Charisi, S. Burke-Spolaor, J. Simon, L. Blecha, T. Bogdanovic, M. Colpi, J. Comerford, D. D'Orazio, M. Dotti, M. Eracleous, M. Graham, J. Greene, Z. Haiman, K. Holley-Bockelmann, E. Kara, B. Kelly, S. Komossa, S. Larson, X. Liu, C. P. Ma, S. Noble, V. Paschalidis, R. Rafikov, V. Ravi, J. Runnoe, A. Sesana, D. Stern, M. A. Strauss, V. U, M. Volonteri, and Nanograv Collaboration, "Multi-Messenger Astrophysics With Pulsar Timing Arrays," *Bull. Am. Astron. Soc.*, vol. 51, no. 3, 490, p. 490, May 2019. arXiv: 1903.07644 [astro-ph.HE].

[105] M. A. McLaughlin, "The North American Nanohertz Observatory for Gravitational Waves," *Class. Quant. Grav.*, vol. 30, p. 224 008, 2013. DOI: 10.1088/0264-9381/30/22/224008. arXiv: 1310.0758 [astro-ph.IM].

[106] S. Barke, Y. Wang, J. Esteban Delgado, M. Tröbs, G. Heinzel, and K. Danzmann, "Towards a gravitational wave observatory designer: sensitivity limits of space-borne detectors," *Class. Quant. Grav.*, vol. 32, no. 9, p. 095 004, 2015. DOI: 10.1088/0264-9381/32/9/095004. arXiv: 1411.1260 [physics.ins-det].

[107] J. Verbiest *et al.*, "The International Pulsar Timing Array: First Data Release," *Mon. Not. Roy. Astron. Soc.*, vol. 458, no. 2, pp. 1267–1288, 2016. DOI: 10.1093/mnras/stw347. arXiv: 1602.03640 [astro-ph.IM].

[108] B. Ryden, *Introduction to Cosmology*. Addison-Wesley, 2003.

[109] C. M. F. Mingarelli, T. J. W. Lazio, A. Sesana, J. E. Greene, J. A. Ellis, C.-P. Ma, S. Croft, S. Burke-Spolaor, and S. R. Taylor, "The local nanohertz gravitational-wave landscape from supermassive black hole binaries," *Nature Astronomy*, vol. 1, pp. 886–892, Nov. 2017. DOI: 10.1038/s41550-017-0299-6. arXiv: 1708.03491 [astro-ph.GA].

[110] R. N. Manchester, G. B. Hobbs, A Teoh, and M Hobbs, "The Australia Telescope National Facility pulsar catalogue," *Astron. J.*, vol. 129, p. 1993, 2005. DOI: 10.1086/428488. arXiv: astro-ph/0412641.

[111] X. Zhu, L. Wen, J. Xiong, Y. Xu, Y. Wang, S. D. Mohanty, G. Hobbs, and R. N. Manchester, "Detection and localization of continuous gravitational waves with pulsar timing arrays: the role of pulsar terms," *Mon. Not. Roy. Astron. Soc.*, vol. 461, no. 2, pp. 1317–1327, 2016. DOI: 10.1093/mnras/stw1446. arXiv: 1606.04539 [astro-ph.IM].

[112] K. Schwarzschild, "Über das Gravitationsfeld eines Massenpunktes nach der Einsteinschen Theorie," *Sitzungsber. Preuss. Akad. Wiss. Berlin (Math. Phys.)*, pp. 189–196, 1916.

Appendix A. Derivation of linearized gravity

The Einstein Field Equations, which describe the curvature of space–time by the effect of matter, are given by,

$$R_{\mu\nu} - \frac{1}{2} R g_{\mu\nu} = \frac{8\pi G}{c^4} T_{\mu\nu}, \tag{A.1}$$

where $R_{\mu\nu}$ is the Ricci tensor, R is the scalar of curvature, $g_{\mu\nu}$ is the metric tensor and $T_{\mu\nu}$ is the energy–momentum tensor. Thus, if a source of matter produce a little perturbation on space–time, e.g. a binary system or a rotating body, we can write the metric tensor as,

$$g_{\mu\nu} = \bar{g}_{\mu\nu} + h_{\mu\nu}, \qquad |h_{\mu\nu}| \ll 1 \tag{A.2}$$

where $\bar{g}_{\mu\nu}$ is the background metric of space–time and $h_{\mu\nu}$ is a symmetric tensor of rank 2. For instance, let us take a minkowskian background, i.e. $\bar{g}_{\mu\nu} = \eta_{\mu\nu}$, such that

$$g_{\mu\nu} = \eta_{\mu\nu} + h_{\mu\nu}, \qquad |h_{\mu\nu}| \ll 1. \tag{A.3}$$

The result of doing perturbation theory on the Field Equations is called *Linearized Theory*. Note that if we choose a reference frame in which (A.3) holds, some residual gauge symmetry remains. For example, consider the transformation,

$$x^\mu \longrightarrow x'^\mu = x^\mu + \xi^\mu(x^\mu), \qquad |\partial_\mu \xi_\nu| \sim |h_{\mu\nu}| \ll 1 \tag{A.4}$$

Using the general coordinate transformation law of a second rank tensor on the metric,

$$g_{\mu\nu}(x^\mu) = \frac{\partial x'^\rho}{\partial x^\mu} \frac{\partial x'^\sigma}{\partial x^\nu} g'_{\rho\sigma}(x'^\mu),$$

and

$$\frac{\partial x'^\rho}{\partial x^\nu} = \delta^\rho_\nu + \partial_\nu \xi^\rho$$

Therefore,

$$
\begin{aligned}
g_{\mu\nu}(x^\mu) &= (\delta^\rho_\mu + \partial_\mu \xi^\rho)(\delta^\sigma_\nu + \partial_\nu \xi^\sigma) g'_{\rho\sigma}(x'^\mu) \\
&= (\delta^\rho_\mu \delta^\sigma_\nu + \delta^\rho_\mu \partial_\nu \xi^\sigma + \partial_\mu \xi^\rho \delta^\sigma_\nu + (\partial_\mu \xi^\rho)(\partial_\nu \xi^\sigma))(\eta'_{\rho\sigma} + h'_{\rho\sigma}) \\
\eta_{\mu\nu} + h_{\mu\nu} &\cong (\delta^\rho_\mu \delta^\sigma_\nu + \delta^\rho_\mu \partial_\nu \xi^\sigma + \partial_\mu \xi^\rho \delta^\sigma_\nu)(\eta'_{\rho\sigma} + h'_{\rho\sigma}) \\
&= \eta'_{\mu\nu} + \eta'{}_{\mu\sigma} \partial_\nu \xi^\sigma + \eta'{}_{\rho\nu} \partial_\mu \xi^\rho + h'_{\mu\nu} + h'_{\rho\sigma}(\delta^\rho_\mu \partial_\nu \xi^\sigma + \partial_\mu \xi^\rho \delta^\sigma_\nu) \\
&\cong \eta'_{\mu\nu} + \eta'{}_{\mu\sigma} \partial_\nu \xi^\sigma + \eta'{}_{\rho\nu} \partial_\mu \xi^\rho + h'_{\mu\nu} \\
h'_{\mu\nu} &= h_{\mu\nu} - (\partial_\mu \xi_\nu + \partial_\nu \xi_\mu) + \mathcal{O}\Big(h^2\Big).
\end{aligned}
\tag{A.5}
$$

As $|\partial_\mu \xi_\nu| \sim |h_{\mu\nu}|$, the condition $|h_{\mu\nu}| \ll 1$ is preserved under the gauge transformation and hence, the slowly varying diffeomorphisms are a symmetry of the linear theory. Besides, as $h_{\mu\nu}$ transforms as a tensor under Lorentz transformations,

$$
h'_{\mu\nu} = \Lambda^\rho{}_\mu \Lambda^\sigma{}_\nu h_{\rho\sigma},
$$

and $h_{\mu\nu}$ is invariant under constant translations,

$$
x^\mu \longrightarrow x'^\mu = x^\mu + a^\mu,
$$

we may say that the linearized theory is invariant under finite Poincaré transformations. We summarize this result as:

Full Theory $\longrightarrow$ Covariant under general coordinate transformation

Linearized Theory $\longrightarrow$ Invariant under infinitesimal local transformation $+$ Poincaré symmetry.

For the next equations, the label $(\cdot)^{(1)}$ indicates that the term is linear in $h_{\mu\nu}$. Therefore, in the linearized theory, the Christoffel symbol is given by,

$$
\begin{aligned}
\Gamma^\rho{}_{\mu\nu} &\equiv \frac{1}{2} g^{\rho\sigma}(\partial_\mu g_{\sigma\nu} + \partial_\nu g_{\sigma\mu} - \partial_\sigma g_{\mu\nu}) \\
\Gamma^{\rho(1)}_{\mu\nu} &= \frac{1}{2} \eta^{\rho\sigma}(\partial_\mu h_{\sigma\nu} + \partial_\nu h_{\sigma\mu} - \partial_\sigma h_{\mu\nu}) + \mathcal{O}\Big(h^2_{\mu\nu}\Big)
\end{aligned}
$$

In the same way, linearized the Riemann tensor reads,

$$
\begin{aligned}
R^{\mu}{}_{\nu\rho\sigma} &\equiv \partial_\rho \Gamma^{\mu}{}_{\nu\sigma} - \partial_\sigma \Gamma^{\mu}{}_{\nu\rho} + \Gamma^{\mu}{}_{\alpha\rho}\Gamma^{\alpha}{}_{\nu\sigma} - \Gamma^{\mu}{}_{\alpha\sigma}\Gamma^{\alpha}{}_{\nu\rho} \\
R^{\mu(1)}_{\nu\rho\sigma} &= \partial_\rho \Gamma^{\mu(1)}_{\nu\sigma} - \partial_\sigma \Gamma^{\mu(1)}_{\nu\rho} + \mathcal{O}\Big(h^2_{\mu\nu}\Big) \\
&= \frac{1}{2}\eta^{\mu\lambda}(\partial_\rho\partial_\nu h_{\lambda\sigma} + \partial_\rho\partial_\sigma h_{\lambda\nu} - \partial_\rho\partial_\lambda h_{\nu\sigma} - \partial_\sigma\partial_\nu h_{\lambda\rho} - \partial_\sigma\partial_\rho h_{\lambda\nu} + \partial_\sigma\partial_\lambda h_{\nu\rho}) + \mathcal{O}\Big(h^2_{\mu\nu}\Big) \\
&= \frac{1}{2}\eta^{\mu\lambda}(\partial_\rho\partial_\nu h_{\lambda\sigma} + \partial_\sigma\partial_\lambda h_{\nu\rho} - \partial_\rho\partial_\lambda h_{\nu\sigma} - \partial_\sigma\partial_\nu h_{\lambda\rho}) + \mathcal{O}\Big(h^2_{\mu\nu}\Big)
\end{aligned}
$$

Hence, the Ricci tensor in the linearized theory reads,

$$
\begin{aligned}
R_{\mu\nu} &\equiv R^{\alpha}{}_{\mu\alpha\nu} \\
R^{(1)}_{\mu\nu} &= R^{\alpha(1)}_{\mu\alpha\nu} \\
&= \frac{1}{2}\eta^{\alpha\lambda}(\partial_\alpha\partial_\mu h_{\lambda\nu} + \partial_\nu\partial_\lambda h_{\mu\alpha} - \partial_\alpha\partial_\lambda h_{\mu\nu} - \partial_\nu\partial_\mu h_{\lambda\alpha}) + \mathcal{O}\Big(h^2_{\mu\nu}\Big) \\
&= \frac{1}{2}\Big(\partial^\lambda\partial_\mu h_{\lambda\nu} + \partial^\alpha\partial_\nu h_{\mu\alpha} - \partial^\lambda\partial_\lambda h_{\mu\nu} - \partial_\mu\partial_\nu h^{\alpha}{}_{\alpha}\Big) + \mathcal{O}\Big(h^2_{\mu\nu}\Big) \\
&= \frac{1}{2}\Big(\partial^\lambda\partial_\mu h_{\lambda\nu} + \partial^\alpha\partial_\nu h_{\mu\alpha} - \Box h_{\mu\nu} - \partial_\mu\partial_\nu h\Big) + \mathcal{O}\Big(h^2_{\mu\nu}\Big),
\end{aligned}
\tag{A.6}
$$

where in the last line we have defined the trace of the metric perturbation,

$$h \equiv \eta^{\mu\nu} h_{\mu\nu} = h^{\mu}{}_{\mu}, \tag{A.7}$$

and $\Box(\cdot)$ is known as the D'Alembert operator, which in flat space–time is given by,

$$\Box(\cdot) \equiv \eta^{\mu\nu}\partial_\mu\partial_\nu(\cdot) = \partial_\mu\partial^\mu(\cdot) \tag{A.8}$$

The Ricci scalar can be obtained at first order in the same way,

$$
\begin{aligned}
R &\equiv g^{\mu\nu} R_{\mu\nu} \\
R^{(1)} &= \eta^{\mu\nu} R^{(1)}_{\mu\nu} + \mathcal{O}\Big(h^2_{\mu\nu}\Big) \\
&= \frac{1}{2}\eta^{\mu\nu}\Big(\partial^\lambda\partial_\mu h_{\lambda\nu} + \partial^\alpha\partial_\nu h_{\mu\alpha} - \Box h_{\mu\nu} - \partial_\mu\partial_\nu h\Big) + \mathcal{O}\Big(h^2_{\mu\nu}\Big) \\
&= \frac{1}{2}\Big(\partial^\lambda\partial^\mu h_{\lambda\mu} + \partial^\alpha\partial^\mu h_{\mu\alpha} - \Box h - \Box h\Big) + \mathcal{O}\Big(h^2_{\mu\nu}\Big) \\
&= \partial^\alpha\partial^\beta h_{\alpha\beta} - \Box h + \mathcal{O}\Big(h^2_{\mu\nu}\Big)
\end{aligned}
$$

Thus, the linearized version of the Einstein Field Equations become,

$$
\begin{aligned}
R^{(1)}_{\mu\nu} - \frac{1}{2}\eta_{\mu\nu}R^{(1)} &= \frac{1}{2}\Big(\partial^\lambda\partial_\mu h_{\lambda\nu} + \partial^\alpha\partial_\nu h_{\mu\alpha} - \Box h_{\mu\nu} - \partial_\mu\partial_\nu h\Big) - \frac{1}{2}\eta_{\mu\nu}\Big(\partial^\alpha\partial^\beta h_{\alpha\beta} - \Box h\Big) + \mathcal{O}\Big(h^2_{\mu\nu}\Big) \\
&= \frac{1}{2}\Big[\partial^\lambda\partial_\mu h_{\lambda\nu} + \partial^\alpha\partial_\nu h_{\mu\alpha} - \Box h_{\mu\nu} - \partial_\mu\partial_\nu h - \eta_{\mu\nu}\partial^\alpha\partial^\beta h_{\alpha\beta} + \eta_{\mu\nu}\Box h\Big] + \mathcal{O}\Big(h^2_{\mu\nu}\Big).
\end{aligned}
$$

In vaccum, we obtain the Fierz–Pauli equation for a massless spin–2 particle,

$$
\partial^\lambda\partial_\mu h_{\lambda\nu} + \partial^\alpha\partial_\nu h_{\mu\alpha} - \Box h_{\mu\nu} - \partial_\mu\partial_\nu h - \eta_{\mu\nu}\partial^\alpha\partial^\beta h_{\alpha\beta} + \eta_{\mu\nu}\Box h = 0 \tag{A.9}
$$

If we define the trace–reversed metric perturbation as,

$$
\bar{h}_{\mu\nu} \equiv h_{\mu\nu} - \frac{1}{2}\eta_{\mu\nu}h, \tag{A.10}
$$

whose trace satisfies,

$$
\bar{h} \equiv \eta^{\mu\nu}\bar{h}_{\mu\nu} = \eta^{\mu\nu}h_{\mu\nu} - \frac{1}{2}\eta^{\mu\nu}\eta_{\mu\nu}h = h - 2h = -h, \tag{A.11}
$$

we can express the usual metric perturbation as,

$$
h_{\mu\nu} = \bar{h}_{\mu\nu} + \frac{1}{2}\eta_{\mu\nu}h = \bar{h}_{\mu\nu} - \frac{1}{2}\eta_{\mu\nu}\bar{h} \tag{A.12}
$$

Therefore, using the trace–reversed perturbation, the Field Equations reads,

$$
\begin{aligned}
R^{(1)}_{\mu\nu} - \frac{1}{2}\eta_{\mu\nu}R^{(1)} &= \frac{1}{2}\Big[\partial^\lambda\partial_\mu\Big(\bar{h}_{\lambda\nu} - \frac{1}{2}\eta_{\lambda\nu}\bar{h}\Big) + \partial^\alpha\partial_\nu\Big(\bar{h}_{\mu\alpha} - \frac{1}{2}\eta_{\mu\alpha}\bar{h}\Big) - \Box\Big(\bar{h}_{\mu\nu} - \frac{1}{2}\eta_{\mu\nu}\bar{h}\Big) \\
&\qquad -\partial_\mu\partial_\nu(-\bar{h}) - \eta_{\mu\nu}\partial^\alpha\partial^\beta\Big(\bar{h}_{\alpha\beta} - \frac{1}{2}\eta_{\alpha\beta}\bar{h}\Big) + \eta_{\mu\nu}\Box(-\bar{h})\Big] \\
&= \frac{1}{2}\Big[\partial^\lambda\partial_\mu\bar{h}_{\lambda\nu} - \cancel{\frac{1}{2}\partial_\nu\partial_\mu\bar{h}} + \partial^\alpha\partial_\nu\bar{h}_{\mu\alpha} - \cancel{\frac{1}{2}\partial_\mu\partial_\nu\bar{h}} - \Box\bar{h}_{\mu\nu} + \cancel{\frac{1}{2}\eta_{\mu\nu}\Box\bar{h}} + \cancel{\partial_\mu\partial_\nu\bar{h}} \\
&\qquad -\eta_{\mu\nu}\partial^\alpha\partial^\beta\bar{h}_{\alpha\beta} + \cancel{\frac{1}{2}\eta_{\mu\nu}\Box\bar{h}} - \cancel{\eta_{\mu\nu}\Box\bar{h}}\Big] \\
&= \frac{1}{2}\Big[\partial^\lambda\partial_\mu\bar{h}_{\lambda\nu} + \partial^\alpha\partial_\nu\bar{h}_{\mu\alpha} - \Box\bar{h}_{\mu\nu} - \eta_{\mu\nu}\partial^\alpha\partial^\beta\bar{h}_{\alpha\beta}\Big]
\end{aligned}
$$

Thus, the trace–reversed metric perturbation satisfies the linearized Field Equations

$$
\Box\bar{h}_{\mu\nu} + \eta_{\mu\nu}\partial^\alpha\partial^\beta\bar{h}_{\alpha\beta} - \partial^\alpha\partial_\nu\bar{h}_{\mu\alpha} - \partial^\alpha\partial_\mu\bar{h}_{\alpha\nu} = -\frac{16\pi G}{c^4}T_{\mu\nu} \tag{A.13}
$$

Using the gauge symmetry of the linearized theory in flat space–time, given by equation (A.5), we can try to fix the gauge through the *Lorenz gauge condition*,

$$
\partial^\nu\bar{h}_{\mu\nu} = 0 \tag{A.14}
$$

To verify this, let us write the gauge transformation of eq. (A.5) in terms of the trace–reversed metric perturbation,

$$
\begin{aligned}
\bar{h}_{\mu\nu} \longrightarrow \bar{h}'_{\mu\nu} = h'_{\mu\nu} - \frac{1}{2}\eta_{\mu\nu}h' &= h_{\mu\nu} - (\partial_\mu\xi_\nu + \partial_\nu\xi_\mu) - \frac{1}{2}\eta_{\mu\nu}(\eta^{\alpha\beta}h'_{\alpha\beta}) \\
&= h_{\mu\nu} - (\partial_\mu\xi_\nu + \partial_\nu\xi_\mu) - \frac{1}{2}\eta_{\mu\nu}\eta^{\alpha\beta}(h_{\alpha\beta} - \partial_\alpha\xi_\beta - \partial_\beta\xi_\alpha) \\
&= \bar{h}_{\mu\nu} - (\partial_\mu\xi_\nu + \partial_\nu\xi_\mu - \eta_{\mu\nu}\partial_\alpha\xi^\alpha),
\end{aligned}
$$

and hence, the Lorenz conditions transforms as,

$$\begin{aligned}\partial^\nu \bar{h}_{\mu\nu} \longrightarrow (\partial^\nu \bar{h}_{\mu\nu})' &= \partial^\nu \bar{h}_{\mu\nu} - \cancel{\partial^\nu \partial_\mu \xi_\nu} - \partial^\nu \partial_\nu \xi_\mu + \cancel{\eta_{\mu\nu}\partial^\nu \partial_\alpha \xi^\alpha} \\ &= \partial^\nu \bar{h}_{\mu\nu} - \Box \xi_\mu\end{aligned}$$

Let us suppose that initially the field $h_{\mu\nu}$ satisfies $\partial^\nu \bar{h}_{\mu\nu} = f_\mu(x^\alpha)$, for an arbitrary continuous function f_μ. Then, in order to obtain coordinates where $(\partial^\nu \bar{h}_{\mu\nu})' = 0$ holds, we must solve

$$\Box \xi_\mu = f_\mu(x^\alpha), \tag{A.15}$$

but actually this equation always admits a solution. If we define $G(x^\alpha)$ as the Green's function of the box operator,

$$\Box_{x^\alpha} G(x^\alpha - y^\alpha) = \delta^{(4)}(x^\alpha - y^\alpha), \tag{A.16}$$

Then, the solution of (A.15) is given by,

$$\xi_\mu(x^\alpha) = \int \mathrm{d}^4x \, G(x^\alpha - y^\alpha) f_\mu(y^\alpha) \tag{A.17}$$

Summarizing, for any initial configuration of the field $h_{\mu\nu}(x^\alpha)$, we can find a corresponding ξ_μ such that exists –locally– a new coordinate system $\{x'^\alpha\}$ in which the Lorenz condition $(\partial^\nu \bar{h}_{\mu\nu})' = 0$ holds. In this sense, the gauge condition (A.14) fixes four equations, reducing the ten independent components of $h_{\mu\nu}$ to six. Therefore, in the Lorenz gauge, the linearized Einstein Field Equations become,

$$\boxed{\Box \bar{h}_{\mu\nu} = -\frac{16\pi G}{c^4} T_{\mu\nu}} \tag{A.18}$$

If we take the partial derivative to both sides and use the Lorenz gauge condition, we get

$$\partial^\nu \Box h_{\mu\nu} = \Box(\partial^\nu h_{\mu\nu}) = -\frac{8\pi G}{c^4} \partial^\nu T_{\mu\nu} = 0 \quad \longrightarrow \quad \partial^\nu T_{\mu\nu} = 0 \tag{A.19}$$

These two results show that:

(i) The metric perturbation $h_{\mu\nu}$ propagates as a wave traveling at speed c, and the source of the wave is described by the energy–momentum tensor.

(ii) The conservation law of the energy–momentum tensor is expressed in terms of partial derivatives, rather than covariant derivatives.

(iii) The approximation of the linearized theory implies that the sources of gravitational waves should move in a flat space–time. For instance, the fact that we are using the background $\bar{g}_{\mu\nu} = \eta_{\mu\nu}$ implies that we can approximately describe the dynamics of self-gravitating systems, e.g. binary stars, using Newtonian gravity.

(iv) Actually, the gauge is not completely fixed. From the Wigner Theorem, we know that any massless particle has two polarizations or degrees of freedom. Thus, as we have at the moment six independent components for $h_{\mu\nu}$, four conditions (or equations) remain to be found. These will be obtained from another gauge–fixing procedure, with the Transverse–Traceless (TT) gauge condition.

Appendix B. Derivation of Friedmann Equations

The components of Stress-Energy tensor for a perfect fluid in thermodynamic equilibrium are given by

$$T_{\mu\nu} = (\rho + p)U_\mu U_\nu + p g_{\mu\nu}, \tag{B.1}$$

where ρ is the rest energy density and p is the isotropic pressure. In the FLRW comoving coordinates it holds that $U^\mu = U_\mu = (-1, 0, 0, 0)$ due to normalization condition $g_{\mu\nu}U^\mu U^\nu = -1$. Thus, in FLRW coordinates it follows that

$$[T_{\mu\nu}] = \begin{bmatrix} \rho & 0 & 0 & 0 \\ 0 & p\,a^2 & 0 & 0 \\ 0 & 0 & p\,a^2 & 0 \\ 0 & 0 & 0 & p\,a^2 \end{bmatrix}. \tag{B.2}$$

Additionally, for several non-interacting fluid components we can define a *equation of state* that relates pressure and energy density

$$p_i = \omega_i \rho_i, \tag{B.3}$$

where i will label the fluid component and ω_i is a constant which characterizes the type of fluid. For example, $\omega = 0$ corresponds to Dust and $\omega = 1/3$ to Radiation.

For the FLRW metric with $K = 0$, the components of Ricci Tensor and scalar curvature in Cartesian coordinates ($\mathrm{d}l^2 = \mathrm{d}x^2 + \mathrm{d}y^2 + \mathrm{d}z^2$) are given by

$$R_{00} = -3\frac{\ddot{a}}{a} \quad R_{ii} = a\ddot{a} + 2\dot{a}^2 \quad R_{ij} = 0 \quad R = 6\left[\frac{\ddot{a}}{a} + \left(\frac{\dot{a}}{a}\right)^2\right] \tag{B.4}$$

where $a = a(T)$ is the factor scale and a dot means derivative respect T. From Stress-Energy tensor of perfect fluid (B.2) and the components of Ricci tensor (B.4) it follows that the 00 component of generalized Einstein Field Equations (1.24) takes the form

$$\begin{aligned} R_{00} - \frac{1}{2} g_{00} R + \Lambda g_{00} &= \kappa T_{00} \\ -3\frac{\ddot{a}}{a} + 3\left[\frac{\ddot{a}}{a} + \left(\frac{\dot{a}}{a}\right)^2\right] - \Lambda &= \kappa \rho_i \\ \left(\frac{\dot{a}}{a}\right)^2 &= \frac{\kappa \rho_i + \Lambda}{3}. \end{aligned}$$

Defining $\rho_\Lambda \equiv \frac{\Lambda}{\kappa}$, we obtain the **1st Friedmann Equation**

$$\left(\frac{\dot{a}}{a}\right)^2 = \frac{\kappa}{3}\left(\rho_i + \rho_\Lambda\right). \tag{B.5}$$

For ii component of generalized EFE (1.24), it follows that

$$\begin{aligned} R_{ii} - \frac{1}{2} g_{ii} R + \Lambda g_{ii} &= \kappa T_{ii} \\ a\ddot{a} + 2\dot{a}^2 - 3a^2\left[\frac{\ddot{a}}{a} + \left(\frac{\dot{a}}{a}\right)^2\right] + \Lambda a^2 &= \kappa\, p_i\, a^2 \\ -2\ddot{a}a - \dot{a}^2 + \Lambda a^2 &= \kappa\, p_i\, a^2. \end{aligned}$$

Dividing by a^2 and using ρ_Λ we get

$$2\left(\frac{\ddot{a}}{a}\right) + \left(\frac{\dot{a}}{a}\right)^2 = \kappa(\rho_\Lambda - p_i).$$

When replacing (B.5) into last equation the **2nd Friedmann Equation** is obtained

$$\left(\frac{\ddot{a}}{a}\right) = \kappa\left(\frac{\rho_\Lambda}{3} - \frac{\rho_i}{6} - \frac{p_i}{2}\right). \tag{B.6}$$

Appendix C. Derivation of Schwarzschild and the SdS metrics

The first exact solution of the Einstein Field Equations was found by Karl Schwarzschild in 1916 [112]. Let us consider the following assumptions for a spacetime metric:

(i) Static: $g_{\mu\nu}$ is not time dependent.

(ii) Spherically Symmetric: Angular terms of the form $r^2(\mathrm{d}\theta^2 + \sin^2\theta \mathrm{d}\phi^2)$.

Thus, the most general metric that satisfies the previous conditions is given by

$$g_{\mu\nu}\mathrm{d}x^\mu \mathrm{d}x^\nu = -A(r)\mathrm{d}t^2 + B(r)\mathrm{d}r^2 + r^2[\mathrm{d}\theta^2 + \sin^2(\theta)\mathrm{d}\phi^2], \tag{C.1}$$

where $A(r)$ and $B(r)$ are unknown functions that depend only of r. If we multiply the Einstein Field Equations by $g^{\mu\nu}$ and sum over follows that

$$g^{\mu\nu}R_{\mu\nu} - \frac{1}{2}Rg^{\mu\nu}g_{\mu\nu} = \kappa g^{\mu\nu}T_{\mu\nu} \to R - 2R = \kappa T \to R = -\kappa T, \tag{C.2}$$

where we used that $R \equiv g^{\mu\nu}R_{\mu\nu}$, from (1.1) $\delta^\mu_\mu = 4$ and $T \equiv T^\mu_\mu$ is the trace of Stress-Energy tensor. Thus, for a vacuum solution $T = 0$, then $R = 0$ and EFE now reads

$$R_{\mu\nu} = 0. \tag{C.3}$$

When computing Ricci tensor components, using (C.1), we obtain

$$R_{rr} = -\frac{A''(r)}{2A(r)} + \frac{1}{4}\left(\frac{A'(r)}{A(r)}\right)\left[\frac{B'(r)}{B(r)} + \frac{A'(r)}{A(r)}\right] + \frac{1}{r}\left(\frac{B'(r)}{B(r)}\right) \tag{C.4}$$

$$R_{tt} = \frac{A''(r)}{2B(r)} - \frac{1}{4}\left(\frac{A'(r)}{B(r)}\right)\left[\frac{B'(r)}{B(r)} + \frac{A'(r)}{A(r)}\right] + \frac{1}{r}\left(\frac{A'(r)}{B(r)}\right) \tag{C.5}$$

$$R_{\theta\theta} = 1 + \frac{r}{2B(r)}\left[\frac{B'(r)}{B(r)} - \frac{A'(r)}{A(r)}\right] - \frac{1}{B(r)} \tag{C.6}$$

$$R_{\phi\phi} = \sin^2(\theta)R_{\theta\theta} \tag{C.7}$$

From (C.3); $R_{rr} = 0$, $R_{tt} = 0$ and $R_{\theta\theta} = 0$. It can be noted that

$$\frac{R_{rr}}{B(r)} + \frac{R_{tt}}{A(r)} = \frac{1}{rB(r)}\left(\frac{B'(r)}{B(r)} + \frac{A'(r)}{A(r)}\right) \stackrel{!}{=} 0, \tag{C.8}$$

then $A(r)B'(r) + B(r)A'(r) = 0$, so

$$\frac{\mathrm{d}}{\mathrm{d}r}\Big(A(r)B(r)\Big) = 0 \to A(r)B(r) = C, \tag{C.9}$$

with C a constant. If we now impose that the spacetime must be asymptotically flat (i.e $\lim_{r\to\infty} g_{\mu\nu} = \eta_{\mu\nu}$) it follows that $C = 1$. Thus, $A(r) = [B(r)]^{-1}$. Replacing the last expression into (C.6) gives

$$R_{\theta\theta} = 1 - \frac{r}{B(r)}\frac{A'(r)}{A(r)} - \frac{1}{B(r)} = 1 - rA'(r) - A(r) = 1 - \frac{\mathrm{d}}{\mathrm{d}r}\Big(rA(r)\Big) = 0. \tag{C.10}$$

Integrating with respect to r, we obtain that $A(r) = 1 + \frac{D}{r}$, with D a constant. At Newtonian limit $g_{tt} \approx -1 - 2\phi = -1 + \frac{2M}{r}$. Comparing, can be inferred that $D = -2M$, where M is the mass of gravitational source. Finally, the **Schwarzschild metric** is

$$g_{\mu\nu}\mathrm{d}x^\mu \mathrm{d}x^\nu = -\left(1 - \frac{2M}{r}\right)\mathrm{d}t^2 + \frac{\mathrm{d}r^2}{1 - \dfrac{2M}{r}} + r^2\mathrm{d}\Omega^2, \tag{C.11}$$

where $\mathrm{d}\Omega^2 = \mathrm{d}\theta^2 + \sin^2(\theta)\mathrm{d}\phi^2$. On the other hand, in a de Sitter spacetime we use the generalized Einstein Field Equations. Thus, following the same steps as before, let multiply (1.24) by $g^{\mu\nu}$ and sum over components

$$R - 2R + 4\Lambda = \kappa T \ \to \ R = 4\Lambda - \kappa T. \tag{C.12}$$

Then, a vacuum solution requires that

$$R_{\mu\nu} = \Lambda g_{\mu\nu}. \tag{C.13}$$

Conveniently we note that

$$\frac{R_{rr}}{B(r)} + \frac{R_{tt}}{A(r)} = \frac{\Lambda g_{rr}}{B(r)} + \frac{\Lambda g_{tt}}{A(r)} = \Lambda \left(\frac{B(r)}{B(r)} - \frac{A(r)}{A(r)} \right) \overset{!}{=} 0, \tag{C.14}$$

and as components of Ricci tensor do not change, the same procedure as before can be done. In particular, from last equation is clearly that again $A(r) = [B(r)]^{-1}$. Then, from (C.10) and (C.13) the $\theta\theta$ component of Ricci tensor must satisfy

$$R_{\theta\theta} = 1 - \frac{\mathrm{d}}{\mathrm{d}r}\Big(rA(r) \Big) = \Lambda g_{\theta\theta} = \Lambda r^2. \tag{C.15}$$

Integrating the last expression and applying the appropriate limits, we obtain

$$A(r) = 1 - \frac{2M}{r} - \frac{\Lambda}{3} r^2. \tag{C.16}$$

Finally, the **Schwarzschild-de Sitter metric** (SdS) is given by

$$g_{\mu\nu}\mathrm{d}x^\mu \mathrm{d}x^\nu = -\left(1 - \frac{2M}{r} - \frac{\Lambda}{3}r^2\right)\mathrm{d}t^2 + \frac{\mathrm{d}r^2}{1 - \dfrac{2M}{r} - \dfrac{\Lambda}{3}r^2} + r^2 \mathrm{d}\Omega^2. \tag{C.17}$$

APPENDIX D. ON THE DERIVATION OF THE $SS\chi$ METRIC

As we have to impose a spherically symmetric geometry we will have the transformation $r^2\,\mathrm{d}\Omega^2 \rightarrow a(T)^2 R^2\,\mathrm{d}\Omega^2$. Using the second rank tensor property of the metric tensor when we perform coordinate transformations,

$$g_{\mu'\nu'} = \frac{\partial X^\mu}{\partial x^{\mu'}} \frac{\partial X^\nu}{\partial x^{\nu'}} g_{\mu\nu}, \tag{D.1}$$

and the requirement that the new metric must be diagonal, we obtain the relation

$$0 = \frac{\partial T}{\partial t}\frac{\partial T}{\partial r} g_{TT} + \frac{\partial R}{\partial t}\frac{\partial R}{\partial r} g_{RR}. \tag{D.2}$$

By computing the partial derivatives we obtain the expressions

$$\frac{\partial R}{\partial r} = -\frac{1}{3}\frac{2r\frac{\partial T}{\partial r} - 3T(\chi_i+1)}{a(T)(\chi_i+1)T} \tag{D.3}$$

$$\frac{\partial R}{\partial t} = -\frac{2}{3}\frac{r\frac{\partial T}{\partial t}}{a(T)(\chi_i+1)T}, \tag{D.4}$$

and from (D.2) we find that

$$\frac{\partial T}{\partial r} = \frac{a(T)^2}{\frac{\partial T}{\partial t}}\frac{\partial R}{\partial t}\frac{\partial R}{\partial r}. \tag{D.5}$$

Thus, from the last equation, $\frac{\partial T}{\partial r}$ becomes

$$\frac{\partial T}{\partial r} = \frac{6rT(\chi_i+1)}{4r^2 - 9(\chi_i+1)^2T^2}, \tag{D.6}$$

and using (D.1) we can obtain the components of the metric,

$$g_{tt} = -\left(\frac{\partial T}{\partial t}\right)^2 \left[\frac{9(\chi_i+1)^2T^2 - 4r^2}{9(\chi_i+1)^2T^2}\right] \tag{D.7}$$

$$g_{rr} = \frac{9(\chi_i+1)^2T^2}{9(\chi_i+1)^2T^2 - 4r^2}. \tag{D.8}$$

From (1.55) we can write the SSχ_i metric as

$$\mathrm{d}s^2 = -\frac{(\partial_t\rho_i)^2}{3\kappa\rho_i^3(\chi_i+1)^2}\left[1 - \frac{\kappa\rho_i r^2}{3}\right]\mathrm{d}t^2 + \frac{\mathrm{d}r^2}{1 - \frac{\kappa\rho_i r^2}{3}} + r^2\,\mathrm{d}\Omega^2, \tag{D.9}$$

but, using (1.55) and (D.6), we get

$$\frac{\partial \rho_i}{\partial r} = \frac{(\chi_i + 1)\kappa \rho_i^2 r}{1 - \frac{\kappa \rho_i}{3} r^2}. \tag{D.10}$$

If we properly redefine $\tilde{\rho}_i \equiv \kappa \rho_i$, the last expression becomes

$$\frac{\partial \tilde{\rho}_i}{\partial r} = \frac{(\chi_i + 1)\tilde{\rho}_i^2 r}{1 - \frac{\tilde{\rho}_i}{3} r^2}, \tag{D.11}$$

but it can be noticed from (D.11) that we can form the expression

$$\frac{\partial}{\partial r}\left[\frac{c + r^2 \tilde{\rho}_i}{\tilde{\rho}_i^n}\right] = 0, \tag{D.12}$$

where c and n are unknown constants. Unfolding the last expression and using the linear independence of r, we obtain that the constants are

$$c = \frac{6}{3\chi_i + 1} \qquad n = \frac{3\chi_i + 1}{3(\chi_i + 1)}. \tag{D.13}$$

Therefore, we can integrate (D.12) and write

$$\frac{c + r^2 \tilde{\rho}_i}{\tilde{\rho}_i^n} = F(t), \tag{D.14}$$

where $F(t)$ is a function of t. By a dimensional analysis, we note that in natural units $[\tilde{\rho}_i] = L^{-2}$ and therefore $[F(t)] = L^{2n}$. As there is no other parameter involved apart from t, and also as $[t] = L$ in natural units, then we set $F(t) = At^{2n}$, with A as a dimensionless arbitrary constant. For any fluid we can expect that at later stage it will be diluted homogeneously, which implies that for $t \to \infty$ the metric (D.9) is almost flat. Then,

$$\lim_{t\to\infty(\rho_i \to 0)} \frac{(\partial_t \rho_i)^2}{3\kappa \rho_i^3 (\chi_i + 1)^2} = 1. \tag{D.15}$$

On the other hand, (D.14) can be written as

$$\frac{c + r^2 \kappa \rho_i}{(\kappa \rho_i)^n} = At^{2n}, \tag{D.16}$$

but when we take the derivative with respect to t and solving for $\partial_t \rho_i$, we obtain

$$\frac{\partial \rho_i}{\partial t} = -\frac{2nAt^{2n-1}(\kappa\rho_i)^n \rho_i}{\kappa\rho_i n r^2 - r^2\kappa\rho_i + cn}, \tag{D.17}$$

and if we square, divide by $3\kappa\rho_i^3$ and replace the previous results, we can found the following equality

$$\frac{(\partial_t \rho_i)^2}{3\kappa\rho_i^3(\chi_i+1)^2} = \frac{4n^2 A^{1/n}(\kappa r^2\rho_i + c)^{\frac{2n-1}{n}}}{3(\chi_i+1)^2[(n-1)\kappa r^2\rho_i + cn]}. \tag{D.18}$$

Computing the limit $\rho_i \to 0$ as the fluid dilutes at distant times, we can set A,

$$\lim_{t\to\infty(\rho_i\to 0)} \frac{(\partial_t \rho_i)^2}{3\kappa\rho_i^3(\chi_i+1)^2} = \frac{4n^2 A^{1/n} c^{\frac{2n-1}{n}}}{3(\chi_i+1)^2(cn)^2}, \tag{D.19}$$

and using that the metric is asymptotically flat, which implies that the previous limit is equal to one, we get the value of A,

$$A = c\left(\frac{3}{4}\right)^n (\chi_i+1)^{2n}. \tag{D.20}$$

Finally, with the constant A known, we can provide an exact expression for the the SSχ metric, which becomes

$$\mathrm{d}s^2 = -\frac{\mathrm{d}t^2}{\left(1-\frac{\kappa\rho_i r^2}{3}\right)\left(1+\frac{\kappa\rho_i r^2(3\chi_i+1)}{6}\right)^{\frac{1-3\chi_i}{1+3\chi_i}}} + \frac{\mathrm{d}r^2}{1-\frac{\kappa\rho_i r^2}{3}} + r^2\left(\mathrm{d}\theta^2 + \sin^2(\theta)\,\mathrm{d}\phi^2\right), \tag{D.21}$$

and from (D.16) we can express the coordinate transformation between the SSχ_i and the FLRW frames in terms of ρ_i y $\rho_{i0} = \rho_i(T_0)$,

$$t = \frac{\left[c + R^2(\kappa\rho_{i0})^{\frac{2}{3(\chi_i+1)}}(\kappa\rho_i)^{\frac{3\chi_i+1}{3(\chi_i+1)}}\right]^{\frac{1}{2n}}}{\left(A^{\frac{1}{2n}}\right)\sqrt{\kappa\rho_i}} \tag{D.22}$$

$$r = R\left(\frac{\rho_{i0}}{\rho_i}\right)^{\frac{1}{3(\chi_i+1)}}. \tag{D.23}$$

APPENDIX E. ON THE ACCURACY IN THE APPROXIMATION OF H_0

In order to simplify the computation, we can omit the geometrical prefactor that appears in (4.20), because it is common to every observation and is H_0–independent. Therefore, we define a reduced timing residual,

$$\tau_{\rm GW}^{\rm red} \equiv \int_{-1}^{0} \frac{1+H_0\left[T_e+\frac{xL}{c}\right]}{Z+xL\cos\alpha}\sin\left(\frac{\pi}{4}+\Theta(x,\alpha)\right)\,\mathrm{d}x \approx R_1+\left(\frac{1+\frac{H_0 Z}{c}}{Z}\right)\int_{-1}^{0}\sin\left(\frac{\pi}{4}+\Theta(x,\alpha)\right)\,\mathrm{d}x, \tag{E.1}$$

with $|R_1| \leq \frac{LH_0}{cZ} \sim 10^{-31}$ s. Then, we take the reduced timing residual from (E.1) and note that R_1 is given by

$$R_1 = \int_{-1}^{0}\mathrm{d}x \sin\left(\Theta(x,\alpha)+\frac{\pi}{4}\right)\left[\frac{1+H_0\left[\frac{Z_e}{c}+\frac{L}{c}x\right]}{Z_e+xL\cos\alpha}-\frac{1+H_0\frac{Z_e}{c}}{Z_e}\right]. \tag{E.2}$$

Thus we can bound the value of R_1 by

$$\begin{aligned} |R_1| &\leq \frac{L}{Z_e}\int_{-1}^{0}\left|\sin\left(\Theta(x,\alpha)+\frac{\pi}{4}\right)\right| \times \left|\frac{H_0\left[\frac{1}{c}x\right]-x\frac{L}{Z_e^2}\cos\alpha - x\frac{L}{Z_e}\cos\alpha H_0\frac{1}{c}}{\left(1+x\frac{L}{Z_e}\cos\alpha\right)}\right|\mathrm{d}x \\ &\leq \frac{LH_0}{2Zc}+\mathcal{O}\left(\frac{L^2}{Z^3}\right) \sim 10^{-31}\ \mathrm{s}. \end{aligned} \tag{E.3}$$

Then we can reasonable neglect R_1 in the equation (E.1). Now we can express $\tau_{\rm GW}^{\rm red}$ in terms of the imaginary part of the complex exponential and write, since $\Theta(x,\alpha)$ is quadratic in x:

$$\tau_{\rm GW}^{\rm red} = \mathrm{Im}\left\{\int_{-1}^{0}\mathrm{d}x\ e^{i\left(\Theta(x,\alpha)+\frac{\pi}{4}\right)}\right\} = \mathrm{Im}\left\{B(\alpha)e^{i\left(\Theta(x^*,\alpha)+\frac{\pi}{4}\right)}\right\}, \tag{E.4}$$

where $B(\alpha)$ is defined as $B(\alpha) \equiv \int_{-1}^{0}\mathrm{d}x\ e^{i\lambda(x-x^*)^2}$, x^* satisfies $\partial\Theta(x,\alpha)/\partial x\ |_{x=x^*} = 0$, thus

$$x^* = \frac{-c+c\cos\alpha+Z_e H_0}{(\cos\alpha^2-2\cos\alpha)\,H_0 L}, \tag{E.5}$$

and λ is given by

$$\lambda = \frac{1}{2}\frac{\partial^2\Theta(x,\alpha)}{\partial x^2} = \frac{1}{2}\frac{\Omega H_0 L^2}{c^2}(\cos\alpha^2-2\cos\alpha). \tag{E.6}$$

The integral $B(\alpha)$ can be written in terms of the error function, giving

$$B(\alpha) = \frac{\sqrt{2\pi}}{4}(1+i)\frac{1}{\sqrt{\lambda}}\left[-\operatorname{erf}\left(\frac{\sqrt{2}}{2}(1-i)u^*\right) + \operatorname{erf}\left(\frac{\sqrt{2}}{2}(1-i)\left(\sqrt{\lambda}+u^*\right)\right)\right], \tag{E.7}$$

where $u^* \equiv \sqrt{\lambda}x^*$. Using the asymptotic expansion of the error functions for $u^* \gg 1$, e.g. see [42], we can write

$$B(\alpha) \approx e^{-z_1^2}\left(1+\frac{1}{2z_1}\right) \qquad z_1 \equiv \frac{\sqrt{2}}{2}(1-i)u^*. \tag{E.8}$$

Inserting the last expression into (E.4), $\tau_{\text{GW}}^{\text{red}}$ becomes

$$\tau_{\text{GW}}^{\text{red}} \approx \sin\left(C+\frac{\pi}{4}\right) + \frac{1}{2|u^*|}\sin C, \tag{E.9}$$

where $C = H_0 Z^2\Omega/2c^2$. From this expression we can see that the maximum of $\tau_{\text{GW}}^{\text{red}}$ clearly happens for $u^* \to 0$. This condition implies, from (E.6), that the angle corresponding to the maximum absolute value of τ_{GW} satisfies $x^* = 0$, or, rearranging the terms, the approximation formula (4.22). In order to justify the validity of the asymptotic expansion, we can explore around $u^* = 0$, finding that for a variation in the angle $\Delta\alpha$, then $u^* \sim i\sqrt{\frac{Z\Omega}{c}}\Delta\alpha \sim 10^4\Delta\alpha$. Thus, the expansion is well defined for $\Delta\alpha \gg 10^{-4}$.

Appendix F. Table of pulsars of the ATNF catalog

Pulsar Name	θ	ϕ	L_i
J0324+5239	$168.5°$	$-31.68°$	2.56 kpc
J0325+67	$145°$	$-1.22°$	1.51 kpc
J0329+1654	$130.31°$	$18.68°$	1.05 kpc
J0332+5434	$150.35°$	$-8.64°$	1.54 kpc
J0332+79	$169.99°$	$-30.04°$	1.30 kpc
J2007+2722	$78.23°$	$2.09°$	2.15 kpc
J2007+3120	$68.86°$	$-4.67°$	2.10 kpc
J2008+2513	$76.89°$	$0.96°$	10.3 kpc
J2009+3326	$87.86°$	$8.38°$	1.83 kpc
J2010-1323	$86.86°$	$7.54°$	2.06 kpc
J1848-1150	$35.26°$	$1.4°$	12.3 kpc
J1848+12	$36.72°$	$2.23°$	8.23 kpc
J1848-1243	$44.99°$	$6.34°$	2.17 kpc
J1848-1414	$46.69°$	$7.29°$	1.22 kpc
J1848-1952	$32.54°$	$-0.33°$	5.45 kpc
J1826-1256	$21.33°$	$0.26°$	4.94 kpc
J1826-1334	$14.6°$	$-3.42°$	5.94 kpc
J1826-1419	$53.34°$	$15.61°$	0.91 kpc
J1826-1526	$29.76°$	$4.25°$	10.3 kpc
J1827-0750	$29.16°$	$3.99°$	3.50 kpc
J1946+14	$66.86°$	$2.55°$	7.47 kpc
J1946+1805	$44.86°$	$-10.55°$	3.94 kpc
J1946+2052	$61.1°$	$-1.17°$	7.27 kpc
J1946+2244	$50°$	$-7.74°$	1.51 kpc
J1946+24	$52.5°$	$-6.58°$	1.59 kpc

TABLE F.1. List of randomly distributed pulsars averaged for an hypothetical source. The galactic longitude is denoted by θ and the galactic latitude by ϕ. More information about the pulsars can be found in *http://www.atnf.csiro.au/research/pulsar/psrcat/*.

Pulsar Name	θ	ϕ	L_i
J1946+24	$30.81°$	$3.73°$	3.35 kpc
J1831-1329	$30.57°$	$3.45°$	4.68 kpc
J1831-1423	$27.04°$	$1.75°$	2.49 kpc
J1832+0029	$25.64°$	$0.96°$	6.30 kpc
J1832-0644	$25.17°$	$0.76°$	8.29 kpc
J2155-3118	$108.64°$	$6.85°$	1.88 kpc
J2155-5641	$89.66°$	$-22.81°$	2.82 kpc
J2156+2618	$87.69°$	$-26.28°$	1.80 kpc
J2157+4017	$106.65°$	$2.95°$	3.00 kpc
J2203+50	$107.15°$	$3.64°$	3.01 kpc
J1840-0809	$30.28°$	$1.02°$	6.97 kpc
J1840-0815	$34.56°$	$3.34°$	5.04 kpc
J1840-0840	$29.08°$	$0.58°$	8.58 kpc
J1840-1122	$35.43°$	$3.85°$	4.33 kpc
J1840-1207	$28.35°$	$0.17°$	3.71 kpc
J1828-2119	$31.25°$	$4.36°$	1.04 kpc
J1829+0000	$24.81°$	$1.07°$	10.4 kpc
J1829-0734	$23.27°$	$0.3°$	5.20 kpc
J1829-1011	$23.11°$	$0.26°$	0.81 kpc
J1829-1751	$21.59°$	$-0.6°$	4.69 kpc
J1848-0511	$32.76°$	$0.09°$	5.63 kpc
J1848-0601	$32.41°$	$0.07°$	6.71 kpc
J1848+0604	$33.25°$	$0.35°$	4.05 kpc
J1848+0647	$32.37°$	$-0.04°$	6.5 kpc
J1848+0826	$34.02°$	$0.96°$	3.39 kpc
J1843-0050	$29.57°$	$0.12°$	6.03 kpc
J1843-0137	$29.52°$	$0.07°$	5.70 kpc
J1843-0211	$29.4°$	$0.24°$	5.26 kpc
J1843-0355	$29.34°$	$0.04°$	5.97 kpc
J1843-0408	$28.79°$	$-0.19°$	5.45 kpc

TABLE F.2. Second part of the table.